

**Deanship of Graduate Studies
Al-Quds University**

**Estimation of Time-Varying MC-DS-CDMA Fading Channels
Based on Kalman Filtering**

Walid Jamal Hassan Hassasneh

M.Sc. Thesis

Jerusalem-Palestine

Jamada El Oula-1428 / May-2007

**Deanship of Graduate Studies
Al-Quds University**

**Estimation of Time-Varying MC-DS-CDMA Fading Channels
Based on Kalman Filtering**

Walid Jamal Hassan Hassasneh

M.Sc. Thesis

Jerusalem-Palestine

Jamada El Oula-1428 / May-2007

**Estimation of Time-Varying MC-DS-CDMA Fading Channels
Based on Kalman Filtering**

**Prepared By:
Walid Jamal Hassan Hassasneh**

B.Sc: Electrical Engineering- Light Current from BerZeit University- Palestine

**Supervisor: Dr. Hanna Abdel Nour
Co-Supervisor: Ali Jamoos**

**A Thesis Submitted in Partial fulfillment of requirements for the degree
of Master of Electronic Engineer and Computer Engineering.**

**Department of Electrical Engineering/ Master Program in
Electronic and Computer Engineering/ Al-Quds University**

Jamada El Oula-1428 / May-2007

Al Quds University
Deanship of Graduate Studies
Graduate Studies/Electronic and Computer Engineering



Thesis Approval

Estimation of Time-Varying MC-DS-CDMA Fading Channels Based on Kalman Filtering

Prepared By: Walid Jamal Hassan Hassasneh
Registration No: 20310020

Supervisor: Dr. Hanna Abdel Nour
Co-Supervisor: Ali Jamoos

Master thesis submitted and accepted, Date:25/05/2007

The names and signatures of the examining committee members are as follows:

1- Dr. Hanna Abdel Nour	Head of Committee	Signature.....
2- Dr. Hussein Jaddu	Internal Examiner	Signature.....
3- Dr. Nasser Hamad	External Examiner	Signature.....

Jerusalem-Palestine
2007

Dedication:

This work is dedicated to most precious one my mother's spirit, Khadijeh, who loved and gave me all hopefulness in life.

Declaration:

I certify that this thesis submitted for the degree of Master is the results of my own research, except where otherwise acknowledged, and that this thesis (or any part of the same) has been submitted for a higher degree to any other university or institution.

Signed:.....

Walid Jamal Hassan Hassasneh

Date: 25/05/2007

Acknowledgments

بِسْمِ اللَّهِ الرَّحْمَنِ الرَّحِيمِ

Thanks to God for this work.

First and foremost, I would like to thank my supervisor Dr. Hanna Abdel Nour, and co-supervisor Ali Jamoos for their efforts, assistance, insight, patience and guidance through my graduate work.

Most of all I would like to thank my friends and my family, father, brothers (Moafag, Nadir and Tawfiq), sisters (Mona and Olfat), and special thanks to my fiancée, Lila, for their encouragements and supports.

I don't forget also all the professors of Computer and Electronic Engineering departments in Al-Quds University, specially, Dr. Hussein Jaddu, Dr Labib Arafeh, and Dr. Abed Al Kareem Ayad. Furthermore, to all Palestinians and people who love peace.

It should be noted that this thesis is the fruit of collaboration with the Signal and Image Group (ESI) at the UMR CNRS 5218 IMS in Bordeaux1 University-France. More particularly, it results from the close cooperation with Mr. A. Jamoos and Dr. E. Grivel who are members of the ESI. This cooperation was made possible with the financial support of the French government through the "Programme d'Action Intégrée" (PAI 2005).

Abstract

Code Division Multiple Access is a common wideband communication system, due to its high data rates, bandwidth efficiency, multiple user services and securities. However, this scheme doesn't treat channel problems perfectly. Hence, the Multi-Carrier (MC-CDMA) of combining Orthogonal Frequency Division Multiplexing (OFDM) with CDMA is found, using the advantages of both schemes. Further advantages can be achieved by combination of MC transmissions with Direct Sequence (DS) CDMA, known as MC-DS-CDMA, which is considered as one important technique for beyond third generation mobile wireless systems. Actually, this technique has been adopted for CDMA2000 third generation cellular standard.

The MC-DS-CDMA better compensates multipath fading problems of non-ideal channels by using adaptive channel estimator filters. Furthermore, this scheme can suppress the Multiple Access Interference (MAI) problem due to cross-correlation properties of its spreading codes, by using adaptive receivers. Indeed, this performance is obtained under certain conditions.

Channel status information are assumed to be perfectly known when considering a receiver structure of a decorrelator along each carrier for suppressing MAI, followed by a Maximum Ratio Combiner (MRC). Unfortunately, the channel coefficients are unknown and must be estimated to compact these fading effects. In reality, the Kalman filter based channel estimator works well in time varying fading channels. However, this requires the *a priori* estimation of the autoregressive (AR) parameters. Based on the well-known Jakes model, AR parameters can be obtained by first fitting AR process autocorrelation function to the Jakes one and then solving the resulting Yule-Walker equations (YWE). But we have to pay attention to the condition number of the autocorrelation matrix of this YWE, which determines the accuracy of the solution.

Due to the band-limited nature of the Jakes Doppler spectrum, severe ill-conditioning problems in solving YWE are unavoidable for all but very small AR model orders. For this reason and for the sake of simplicity, we find previous studies focus only on first and second order AR models. To avoid the ill-conditioning problem, a very small positive bias is added to the main diagonal of the autocorrelation matrix in the YWE. Indeed, this can remove band-limitation of the original spectrum.

As the ill-conditioning can be solved investigating the relevance of high order AR models can be done, hence, better approximations to the Rayleigh fading channel could be achieved. However, the higher AR model orders the higher computational costs. Thus, a compromise between the model accuracy and the computational cost has to be found.

In this work we investigate high AR model orders using Kalman filtering based channel estimator for a synchronous MC-DS-CDMA scheme in time varying fading channels.

Simulation results of BER performance for different channel estimators under realistic Jakes fading channel is presented, which investigates the relevance of high AR model

orders for retrieving transmitted data sequences using the Kalman filtering based channel estimator.

Furthermore, we consider the high order AR models with known Doppler rates, or equivalently, mobile speed, with different fading rate scenarios.

For the purpose of comparative study, we also carry out channel estimation by Least Mean Square (LMS) and Recursive Least Square (RLS) channel estimators, followed by MRC. Simulation results show that the Kalman filter based channel estimator provides better results than those based on LMS or RLS, especially in high Doppler rate environments. In addition, increasing the AR model order yields better modeling approximation to the fading channel and provides lower BER. Furthermore, a fifth order AR model can provide a trade-off between the accuracy of the model and the computational cost.

المخلص

يستخدم نظام MC-DS-CDMA في الجيل الثالث من الاتصالات, وذلك بسبب سعة عرض النطاق الترددي, ودعمه لعدد كبير من المستخدمين, بالإضافة للخدمات التي تحتاجها الانظمة الحديثة للإتصالات اللاسلكية. بالحقيقة هذا النوع من الانظمة أعتد للأجهزة الخلوية التي تستخدم ب 3G CDMA 2000.

بإستخدام المرشحات الحديثة لهذا النوع من الأنظمة يمكن حل مشاكل تعدد المسارات للموجات الكهرومغناطيسية والذي ينتج عنه ما يعرف بمشكلة التضائلات Multipath Fading , كما ويقاوم هذا النظام مشاكل تداخل المستخدمين MAI بكفاءة عند إستخدام مرشحات متطورة مثل ما يسمى مستقبل الديكورريلاتور Decorrelator Receivers.

إن مرشح الكلمان Kalman Filter ذو كفاءة عالية مقارنة مع الانواع الأخرى مثل LMS و RLS. ولتطبيق هذا المرشح نحتاج الى ما يعرف بنموذج التردد التلقائي Autoregressive Model. والذي يحتاج بدورة برمترات AR parameters التي قد نجدها من حل معادلة ما يعرف ب يل ولكر Yule-Walker Equation.

على اي حال, حل هذه المعادلة بسبب ضمام الطبيعة للوسط ذو الطيف المحدود يعاني مما يعرف بمشكلة العصابة Ill-conditioning لجميع الدرجات ما عدا القليل منها. ولهذا نجد السابقين في الموضوع درسوا لدرجات منخفضة أقصاها الدرجة الثانية. وللتعامل مع هذا النوع من المشاكل "حل يل ولكر" نحيز مصفوفة الترابط التلقائي Autocorrelation matrix بإضافة رقم موجب صغير على قطرها. مما يزيل العصابة في الطيف الأصلي.

هنا بهذا البحث نقدم مرشح كلمان لتقدير الوسط - ظاهرة التضائلات- على درجات التردد التلقائي دون حد أقصى. مع إستخدام الديكوروليتر لحل مشكلة تداخل المستخدمين. توضح نتائج البحث أن الدرجة الخامسة مقبولة للدقة وتعقيد الحسابات.

TABLE OF CONTENTS

Dedication	I
Declaration	II
Acknowledgments	III
Abstract	IV
Table of Contents	VI
List of Figures	VIII
List of Tables	IX
List of Acronyms	X
Chapter 1	
Introduction	
1.1 Wireless Mobile Communications.....	1
1.2 Motivation.....	5
1.3 Summary of Contribution.....	6
1.4 Thesis Outline.....	7
Chapter 2	
MC-DS-CDMA Mobile Wireless Systems	
2.1 Multiple Access Techniques.....	8
2.2 Basics of CDMA.....	14
2.2.1 Spreading Sequences.....	14
2.3 DS-CDMA.....	20
2.4 MC-DS-CDMA.....	21
2.4.1 Why MC-DS-CDMA.....	22
2.4.2 MC-DS-CDMA Transmitter.....	23
Chapter 3	
Mobile Wireless Fading Channels	
3.1 Introduction.....	25
3.2 Channel Parameters.....	27
3.3 Channel Classifications.....	29
3.3.1 Frequency Non-selective versus Frequency Selective.....	29
3.3.2 Slow Fading versus Fast Fading.....	30
3.3.3 Frequency Non-selective Fading Channel.....	31
3.3.4 Frequency Selective Fading Channel.....	33
3.4 Diversity Techniques for Multipath Fading Channels.....	33
3.5 Jakes Model.....	33
3.6 AWGN Channel Model.....	35
Chapter 4	
Receiver Design	
4.1 Introduction.....	37
4.2 Conventional MC-DS-CDMA Receiver.....	37
4.3 Decorrelator Detector Based Receiver.....	39
4.4 Simulation Results.....	42
4.5 Conclusion.....	44
Chapter 5	
Channel Estimation	
5.1 Introduction.....	45

5.2 Autoregressive Model.....	48
5.2.1 Autoregressive Model Background.....	48
5.2.2 Autoregressive Modeling of Rayleigh Fading Channels.....	50
5.3 Kalman Filtering	48
5.3.1 Kalman Filter Background.....	58
5.3.2 Kalman Filtering Based Channel Estimation.....	61
5.4 LMS Channel Estimator.....	63
5.5 RLS Channel Estimator.....	64
5.6 Simulation Results.....	66
5.6.1 Simulation Protocols.....	66
5.6.2 Results And Comments.....	66
5.7 Conclusion.....	70
Chapter 6	
Conclusions and Future Works.....	71
References.....	73
Annex- Related Published Papers.....	77

List of Figures

Figure 1-1	Evolution of wide area cellular networks-WWAN.	2
Figure 1-2	Evolution of current networks to the 3G of wireless networks.	3
Figure 1-3	Data rate versus range for various applications.	4
Figure 1-4	Data rate versus mobility for various applications.	4
Figure 2-1	FDMA scheme.	8
Figure 2-2	TDMA scheme.	9
Figure 2-3	The OFDM orthogonal carriers.	10
Figure 2-4	Principle of CDMA scheme.	11
Figure 2-5	Classification of CDMA schemes according to the modulation method.	12
Figure 2-6	Generation of m-sequences using shift register.	16
Figure 2-7	Gold sequence generator of 31 sequence length.	18
Figure 2-8	Aperiodic autocorrelation plot of Gold sequences corresponds of length 31.	18
Figure 2-9	Aperiodic crosscorrelation plot of Gold sequences corresponds of length 31.	19
Figure 2-10	CDMA downlink channel model.	19
Figure 2-11	CDMA uplink channel model.	20
Figure 2-12	Direct spread CDMA transmitter.	21
Figure 2-13	Multicarrier single user DS-SS transmitter.	22
Figure 2-14	The mth carrier of MC-SS transmitter.	23
Figure 2-15	Spectrum of (a) wideband single DS-SS (b) orthogonal MC-SS signals.	24
Figure 3-1	Illustration of wireless propagation mechanisms.	26
Figure 3-2	Channel model.	27
Figure 3-3	Illustrate multipath spread concept.	28
Figure 3-4	Flat fading characteristics.	29
Figure 3-5	Probability density function of Rayleigh distribution.	32
Figure 3-6	Rayleigh fading channel envelope.	32
Figure 3-7	PSD of the Jakes model.	35
Figure 3-8	Normalized ACF of Jakes model.	36
Figure 4-1	Correlator receiver; consisting of a correlator along each carrier followed by MRC.	38
Figure 4-2	Decorrelator receiver; consisting a decorrelator along each carrier.	41
Figure 4-3	The BER of the conventional decorrelator, correlator receivers with NF.	43
Figure 4-4	The BER of the conventional decorrelator, correlator receivers with MAI.	43
Figure 4-5	BER performance versus number of users, at SNR=15 dB, for 2 carriers.	44
Figure 5-1	Coupled Kalman filter.	46
Figure 5-2	Driving process variance versus the model order with different Doppler rate scenarios.	53
Figure 5-3	ACF of the Jakes model fitted AR (p) process with p=1, 2.	54
Figure 5-4	PSD of the Jakes model and that of the fitted AR(p) process with p=1, 2.	55
Figure 5-5	ACF of the Jakes model and that of the fitted AR (p) process with p=50, 100, and 200.	55
Figure 5-6	PSD of the Jakes model and that of the fitted AR(p) process with p=50, 100 and 200.	56
Figure 5-7	ACF of the Jakes model fitted with AR (p) process with p=1, 2, 5, 20, and 100.	56
Figure 5-8	PSD of the Jakes model and that of the fitted AR(p) process with p=1, 2, 5, 20, and 100.	57
Figure 5-9	Simulation time with AR model.	57
Figure 5-10	Recursive Kalman algorithm.	61
Figure 5-11	Kalman filtering channel estimator.	63
Figure 5-12	LMS filter channel estimator.	64
Figure 5-13	RLS filter channel estimator.	65
Figure 5-14	BER performance vs SNR with channel estimators for number of carriers M=1 and M=3.	68
Figure 5-15	BER performance with the various channel estimators versus the Doppler rate, M=1, and M=3.	68
Figure 5-16	Accuracy of square (BER) vs AR model orders, max of p is 20.	69
Figure 5-17	Accuracy of square (BER) vs AR model orders, max of p is 100.	69
Figure 5-18	Envelope and phase of the estimated fading process along the first carrier.	70

List of Tables

TABLE 1-1	MAJOR MOBILE STANDARDS IN NORTH AMERICA.	3
TABLE 1-2	MAJOR MOBILE STANDARDS IN NORTH EUROPE.	3
TABLE 1-3	DATA CHARACTERISTICS OF UMTS SERVICES.	4
TABLE 2-1	FREQUENCY OF OCCURRENCE OF VALUES FOR GOLD SEQUENCES.	17
TABLE 3-1	DECISION CRITERIA FOR THE TYPES OF CHANNEL MODEL TO USE.	31
TABLE 5-1	TYPICAL VALUES OF THE ADDED BIAS FOR DIFFERENT DOPPLER RATES.	54
TABLE 5-2	AR PARAMETERS OF THE 5TH ORDER WITH VARIOUS MOBILE VELOCITIES.	58
TABLE 5-3	MULTI-DIMENSIONAL KALMAN RECURSIVE EQUATIONS.	59
TABLE 5-4	SUMMARY OF THE KALMAN VECTOR AND MATRIX VARIABLES.	59
TABLE 5-5	COMPLEXITY CALCULATION OF THE KALMAN ALGORITHM PER ITERATION.	60

List of Acronyms and Abbreviations

1G	First Generation
2.5G	Two and Half Generation
2G	Second Generation
3G	Third Generation
3GPP	Third Generation Partnership Project
4G	Forth Generation
ACF	Autocorrelation Function
AMPS	Advanced Mobile Phone Service
APA	Affine Projection Algorithms
AR	AutoRegressive
ATM	Asynchronous Transfer Mode
AWGN	Additive White Gaussian Noise
B3G	Beyond Third Generation
BER	Bit Error Rate
B-ISDN	Broadband Integrated Services Digital Network
BRLS	Block Recursive Least Mean Square
BS	Base Station
CCL	Cross-correlation
CDMA	Code Division Multiple Access
CEPT	Conférence Européenne des Postes et Télécommunication
CT2	British cordless telephone system
DA	Data Aided
DAMPS	Digital-AMPS
dB	Decibel
DD	Decision Directed
DECT	Digital Enhanced Cordless Telecommunication
DFE	Decision Feedback Equalizer
DNR	Preliminary Draft of New Recommendation
DS-CDMA	Direct Sequence -CDMA
EDGE	Enhanced Data Rates for GSM Evolution
EM	Expectation Maximization
F	Frequency
FDMA	Frequency Division Multiple Access
FFH	Fast Frequency Hopping
FH-CDMA	Frequency Hopping CDMA
FM	Frequency Modulation
GPRS	General Packet Radio Service
GSM	Global System for Mobile Telecommunication
HDTV	High Definition Television

iid	Independent and Identical Distributed
IMT-2000	International Mobile Telecommunications 2000
IS	Interim Standard
IS-54	The Pan-American DAMPS TDMA Mobile
IS-95	The Pan-American CDMA Mobile Radio
ISDN	Integrated Services Digital Network
ISI	Intersymbol Interference
ITU	International Telecommunication Union
KF	Kalman Filter
LAN	Local Area Network
LMS	Least Mean Square
LOS	Line-of-sight
MA	Multiple Access
MAI	Multi-access Interference
MC-DS-CDMA	Multi-Carrier Direct Sequence CDMA
MC-CDMA	Multi-Carrier CDMA
MF	Matched Filter
MMSE	Minimum Mean Square Error
MRC	Maximum Ratio Combiner
MS	Mobile Station
MSE	Mean Square Error
MT-CDMA	Multi-Tone CDMA
NAMPS	Narrowband AMPS
NDA	Non Data Aided (Blind technique)
NLMS	Normalized Least Mean Square
NMT	Nordic Mobile Telephone
NMTS	Nordic Mobile Telephone System
NTT	Nippon Telegraph and Telephone Company
OFDM	Orthogonal Frequency Division Multiplexing
PDC	Personal Digital Cellular
Pdf	Probability Density Function
PHP	Personal Handy Phone
PLMR	Public Land Mobile Radio
PN	Pseudo Noise
PSD	Power Spectral Density
QoS	Quality of Service
RLS	Recursive Least Square
SC-DS-CDMA	Single-Carrier DS-CDMA
SFH	Slow Frequency Hopping
SIR	Signal to Interference Ratio
SNR	Signal to Noise Ratio

SSMA	Spread Spectrum Multiple Access
T	Time
TD-CDMA	Time Division Code Division Multiple Access
TDMA	Time Division Multiple Access
TH-CDMA	Time Hopping CDMA
UMTS	Universal Mobile Telecommunications System
USDC	U.S. Digital Cellular
VLSI	Very Large Scale Integration
WCDMA	Wideband Code Division Multiple Access
WLAN	Wireless Local Area Network
WSS	Wide Sense Stationary
WSSUS	Wide-sense Stationary Uncorrelated Scattering
YWE	Yule-Walker Equations

Chapter 1

Introduction

1.1 Wireless Mobile Communications

Recently, Wireless communications are going under explosive growth, due to the fact that the wired phones suffer from serious problems of installations and costs. The first Generation (1G) systems were introduced with Advanced Mobile Phone Service (AMPS) in the 1980s [1], then the Nordic mobile telephone system (NMTS) in Scandinavia in 1981. The first British system was Total Access Communication System (TACS), operated by Cellnet and Vodafone, NMT-900, C-450, RTM, and Radiocom-2000, respectively, introduced in Germany, Italy, and France. The Japanese introduced NTACS. Nevertheless, all of these systems were based on analog FM using digital network control; as Frequency Division Multiple Access (FDMA). However, they did not support international roaming. In addition, these systems only provided voice communications, and they also suffered from a low user capacity, and security problems due to the simple radio interface used.

The Conference “Conférence Européenne des Postes et Télécommunication” (CEPT), the main governing body of the European postal, telephone, and telegraph organizations, created the Group Spécial Mobile (GSM) in 1982 [2, 3], for standardizing a digital cellular pan-European public mobile communications system to operate in the 900-MHz band. Hence, the 2G systems were introduced in 1990s as PLMR system which was designed for the worst case propagation scenario of high-elevation antennas’ providing radio coverage for large rural cells. Further modifications were introduced. Among of these systems are Digital-AMPS (DAMPS), Japanese Personal Digital Cellular (PDC) [4], and Interim Standard (IS)-45 [5], which are all based on digital technologies for voice-oriented traffic, data, and multimedia traffic, mixed-circuit and packet-switched network [6, 7]. This generation provided an increase in the user capacity about three times [8], using more modified techniques like compressing the voice waveforms before transmission [9]. Another 2.5G subcategory is added to the previous; such as the GPRS systems [10]. The 2.5G systems, developed as an overlay technology upon the existing 2G networks, provide transmission speeds from 64 kbps to 144 kbps, with allowing larger text messaging and emails as well as limited web browsing. Actually, the major improvement of 2.5G over 2G was the implementation of packet switching technology.

The first 3G systems were introduced in Oct. 2001 in Japan [11], these systems are considered as an extension of the second-generation systems. The immediate goal of this generation is to raise transmission speeds from 125 Kbps up to 2Mbps for global roaming and video transmissions. Moreover, the capacity of third generation systems is about over ten times the original first generation systems [12]. This is going to be achieved by using multiple access techniques such as CDMA [13-17], or an extension of TDMA [13-17]. Further improving flexibility of services are also available. We may summarize in Fig. 1-1 the evolution of the wide area cellular networks.

The 3G researchers progressed in Universal Mobile Telecommunication Systems (UMTS) [15], with the following standards [18]: wide-band CDMA[19, 20], adaptive TDMA [21], hybrid TDMA/CDMA [22], OFDM [23, 24], and opportunity driven multiple access. We find the Nokia testbed portrayed in [20] was designed with video transmission capabilities of up to 128 kbits/s. Similarly, less bandwidth Japanese wide-band CDMA proposal was in [25] for the intelligent mobile terminal (IMT-2000) emerging from NTT DoCoMo.

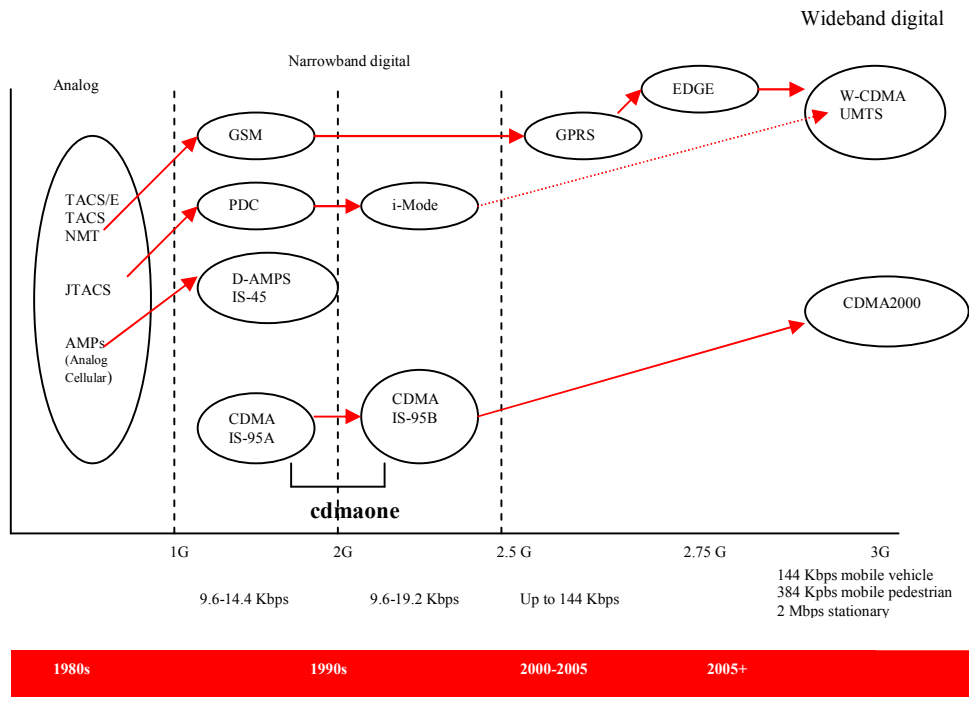


Figure 1-1: Evolution of wide area cellular networks-WWAN [26].

A number of projects dealing with multimedia, source and channel coding, modulation, and multiple access techniques for both cellular and wireless LAN's are developed [27]. These studies interest in designing the architecture and producing demonstrative models for studying UMTS. Specifically, fixed networks are evolving from the basic 2.048 Mbit/s ISDN toward higher rate B-ISDN. A portability of a higher grade of mobility is a feature of cordless telephones, such as the DECT, CT2, and PHP systems. Furthermore, WLAN's can support bit rates up to 155 Mbits/s in order to extend existing ATM links to portable terminals, but they usually do not support full mobility functions, such as location update or handover from one BS to another. These systems exhibit the highest grade of mobility, including high-speed international roaming capabilities. More considerations of this 3G, two main standards were established: 3GPP (Third Generation Partnership Project) which is a collaboration agreement was established in Dec. 1998 (supported by China, Europe, Japan, and some American companies), besides, 3GPP2, which specifies standards for IS-95 (CDMA2000), (supported by another faction of American companies) [28].

We may summarize some of the major cellular mobile phone standards in both North America and Europe respectively in TABLE 1-1, and TABLE 1-2 from mid of 80s until 2000s.

TABLE 1-1: MAJOR MOBILE STANDARDS IN NORTH AMERICA [8].

CELLULAR SYSTEM	YEAR OF INTRODUCTION	TRANSMISSION TYPE	MULTIPLE ACCESS TECHNIQUE	CHANNEL BANDWIDTH	SYSTEM GENERATION
Advanced Mobile Phone System (AMPS)	1983	Analog	FDMA	30kHz	First
Narrowband AMPS (NAMPS)	1992	Analog	FDMA	10kHz	First
U.S. Digital Cellular (USDC)	1991	Digital	TDMA	30kHz	Second
U.S Narrowband Spread Spectrum (IS-95)	1993	Digital	CDMA	1.25MHz	Second
Wideband cdmaOne	2000	Digital	CDMA	5 MHz	Third

TABLE 1-2: MAJOR MOBILE STANDARDS IN NORTH EUROPE [8].

CELLULAR SYSTEM	YEAR OF INTRODUCTION	TRANSMISSION TYPE	MULTIPLE ACCESS TECHNIQUE	CHANNEL BANDWIDTH	SYSTEM GENERATION
E-TACS	1985	Analog	FDMA	25kHz	First
NMT-900	1986	Analog	FDMA	12.5kHz	First
Global System for Mobile (GSM)	1990	Digital	TDMA	200kHz	Second
Universal Mobile Telecommunications System (UMTS)	>2000	Digital	CDMA/ TDMA	5 MHz	Third

Actually, these system generations are also distinguished by many service types. Figure 1-2 shows the evolution of current services and networks to the aim of combining them into a unified third generation network. Many currently separate systems and services such as radio paging, cordless telephony, satellite phones, and private radio systems for companies etc., will be combined so that all these services will be provided by third generation telecommunications systems.

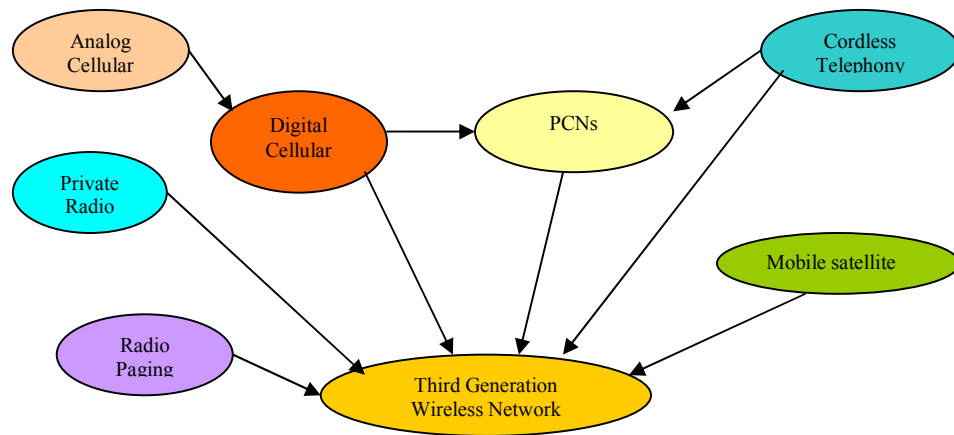


Figure 1-2: Evolution of current networks to the 3G of wireless networks [29].

Furthermore, different applications have different service requirements. Among most important of these requirements are *data rate in Mb/sec*, cell size or range distance between BS - MS and number of users see Fig. 1-3, moving *Mobility* see Fig. 1-4, in addition,

service quality which is a measure of reliability and allowable bit error rate (BER), and real time transfer rate.

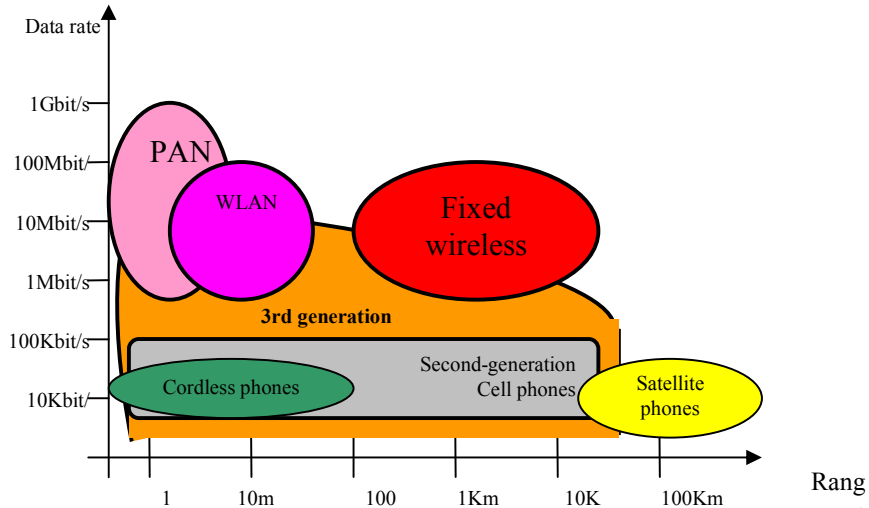


Figure 1-3: Data rate versus range for various applications [30].

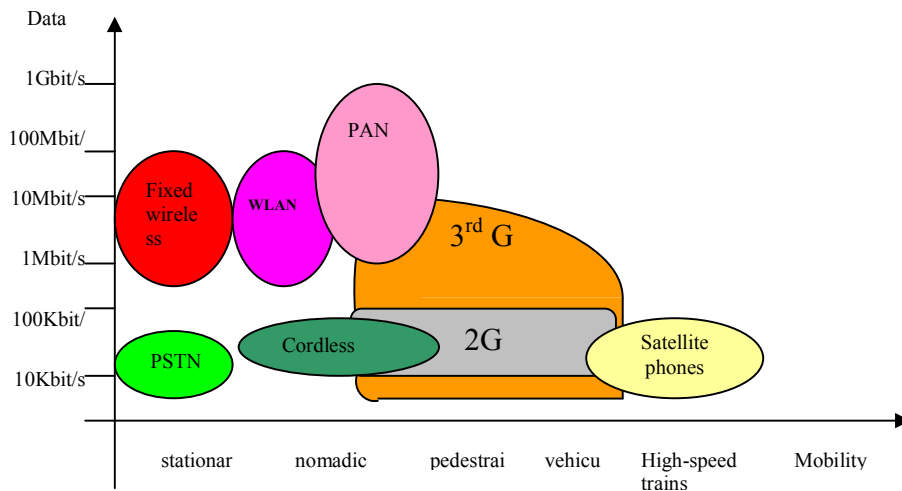


Figure 1-4: Data rate versus mobility for various applications [30].

System services have different characteristics in terms of delay tolerance and allowable bit error rates. TABLE 1-3 shows these characteristics for some of the UMTS services [31].

TABLE 1-3: DATA CHARACTERISTICS OF UMTS SERVICES.

Applications or Services	Data Rate Required	Quality of service required	Time critical data
Messaging (email, etc)	Low (1-10kbps)	High	No
Voice	Low (4-20kbps)	Low (BER < 1e-3)	Yes
Web browsing	As high as possible (>10kbps-100kbps)	High (BER < 1e-9)	Depends on material. Generally not time critical.
Videoconferencing	High (100kbps-1Mbps)	Medium	Yes
Video Surveillance	Medium (50-300kbps)	Medium	No
High Quality Audio	High (100-300kbps)	Medium	Yes
Database access	High (>30kbps)	Very High	No

The 4-G systems or "beyond 3G" may be put in service around 2010. Besides, in [32, 33] a new vision can be found with Preliminary Draft of New Recommendation (DNR) of ITU-R WP8F, getting a steady and continuous evolution of IMT-2000 in order to support new applications, products, and services; such as providing interactive multimedia and wireless internet with transmission speeds, with a capacity up to 30 Mbps. For the systems beyond 3G [beyond IMT-2000 in the International Telecommunication Union (ITU)], there may be a requirement for a new wireless access technology for the terrestrial component around 2010, with approximately 100 Mbps for high mobility and 1Gbps for low mobility.

Higher data rates are possible at lower mobilities or decreased cell size. This is due to two considerations. The first (and main) consideration is that at smaller distances the propagation loss is less and thus for a given power level, higher values of E_b/N_0 , received signal-to-noise ratio, are possible. Another effect is that at high mobilities the channel is harder to estimate and thus proper demodulation/decoding becomes more difficult. However, these channel's effects can be compensated to a certain extent, by the fact that generally error control coding works better (for a fixed block length) when the channel is memory-less (independent fading on different symbols).

One of the main issues involved in the development of the beyond 3G (B3G) systems is the choice of multiple access (MA) technology to efficiently share the available bandwidth among a large number of users. Choice of MA technique could significantly enhance or lower the service quality delivered to end users. It is known that the existing MA techniques used in 2G/3G systems, including those based on time-division (TDMA) and direct sequence code-division (DS-CDMA) [4], and possible combinations of the two schemes are basically suitable for voice communications but not for burst data traffic, which would be the dominant portion of the traffic load in B3G systems. Therefore, need to develop new multi-access (MA) techniques for B3G becomes imperative [34].

1.2 Motivation

From previous discussion, we conclude that the future cellular mobile systems' generations will aim to support a wide range of services and bit rates by employing a variety of techniques capable of achieving the highest possible spectrum efficiency usage [34]. Among of the existing, Code-division multiple access (CDMA) schemes which have been considered as attractive multiple access schemes in both second-generation (2G) and third-generation (3G) wireless systems. Recently, more interests in wireless communications has been shifting in the direction of broadband systems [34, 35]. This is mainly due to the expected spread of the wireless Internet and the continued dramatic increase in demand for all types of advanced wireless multimedia services, including voice and data transmissions. Furthermore, future generations of broadband wireless systems are expected to support ubiquitous communications, regardless of the propagation environment with maintaining the required quality of service (QoS). The CDMA without the assistance of frequency/time hopping- mainly multiple access options include single-carrier direct sequence CDMA (SC-DS-CDMA) using time domain (T-domain) DS spreading [34]- suffers when a transmitted signal from a transceiver passes through non-ideal channel. Actually, the non-ideal channels has complicated propagation process of diffraction, multiple reflections, and scattering mechanisms. Hence, the SC-DS-CDMA suffers from the so-called a multipath

fading problem, which refers to time-varying channel conditions [36]. For the purpose of compensating these multipath effects a combining of OFDM with CDMA is considered as a one of the best techniques which is known as multi carrier CDMA (MC-CDMA) using frequency- domain (F-domain) spreading [34, 37]. However, high data rate results in frequency selective fading that can be mitigated by using multi-carrier transmission while achieving high data rate. Beside, high user mobility results in Doppler spread and time-varying fading which should be estimated and compensated for achieving optimal possible reliable communications. Thus, combining MC with DS to produce multi carrier DS-CDMA (MC-DS-CDMA) using T-domain DS spreading of the individual sub-carrier signals has taken place. Indeed, for MC-DS-CDMA system, we successfully compensate the frequency selective channels using multi-carrier transmission, while in the time-varying fading processes we estimate, track, and compact the process using a channel estimator as Kalman filtering (KF).

Another problem is added for the systems which are based on the CDMA (spread) transmission is so-called multi-access interference (MAI). This phenomenon is due to the nature of spreading information known as spreading sequences and their related cross correlation property, which has to be designed with zero cross-correlation for orthogonality transmission purposes, or the code possesses appropriate cross-correlation property that minimizes the multiple access interference (MAI) in time varying mobile channels [36]. Furthermore, the MAI becomes more severe in a near-far scenario where far users from the base station receive lower power than users who are near the base station, which severely degrades the performance of the system. One successful technique is using the multiuser decorrelator detector [36] as will be discussed in more details in Chapters 4, and Chapter 5. Further treatment techniques also could be used like channel estimators to improve the system performance [37-45].

1.3 Summary of Contribution

The design of receivers usually requires channel state information to achieve optimal diversity combining and coherent symbol detection. When considering the conventional MC-DS-CDMA receiver proposed in [39], which consists of a correlator along each carrier followed by a maximal ratio combiner (MRC), there are still two problems to be solved. First, the channel fading processes are assumed to be perfectly known at the receiver which is not the case in practice and should be estimated. In addition, the multiple access interference (MAI) cannot be eliminated.

By this thesis, we first consider a MC-DS-CDMA receiver structure consisting of [40, 42]:

1. a decorrelator multiuser detector for the purpose of suppressing the MAI and resisting the near-far problem,
2. a Kalman filter based channel estimator for the purpose of estimating the fading processes over all carriers,
3. a Maximal Ratio Combiner (MRC) for the purpose of fading channel compensation.

Our contribution is then two folds:

Firstly, we propose to investigate the relevance of high order AR models in the Kalman filter based channel estimator [46].

Secondly, we carry out comparative study with existing LMS and RLS channel estimators in realistic Jakes channels with different Doppler rate scenarios [47].

1.4 Thesis Outline

Investigation of MC-DS-CDMA Technology is considered in Chapter 2, where we introduce the evolution of multiple access techniques. Moreover, we introduce the spread spectrum with Gold spreading codes. In addition, developing the MC-DS-CDMA technology model with its advantages are also involved, and discussing MAI problems in more details.

In Chapter 3, we introduce multipath fading of mobile wireless channels in the MC-DS-CDMA technology, with some backgrounds for the channel parameters, and classifications. Rayleigh fading and the Jakes model for representing the channel is also discussed with their important parameters like Doppler spread, autocorrelation, and power spectral densities etc.

The Receiver design concepts are illustrated in Chapter 4, with introducing some backgrounds and details for the conventional correlator receiver by Milstein [39], and decorrelator multiuser detector, with its advantages for suppressing MAI, and resisting near-far problems. We also present some simulation results for these receivers. Finally, we offer our conclusions.

In Chapter 5, we introduce channel estimation, AR modeling the Rayleigh Fading channels, and Kalman channel estimator based high order AR models is investigated and its advantages over other MMSE channel estimators like LMS, and RLS. Furthermore, simulation results and conclusions are discussed.

Finally, in Chapter 6 we conclude our works and present several open problems through suggested future works.

Chapter 2

MC-DS-CDMA Technology

2.1 Multiple Access Techniques

Many users in one geographic region share a medium radio channel. Mobile stations compete with one another for the frequency resource to transmit their information streams. Without any other measures to control simultaneous access of several users, collisions can occur (a multiple access problem) [48]. Since collisions are very undesirable for a connection-oriented communication like mobile telephony, the individual subscribers/mobile stations must be assigned dedicated channels on demand. In order to divide the available physical resources of a mobile system, i.e. the frequency bands, into voice channels, special multiple access procedures are used. There are mainly three multiple access techniques adopted by the third Generation Partnership Project (3GPP): Frequency Division Multiple Access (FDMA), Time Division Multiple Access (TDMA), and Code Division Multiple Access (CDMA).

2.1.1 Frequency Division Multiple Access (FDMA):

Enables many users to share same radio spectrum, i.e., each user is allocated a different frequency [49]. In addition, Guard bands are used between adjacent signal spectra to minimize crosstalk between channels. Figure 2-1 shows how this technique treats the available bandwidth to be subdivided into separate frequency channels, each assigned to a user.

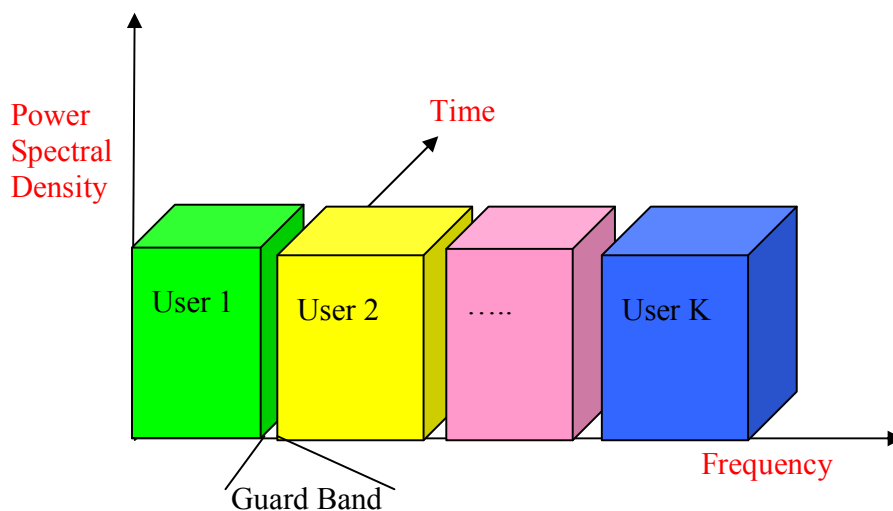


Figure 2-1: FDMA scheme.

This scheme increases the bandwidth usage, with a low inter-symbol interference (ISI), due to use low bit rates (large symbol time) compared to average delay spread. Furthermore, it

is simple to be equalized, and implemented in technological advances. In addition, since the transmission is continuous, less number of bits are needed for synchronization and framing. On the other hand, the capacity depends on reducing Signal-to-Interference Ratio (SIR), or Signal-to-Noise Ratio (SNR). The maximum bit rate per channel is fixed and small due to bandwidth usage. Furthermore, the guard bands result in wastage of capacity. Hardware involves narrow band filters, which cannot be realized in Very Large Scale Integration (VLSI), and thus increases cost for using this VLSI technology.

2.1.2 Time Division Multiple Access (TDMA):

It is a more complex technique, due to a highly accurate synchronization between a transmitter and a receiver is needed [49]. In this technique many users share the same radio spectrum by transmitting information in different time slots, each assigned to a single user. The TDMA scheme is illustrated in Fig. 2-2. As shown the transmission time is divided into multiple slots with assigning each time slot for a user.

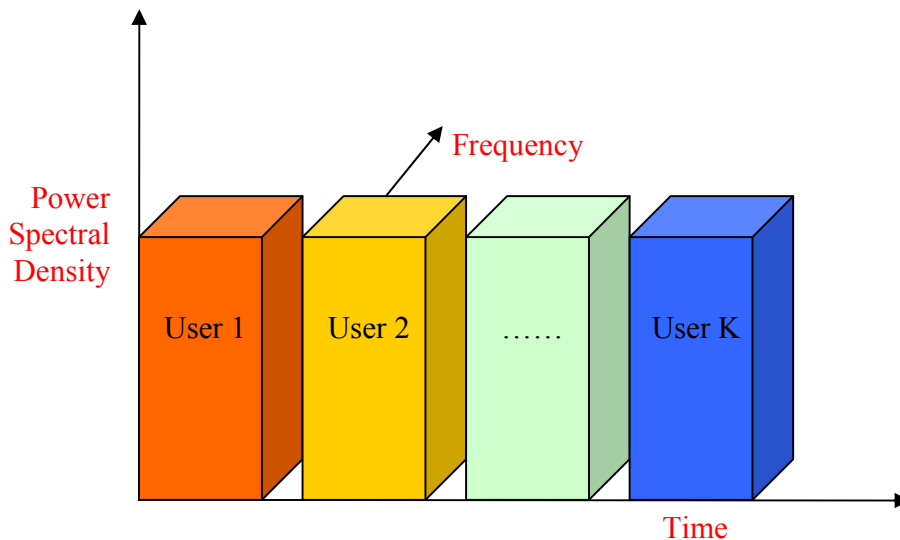


Figure 2-2: TDMA scheme.

Furthermore, in most cases the whole system bandwidth for a time slot is not assigned to a one station, but system frequency is subdivided into sub bands, and TDMA is used for multiple accesses to each sub band. Sub bands are known as carrier frequencies, and the mobile system using the technique are designated as multiple carrier systems. The pan-European digital system GSM (Global System for Mobile communication) employs such a combination of FDMA and TDMA. A frequency range of 25 MHz holds 124 single channels (carrier frequencies) of 200 kHz bandwidth each; with each of these frequency channels containing again 8 TDMA conversation channels. Thus, the sequence of time slots and frequency assigned to a mobile station represents the physical channels of a TDMA system. In each time slot, mobile station transmits a data burst. The period assigned to a time slot for a mobile station thus also determines the number of TDMA channels on a carrier frequency. The time slots of one period are combined into a so-called TDMA frame.

The TDMA signal transmitted on a carrier frequency in general requires more bandwidth than an FDMA signal, because of multiple time use, the gross data rate has to be correspondingly higher. The TDMA, permits flexible bit rates (i.e., multiple time slots can be assigned to a user, e.g., if each time slot translates to 32Kbps, then a 64Kbps user gets assigned 2 slots per frame). Also, it can support bursts or variable bit rate traffic. Number of slots assigned to a user can be changed frame by frame (e.g., 2 slots in frame 1, 3 slots in frame 2, 1 slot in frame 3, 0 slots in frame 4, etc.). Moreover, no guard bands required for wideband system. In addition, no narrowband filters required for wideband system. On the other hand, The TDMA suffers from high bit rates of wideband systems which require complex equalization. Because of burst mode operation, a large number of overhead bits for synchronization and framing are required. Besides, guard time is required in each slot to accommodate time inaccuracies because of clock instability. Electronics operating at high bit rates increase power consumption. Furthermore, complex signal processing is required for synchronize within a short slot time.

2.1.3 Orthogonal Frequency Division Multiplexing (OFDM):

In OFDM, the available spectrum is divided into orthogonal carriers, each one being modulated by low data rate stream [49]. The orthogonal carriers are overlapping in a synchronized orthogonal shape as shown in Fig. 2-3. Among the advantages of this multiple access technique are the following: it doesn't need complex equalizers due to the orthogonality, also, this technique benefits from a frequency diversity techniques, furthermore, it has immunity to frequency selective fading, and multipath delay spread tolerance, in addition, it has a high spectral efficiency, with higher data rates. Unfortunately, this MA suffers from Inter-symbol interference (ISI), and sensitive to frequency offsets, and sub-carrier synchronizations, with clipping due to high Peak-to-Average ratio.

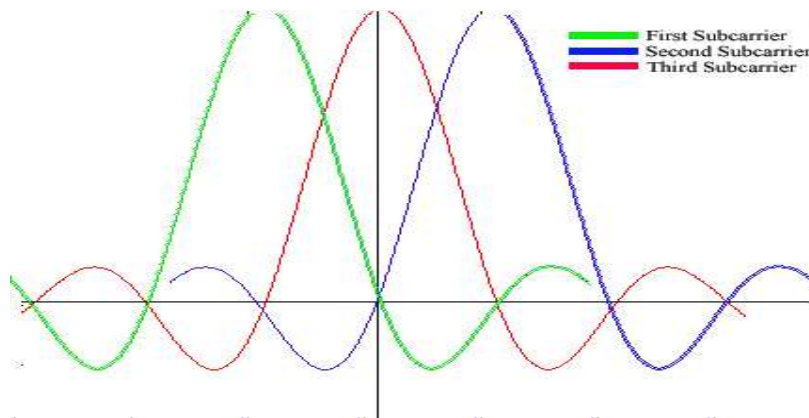


Figure 2-3: The OFDM orthogonal carriers [50].

2.1.4 Code Division Multiple Access (CDMA):

Both the FDMA and TDMA techniques have fixed channel or time slots for a given system. Furthermore, they have fixed number of services, and lack of efficiency. As the number of

user increases exponentially a new dynamic technique of CDMA has been considered which allows many users to share the same radio spectrum, based on a sequence of pseudo-random chips [49]. In reality, these codes are used to distinguish between users, and spread the information signal over a much larger range of frequencies than is occupied by the original information signal, and so sometimes the term Spread Spectrum Multiple Access (SSMA) is also used interchangeably with the term CDMA. Figure 2-4 shows the CDMA scheme with its whole spectrum is available to all users for whole time with separating users information using the spreading codes.

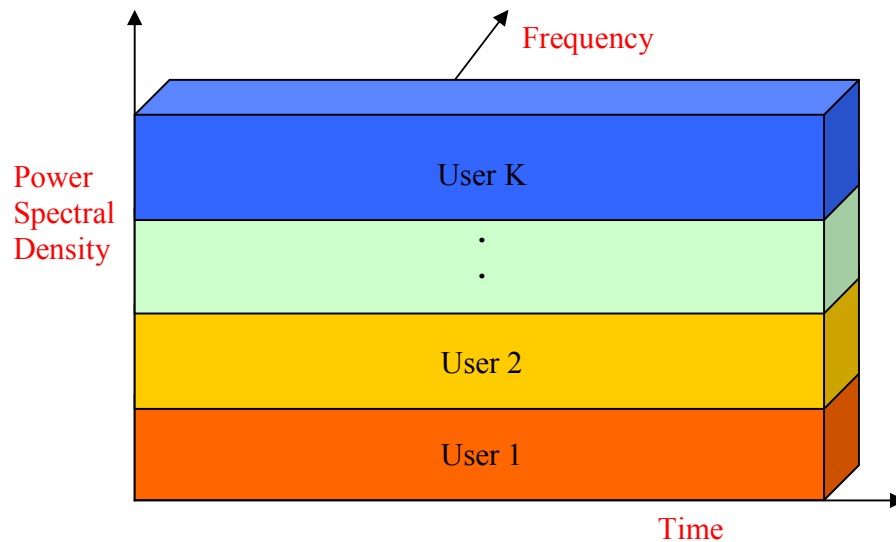


Figure 2-4: Principle of CDMA scheme.

This scheme is classified into various types, which are different in the way that the information signal is transformed to produce a high-bandwidth spread shown in Fig. 2-5 as follows:

- ◆ Direct Sequence CDMA (DS-CDMA), a pseudo-random sequence as a spreading code having a higher bandwidth than the information signal is used to modulate the information signal directly.
- ◆ Frequency Hopping CDMA (FH-CDMA), the transmission bandwidth is divided into frequency sub-bands, where the bandwidth of each sub-band is equal to the bandwidth of the information signal. A pseudo-random code is then used to select the sub-band, in which the information signal is transmitted and this sub-band changes periodically according to the code. There are two sub-categories of FH-CDMA, namely, Slow Frequency Hopping (SFH) [6] and Fast Frequency Hopping (FFH) [6]. In FFH, the frequency subband used to transmit one bit of information is changed multiple times within the bit-duration, while in SFH, the sub-band is changed only after multiple bits have been transmitted.
- ◆ Time Hopping CDMA (TH-CDMA) [6] transmits the information signal in short bursts. These short bursts render the transmission bandwidth high. The start of each burst for one user is determined by a pseudo-random code.

- ◆ Hybrid CDMA [6] encompasses a group of techniques that combine two or more of the other techniques already described. One of these hybrid techniques is known as Multi-Carrier CDMA (MC-CDMA) [6], which is due to combining of CDMA and OFDM where each symbol of a user modulates multiple closely spaced narrowband orthogonal subcarriers [51]. Thus, it has frequency diversity techniques with less sensitivity to the ISI for the CDMA. Furthermore, Multicarrier CDMA techniques can be divided into two main groups according to the way of spreading. Namely, time domain spreading and frequency domain spreading Multicarrier CDMA. These techniques will be discussed in depth in the next subsections.

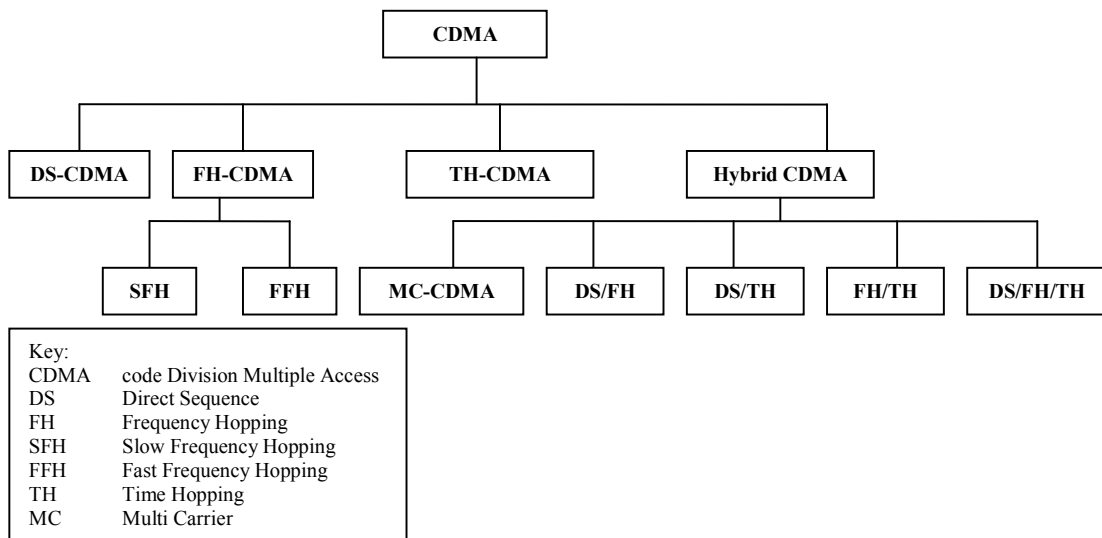


Figure 2-5: Classification of CDMA schemes according to the modulation method.

By using CDMA technique, we get more hiding for information transmission and security due to spreading code, which is superimposed on the information signal, making the signal appear noise-like to all the other users. And, only the intended receiver which has a replica of the same code can retrieve data, by extracting spread information signal, this is due to its autocorrelation behaviors which has optimal value for just corresponding spreading sequences. This also allows the sharing of the same spectrum by multiple users with causing lower MAI effects. Another major property contributes suppressing MAI is the spreading code cross-correlation property, which has to be designed with zero cross-correlation. Unfortunately, even if the codes are designed to be orthogonal, the multi-path fading destroys this orthogonality resulting in severe MAI. In addition, multipath spreading of the CDMA signal results in ISI, which severely degrades the system performance. Thus, the code possesses appropriate cross-correlation property to minimize the multiple access interference (MAI) in time varying mobile channels [36]. Indeed, the 2G CDMA systems, specifically, in Qualcomm IS-95 CDMA standard [52, 53], treats the MAI as noise. In addition, the CDMA is interference-limited, and bandwidth independent rather than the FDMA, and TDMA, which are dependent on the bandwidth, so they are a cost resource, and bandlimited for the capacity. Beside, an important advantage of CDMA schemes is that the multipath propagation can be exploited to give multipath diversity gains by using multipath combining [21]. Although the fading effects are considered as a detrimental effect for time varying mobile channels, which results a received signal having a large

variance about its mean, again resulting in a degraded performance, the CDMA has unique spreading codes for each user which contributes privilege of privacy. In spite of, existing MAI due to increase number of users, which serve a more degradation of performance in presence of near-far problems, the power control [54] can be used with the CDMA to improve performance.

2.1.5 Multi Carrier Code Division Multiple Access (MC-CDMA):

There is an increased urgency to define the next generation of Wireless Broadband Communication Systems. Rapid growth of video, voice and data transmission via the internet and the increased use of mobile telephony today have defined the necessity for higher data rate transmissions over the wireless channels. Though the current 3G systems use considerably higher data rates of 64kbps – 2Mbps as compared to 9.6kbps – 14.4kbps used by their 2G counterparts, the 4G systems that include broadband wireless services like High Definition Television (HDTV) require data rates up to 20Mbps. This also emphasizes the need for improved spectral efficiency and higher Quality of Service (QoS) over current systems.

Above requirements are seen as the primary driving force for more research on multicarrier modulation techniques. Single carrier systems give good data rates but are limited in performance in fading channels and any attempt to mitigate these effects results in an increased system complexity. Improved performance in bad channel conditions, high data rates and efficient bandwidth usage are the primary advantages of multicarrier modulation.

Multi-carrier systems employing CDMA are categorized mainly into two groups depending on the type of spreading. One spreads the original data stream using a given spreading code and then modulates a different sub-carrier with each chip. This is called *Frequency Domain Spreading*. The other spreads the serial to parallel converted data streams using a given spreading code and then modulates a different sub-carrier with each of the data streams. This is called *Time Domain Spreading*.

The major classifications of multicarrier CDMA techniques, which are based on spreading operation in time or frequency domains, are three types [39].

- Multicarrier CDMA (MC-CDMA) Scheme

This scheme is a combination of Frequency domain spreading and Multicarrier modulation [39]. The multi-carrier transmitter spreads the original data stream over different sub-carriers using a spreading code in the frequency domain. In other words, a fraction of the symbol corresponding to a chip of the spreading code is transmitted through a different sub-carrier, which refers to odd number of the spreading sequences.

- Multitone CDMA (MT-CDMA) Scheme [4,39]

The MT-CDMA transmitter spreads the Serial to Parallel converted data streams using a spreading code in the time-domain so that the spectrum of each sub-carrier prior to spreading can satisfy the orthogonality condition with minimum frequency separation. Therefore, the resulting spectrum of each sub-carrier no longer satisfies the orthogonality condition.

- MC-DS-CDMA- Multicarrier/DS-CDMA [37, 39]

The multi-carrier DS-CDMA transmitter spreads the Serial to Parallel converted data streams using a given spreading code in the time-domain so that the resulting spectrum of each sub-carrier can satisfy the orthogonality condition with minimum carrier separation.

2.2 Basics of CDMA

In CDMA scheme, the digital data information of rate T_b , and a bandwidth $DR=1/T_b$ is spread into much larger bandwidth W , using wideband PN sequences of bandwidth $W_c=1/T_c$, where the T_c is the *chip interval* of a *chip* spreading rectangular pulse [55]. This spectrum spreading is achieved by either multiplying the data signal directly with the spreading sequence called Direct Sequence-Code Division Multiple Access (DS-CDMA) or the spectrum of a data-modulated carrier is widened by changing the carrier frequency in a pseudo-random manner called Frequency-Hop Code Division Multiple Access (FH-CDMA). Originally, CDMA was conceived as a single-carrier scheme covering a wide-band. But, a development in the wide-band DS-CDMA was the usage of multiple-carriers for modulation thereby leading to narrow-bands around each carrier. As time passed-by many types of multi-carrier modulation techniques have assumed importance.

2.2.1 Spreading Sequences:

One main important process in generating CDMA scheme is the spreading sequences [56]. Here in this section we discuss these sequences, their properties and generation. These sequences are pseudo-noise (PN) sequences. A binary sequence $\{0,1\}$ is mapped into a corresponding sequence of positive and negative pulses according to the relation

$$p_i(t) = (2q_i - 1)p(t - iT_c), \quad (2.1)$$

where $p_i(t)$ is the pulse corresponding to the element q_i in the sequence with elements $\{0,1\}$. Spreading sequences can be *bipolar* or *poly-phase*. Different sequences can be used as spreading sequences as Gold sequences, Kasami sequences, Polyphase sequences, Four Phase sequences, Mutually Orthogonal Complementary sets of sequences, Dual-BCH sequences. Here, in the following subsection we describe the bipolar Gold sequences [49] due to its advantage properties, as we will be discussed.

Binary shift register sequences

Starting with defining the polynomial

$$f(x) = d_0x^n + d_1x^{n-1} + \dots + d_{n-1}x + d_n, \quad (2.2)$$

in the discrete field with two elements $d_i \in (0,1)$, and $d_0 = d_n = 1$, Then a binary sequence u is said to be a *sequence generated by* $f(x)$ if, for all integers j ,

$$d_0u_j \oplus d_1u_{j-1} \oplus d_2u_{j-2} \oplus \dots \oplus d_nu_{j-n} = 0, \quad (2.3)$$

where \oplus =addition modulo 2.

If we formally change the variables

$$j \rightarrow j + n, \text{ and } d_0 = 1, \text{ we get}$$

$$u_{j+n} = d_nu_j \oplus d_{n-1}u_{j+1} \oplus \dots \oplus d_1u_{j+n-1}, \quad (2.4)$$

which simply represent n -stage binary linear feedback shift register generating the sequence u , where the notation, u_j is the j^{th} bit (called a chip).

Gold Sequences

Gold sequences are maximal length sequences [55], which are generated from appropriately chosen maximal-length (m) sequences with better correlation properties.

Generation of m -Sequences:

m -sequences are generated by using an n -stages of a shift register with feedback as appeared in Fig. 2-6. For the purpose of generating a code word, the n bits are loaded into the shift register, which shifts its contents of the shift register to the left, one bit at a time, i.e., the total number of shifting is 2^n-1 shifts. Indeed, this operation generates a sequence of length $N=2^n-1$. All sequences generated by the shift register are different cyclic shifts of a single sequence. When the shift register is loaded initially and shifted 2^n-1 times, it will cycle through all possible 2^n-1 states. Hence, its original state is repeated after 2^n-1 shifts. Consequently, the output shift register sequence is periodic with length $N=2^n-1$. Due to existing 2^n-1 possible states, this length corresponds to the largest possible period. In reality, when the shift register sequences are with the length 2^n-1 , we called this type as an m -sequence, i.e., maximum-length shift register sequences are achieved.

Properties of m -Sequences:

1. The period of the sequence d is $N = 2^n - 1$

- Let T^i denote the operator which shifts the sequences cyclically to the left by i places. There are exactly N nonzero sequences generated using $f(x)$, and they are just the N different phases of d , i.e., $d, Td, T^2d, \dots, T^{N-1}d$.

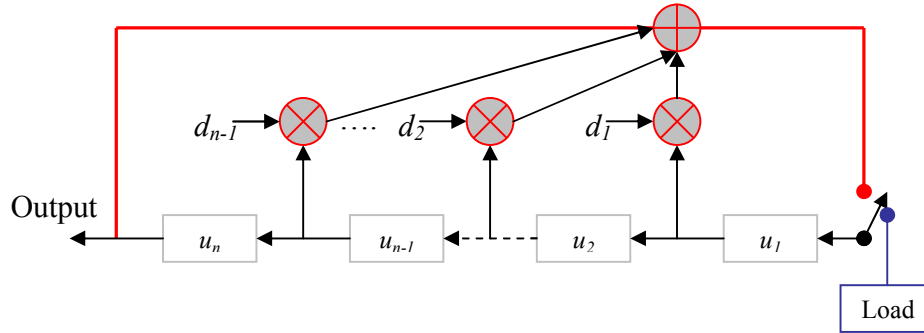


Figure 2-6: Generation of m-sequences using shift register.

- Shift-and-add property: Given distinct integers i and j , $0 < i, j < N$, there is a unique integer k , distinct from both i and j , such that $0 \leq k < N$ and $T^i d \oplus T^j d = T^k d$.
- $wt(d) = \frac{N+1}{2}$, wt is the weight i.e. the number of non-zero elements in d .
- If R_b is the autocorrelation of b ,

$$R_b(l) = \begin{cases} N & \text{if } l \bmod N = 0 \\ -1 & \text{if } l \bmod N \neq 0 \end{cases} \quad (2.5)$$

Thus the autocorrelation function of binary m -sequences have the two optimal values $\{-1, N\}$.

- Cross correlation of m -sequences: Let b_1 and b_2 denote m -sequences of period $2^n - 1$, and let $t(n)$ be defined as

$$t(n) = 1 + 2^{\lfloor (n+2)/2 \rfloor}, \quad (2.6)$$

where $\lfloor \cdot \rfloor$ denotes to the greatest integer value. Then, there exist some sequences with,

$$R_{b_1 b_2}(l) = \begin{cases} -1 \\ -t(n) \\ -t(n) - 2 \end{cases} \quad \forall l \bmod 4 \neq 0 \quad (2.7)$$

A cross correlation function taking on these values is called a *preferred three-valued cross correlation function* and the corresponding pair of m -sequences is called a *preferred pair*.

In addition, a largest possible connected set for these sequences is called a maximal connected set.

Generation of Gold Sequences:

Given a shift register polynomial $f(x)$ factors into $g(x)\hat{g}(x)$, where $g(x)$ and $\hat{g}(x)$ have no factors in common. Then the set of all sequences generated using $f(x)$ which is the set of all sequences of the form $a \oplus b$ where a is a sequence generated by $g(x)$, and b is a sequence generated by $\hat{g}(x)$. If $g(x)$ and $\hat{g}(x)$ are two different primitive polynomials of degree n that generate the pair of m -sequences u and v respectively of period $N = 2^n - 1$. The nonzero sequence generated by $f(x) = g(x)\hat{g}(x)$ is given by:

$y = \{T^i u, T^j v, T^i u \oplus T^j v \quad 0 \leq i, j \leq N-1\}$. There exists some set $G(u, v) \in y$ defined by $G(u, v) = \{u, v, u \oplus T^l v, \dots, u \oplus T^j v\}$, the $G(u, v)$ is called the set of *Gold sequences* if the sequences u and v , used to generate G are *preferred pair* of m -sequences. In addition, $G(u, v)$ contains $N+2$ sequences of period N . The peak correlation parameters R_a and R_c for $G(u, v)$ satisfy

$$R_a = R_c = \max \{R_{u,v}(l) : 0 \leq l \leq N-1\}. \quad (2.8)$$

Thus using a pair of m -sequences u and v with peak periodic crosscorrelation magnitude M , we can construct a set of $N+2$ sequences with peak periodic crosscorrelation magnitude and peak out-of-phase autocorrelation magnitude equal to M . If $\{u, v\}$ is any preferred pair of m -sequences, then $G(u, v)$ has peak correlation parameters $R_a(\text{off-peak}) = R_c = t(n)$. Thus the cross correlation values of Gold sequences take on the three preferred values only. This maximum value of cross correlation R_{\max} is given by $\{-1, -t(n), t(n) - 2\}$, where

$$t(m) = \begin{cases} 2^{(m+1)/2} + 1 & \text{odd } m \\ 2^{(m+2)/2} + 1 & \text{even } m \end{cases}. \quad (2.9)$$

With the exception of sequences u and v , the set of Gold sequences is not m -sequences. The frequency of occurrence of the cross-correlation values for Gold sequences of length $N = 2^n - 1$, n odd is

TABLE 2-1: FREQUENCY OF OCCURRENCE OF VALUES FOR GOLD SEQUENCES.

Cross correlation value	Frequency of occurrence
-1	$2^{(n-1)} - 1$
$-[2^{(n+1)/2} + 1]$	$2^{(n-2)} - 2^{(n-3)/2}$
$[2^{(n+1)/2} - 1]$	$2^{(n-2)} + 2^{(n-3)/2}$

Example

Generation of Gold sequences of length $31=2^5-1$.

The two preferred sequences used for the generation are $g(p) = p^2 + p^3 + 1$, $\hat{g}(p) = p^5 + p^4 + p^3 + p + 1$. The shift registers for generating the m -sequences and the corresponding Gold sequences are in Fig. 2-7.

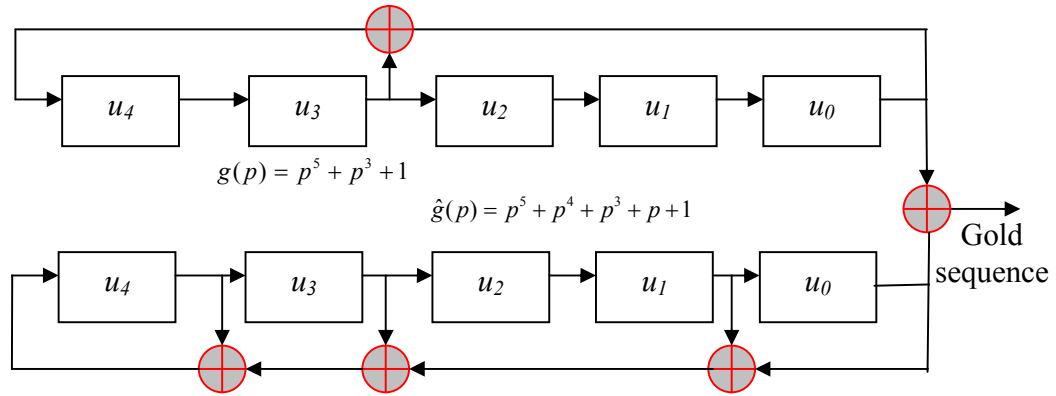


Figure 2-7: Gold sequence generator of 31 sequence length.

The following Fig. 2-8, and Fig. 2-9 are the auto-correlation and cross-correlation plots for gold sequences of length 31, divided by \sqrt{N} using Matlab correlation function. As seen from the two figures we can conclude the autocorrelation of the gold sequences has optimal values when using the same gold sequence, while the cross-correlation (CCL) characterizes like a random function which is necessary for the CDMA systems.

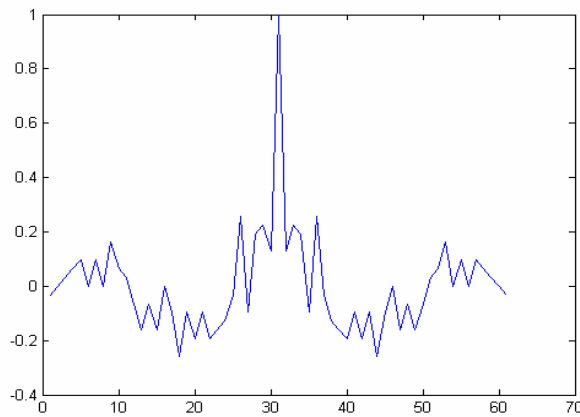


Figure 2-8: Aperiodic autocorrelation plot of Gold sequences corresponds of length 31.

The transmitted signal passes through a mobile communication channel, in which we call propagating of a signal from the base station to a mobile user as the *downlink -forward link*, while propagating for a signal from a mobile to the base station as *uplink -reverse link*.

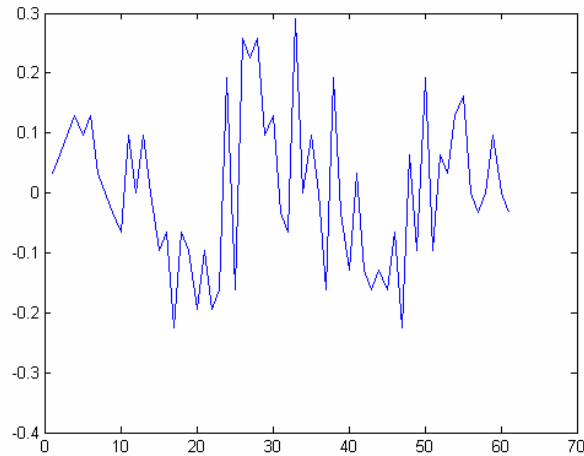


Figure 2-9: Aperiodic crosscorrelation plot of Gold sequences corresponds of length 31.

- *CDMA Downlink Channel*

In the downlink, spread signals are transmitted from a same basestation, thus they can be synchronized. Furthermore, these signals may be considered to pass through a same multipath channel, the same propagation path loss, and fade simultaneously. Figure 2-10 shows the CDMA downlink channel model, where $b_k(t)$ is the k^{th} user data sequence, $c_k(t)$ is the spreading waveform of the k^{th} user, $\eta(t)$ is AWGN, and $x_k(t)$ is the despread (after spreading back the transmitted signal by spreading codes) data sequence for further treatments by a designed receiver.

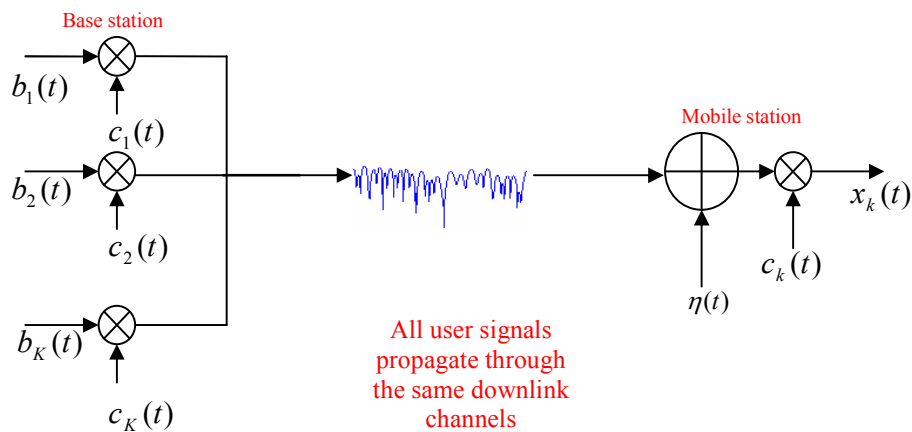


Figure 2-10: CDMA downlink channel model.

- *CDMA Uplink Channel*

In the uplink, the synchronization in transmissions from different users to a basestation can not be established, due to the fact that it is difficult to synchronize users' transmissions. Therefore, the orthogonal spreading codes usually not recommended. Different mobile signals pass through different multipaths, different path losses, and fadings. The following Fig. 2-11 shows the uplink model, due to that MAI exists in the uplink.

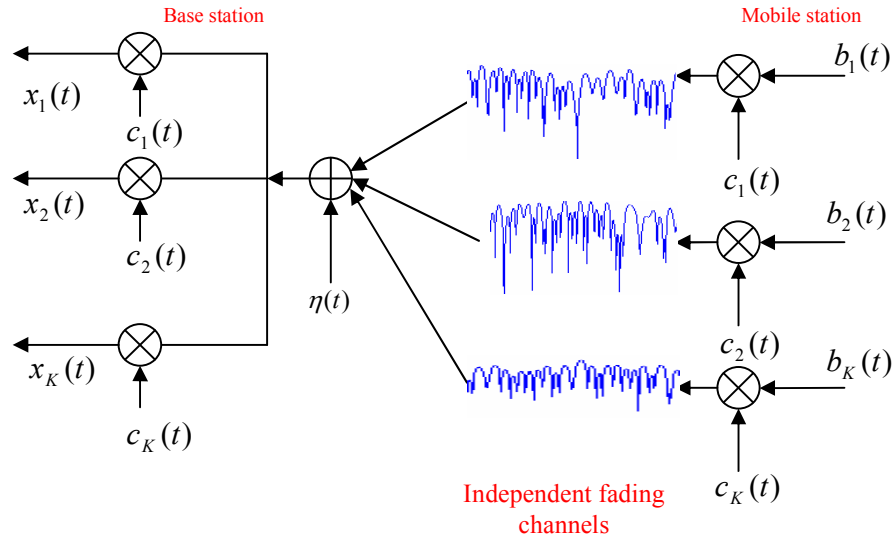


Figure 2-11: CDMA uplink channel model.

2.3 DS-CDMA

In Direct sequence code division multiple access or SC-DS-CDMA, we directly multiply (spread) the data sequences with spreading codes. The narrowband data sequences for the first user as an example $b_1(t)$ is spread on a wideband spectrum using wideband spreading codes $c_1(t)$, which its bandwidth = $\frac{1}{T_c}$ as obvious in above part of Fig. 2-12, which shows this spreading process, and PSD of each transmitter stage. In addition, the lower part shows this process in frequency and time domains, as can be seen, the spreading code of a chip interval T_c and processing gain N , such that $N \times T_c = T_b$ is used for generating the spread information's of the first user, such that the transmitted signal $S_1(t)$ in the time domain has a chip interval T_c . Furthermore, the transmitted bandwidth is nearly equal to the wideband spectrum bandwidth of the spreading codes. Consequently, the transmitted spectrum is much wider in the frequency domain than the data sequences $b_1(t)$ bandwidth.

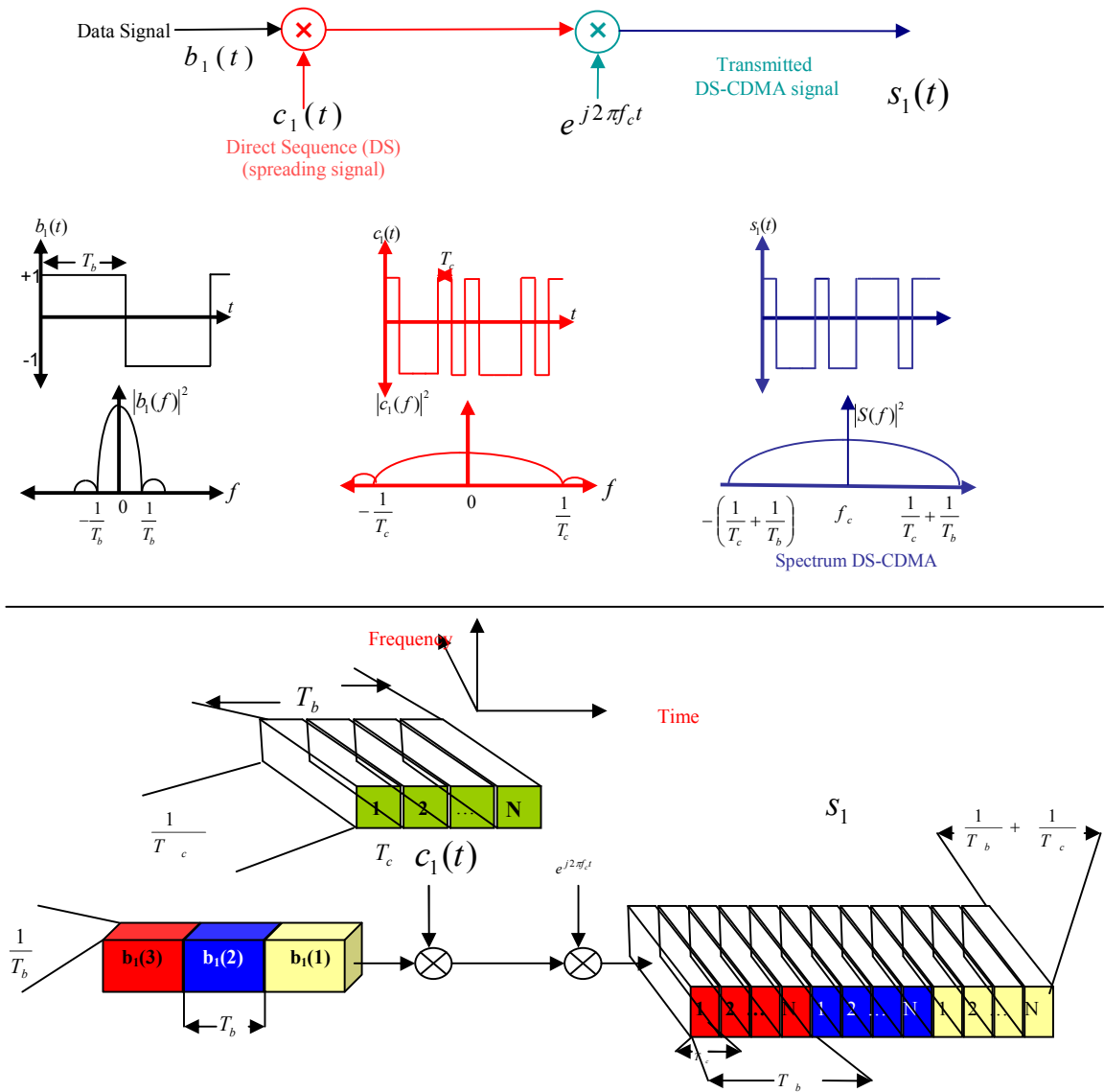


Figure 2-12: Direct spread CDMA transmitter.

2.4 MC-DS-CDMA

Combining of MC-CDMA and DS-CDMA has received much attention to introduce the so-called Multicarrier DS-CDMA (MC-DS-CDMA) scheme as one promising MA scheme for B3G systems [57]. From previous subsections, we know that this scheme spreads data sequences into a wide band with modulating by using M carrier frequencies.

Figure 2-13 shows a first user information signal is spread using direct sequence spreading codes, then the wideband output is modulated with M carriers, for the purpose of using frequency diversity techniques, where we carry the spread signal over more than a carrier, in order to useful from its subdivided spectrum, as will discussed in next Chapter. Furthermore, the power spectral density of each stage is shown below the Fig. 2-13.

2.4.1 Why MC-DS-CDMA:

It is important to indicate that SC-DS-CDMA suffers from weak multipaths. Because of the large number of weak peaks, actually, we face a difficulty of achieving coherent RAKE combination, and consequently cannot obtain enough diversity from this RAKE diversity as an optimal combiner. In addition, the influence of multipath tends to mitigate high-speed communications due to the transmission rate on MC-CDMA channels, which is slower than that of DS-CDMA. Indeed, on uplinks utilizing MC-CDMA, transmitting a signal from each user is affected by its own fading, and each subchannel has also its own fading effect. It is difficult to introduce an actual compensation method for the fading effect of every user and every subchannel. Although CDMA is essentially capable of becoming the MA technique for B3G, the current CDMA schemes unfortunately do not satisfy the requirements of B3G [58].

Hence, combing both techniques into the MC-DS-CDMA can achieve very-high-data-rate transmissions with the advantages of both schemes. We can obtain the RAKE diversity effect even at high-data-rate transmissions and improve performance in multipath fading environment. Furthermore, similar to MC-CDMA, MC-DS-CDMA is robust against frequency-selective fading. Besides, for the purpose of obtaining a certain processing gain, which is a measure of gained spectrum in DS-CDMA, we may decide the chip rate according to the processing gain, and so, we have other impressive advantage of this scheme to be more flexible of assigning spreading codes to the two domains (i.e., time and frequency). Similarly, the processing gain determines the number of subcarriers in MC-CDMA. In contrast with both schemes, in MC-DS-CDMA we have the freedom in decision of such parameters according to the fading effect, system requirements, and so on. Of course, MC-DS-CDMA has some disadvantages with respect to DS-CDMA and MC-CDMA. For example, similar to MC-CDMA, MC-DS-CDMA requires an amplifier with high linearity, which results in power inefficiency.

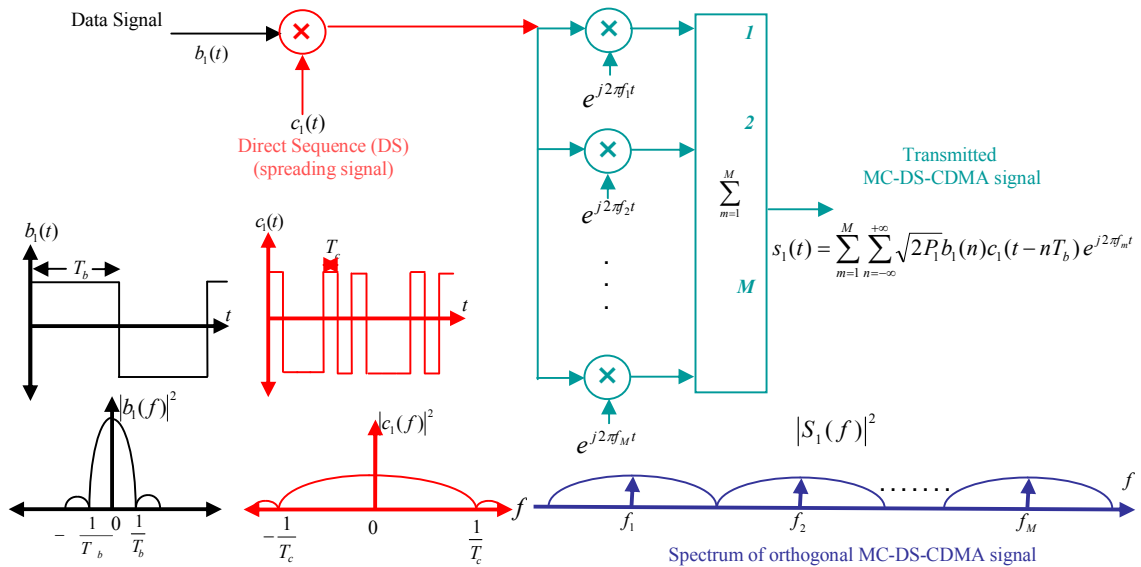


Figure 2-13: Multicarrier single user DS-CDMA transmitter.

2.4.2 MC-DS-CDMA Transmitter:

In this section we explain the MC-DS-CDMA [39] transmitter model using simple mathematical expressions that make it easy to understand the main features of this scheme. This discussion could also be used for future implementation of the MC-DS-CDMA transmitted signal. The transmitted signal of a k^{th} user for the m^{th} carrier can be expressed in complex form as

$$s_m(t) = \text{Re} \left[\sum_{n=-\infty}^{\infty} \sum_{k=1}^K \sqrt{E_{b_k}} b_k(n) c_k(t - nT_b) e^{j2\pi f_m t} \right] \quad (2.10)$$

Where E_{b_k} is the k^{th} bit energy, T_b is the bit duration and f_m is the m^{th} carrier frequency. With using the spreading code

$$c_k(t) = \sum_{i=0}^{N-1} s_k(i) \psi(t - iT_c), \quad (2.11)$$

where T_c is the chip duration, $N = T_b / T_c$ is the spreading code processing gain, $s_k(i) = \{\pm 1/\sqrt{N}\}$ with $i = 0, 1, \dots, N-1$ is the normalized spreading sequence and $\psi(t)$ is the unity chip pulse shape [36]. The different spreading codes can be used, here in our project we use gold sequences as a spreading codes [39]. This m^{th} carrier model is illustrated in Fig. 2-14.

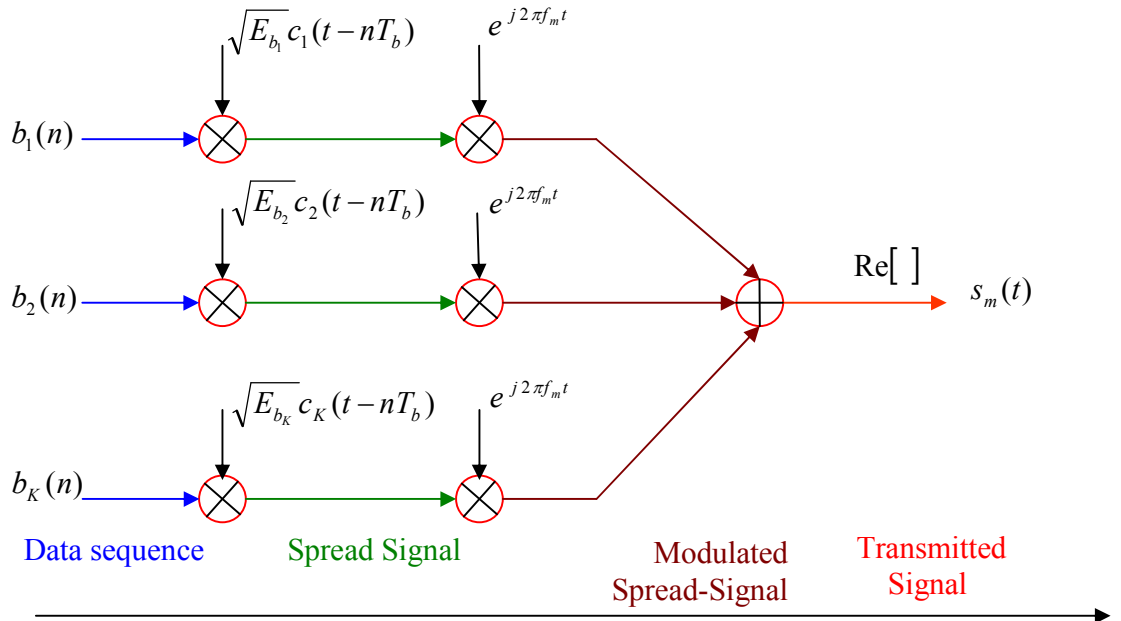


Figure 2-14: The m^{th} carrier of MC-DS-CDMA transmitter.

It is important to denote the coded signals are modulated with M carriers, whose bandwidth is approximated as $BW_m = \frac{1}{MT_c}$. The spectrum of the single and multi carriers DS-CDMA as in the Fig. 2-15, which contributes with using wide sense stationary uncorrelated scattering (WSSUS) model, for assuming the frequency selective wideband fading is subdivided in narrow band fading for the MC transmissions for using better channel models. Furthermore, by suitably choose the M number of carriers separating with the bandwidth of the chips of the spreading codes, a one can assume that, these narrowband fading processes undergo independently. As seen the entire bandwidth for the MC is divided into M equi-width non-overlapping sub-bands with the bandwidth of each sub-band $= \frac{1}{MT_c}$, hence the total bandwidth is $BW = \frac{1}{T_c}$ [39], this discussion may will be more clearly in coming Chapters.

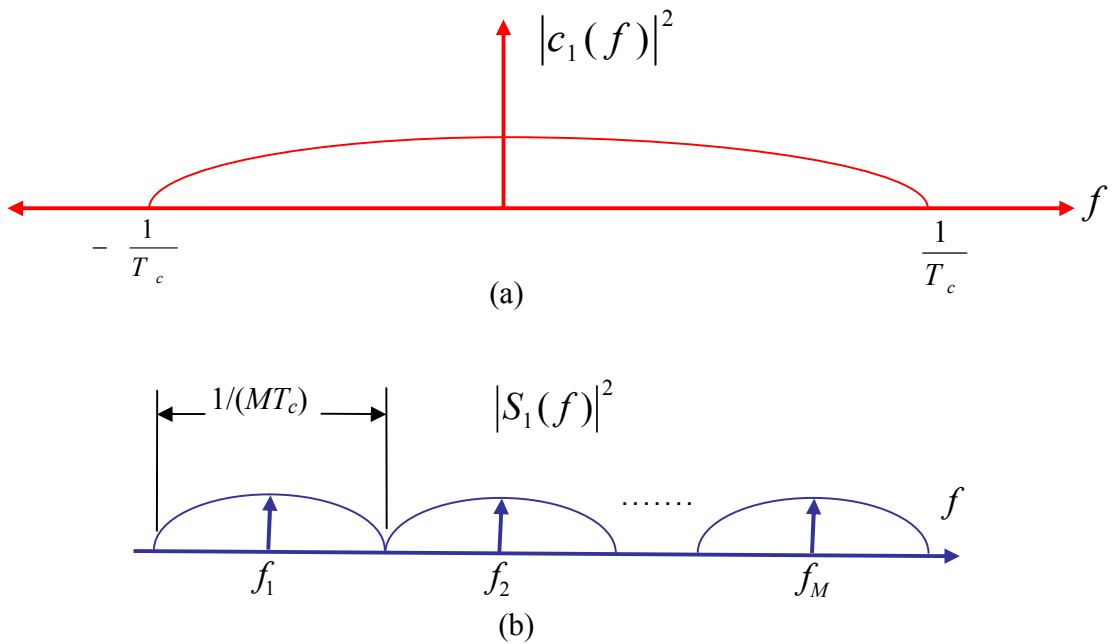


Figure 2-15: Spectrum of (a) widband single DS-CDMA (b) orthogonal MC-DS-CDMA signals.

Chapter 3

Mobile Wireless Channels

Understanding the mobile channels impairments are very important, in order to serve in treating channel introducing distortions. Furthermore, sophisticated signal design and smart transmission and reception technologies are required to maintain a reliable communication [59, 60].

In this chapter, we present an introduction to mobile wireless losses in Section 3.1, channel parameters in Section 3.2, its classifications in Section 3.3, and Rayleigh fading channel, frequency diversity techniques in Section 3.4, in addition, the Jakes model representing the Rayleigh one in Section 3.5, finally, in Section 3.6 we assume AWGN disturbs the mobile channel.

3.1 Introduction

Mobile communication is burdened with particular propagation complications, making reliable wireless communications more difficult than fixed ones, particularly, for positioned antennas. As the antenna is expected to have very little ‘clearance’ due to its height at a mobile terminal which is usually very small, typically less than a few meters. Thus, obstacles and reflecting surfaces in the vicinity of the antenna have a substantial influence on the characteristics of the propagation path. Moreover, the propagation characteristics change from place to place, specially, if the terminal moves from time to time. A transmitted signal from a transceiver passes through complicated propagation processes of diffraction, multiple reflections, and scattering mechanisms as shown in Fig. 3-1. The three propagation effects lead to fluctuation of the received signal are: First, reflection which occurs when a radio signal propagates and incidents onto a smooth surface with large dimensions compared to the signal wavelength. Second, diffraction occurs when a large body obstructs the radio path causing secondary waves to be formed behind the obstructing body and continue propagation to the receiver. Third, scattering occurs when the signal incidents onto a large rough surface, causing the reflected waves to spread out in various directions.

As the arrived signals to the receiver at the base station are the combinations of multipaths. The superposition of amplitudes and time delays can be constructive or destructive, depending on the phases. If the user is considered stationary, the received signal is constant for the multipaths, depending on the base station position, while the scattering and reflecting objects are stationary. However, when a user is in motion, the received signals are considered to fluctuate as a function of time. Actually, the discussed channel effects produce a problem which is so-called multipath fading. The total losses of these effects can be evaluated as

$$L(t) = L_p(d) + m(t) + \beta(t), \quad (3.1)$$

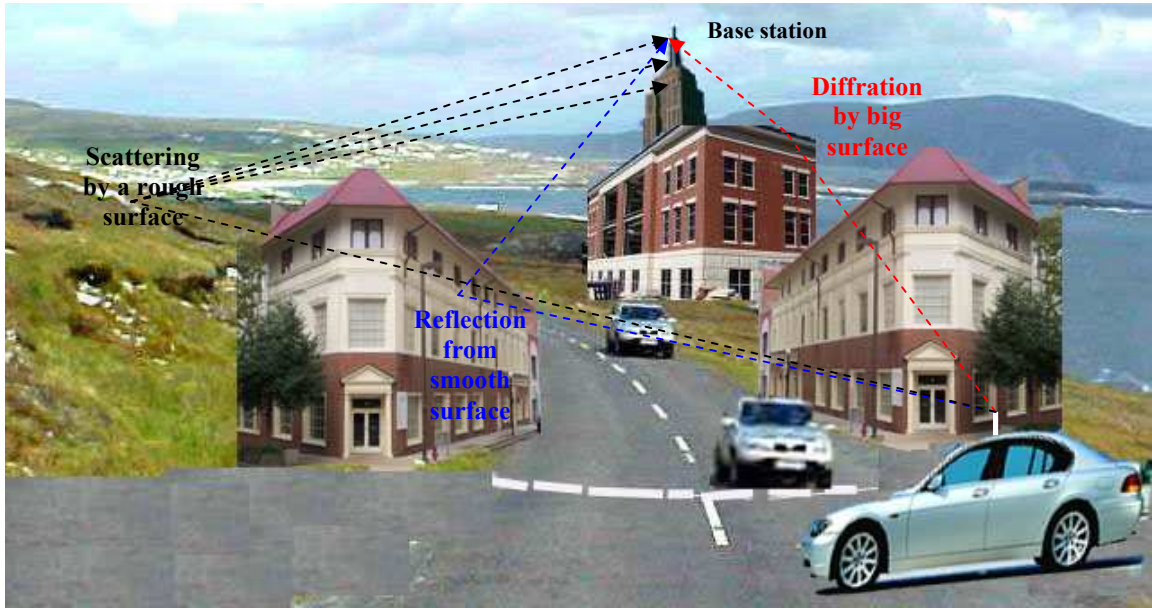


Figure 3-1: Illustration of wireless propagation mechanisms.

where $L_p(d)$ is the mean path loss as a function of the separation distance d between the transmitter and receiver. $m(t)$ is the shadowing variation, and $\beta(t)$ is the fading fluctuation. Indeed, we refer to $L_p(d) + m(t)$ as *the large scale propagation path loss* which can be represented in terms of the mean path and its variation around this mean due to the shadowing. Moreover, $\beta(t)$ is called the *small scale propagation path loss*, which represents the dramatic and rapid changes of the amplitude and phase of the signal, where small and large are considered as respecting to the wavelength of the signal.

- *Large Scale Path Loss*

The large-scale effects (area-mean power) reflect a power level averaged over an area of tens or hundreds of meters. In addition, shadowing introduces fluctuations, so the received local-mean power varies around the area-mean. The term 'local-mean' is used to denote the signal level averaged over a few tens of wave lengths, typically 40 wavelengths. This ensures that the rapid fluctuations of the instantaneous received power due to multipath effects are largely removed.

We express the large scale path loss in dB as [61]:

$$L_p(d) = L_{d_0} + 10n \log\left(\frac{d}{d_0}\right) \quad (3.2)$$

where L_{d_0} is the mean path loss at a reference distance d_0 , n is the path loss exponent.

The large scale path loss has a lognormal distribution due to shadowing, and the received signal level follows a normal distribution. So $m(t)$ is a zero mean Gaussian with σ_m^2 variance [57].

- *Small Scale Path Loss*

If the vehicle moves over a distance in the order of a wave length or more, fading leads rapidly constructive or destructive fluctuations of the phase and amplitude. Thus, the multipath fading problem is appeared which is considered as a 'small-scale' effect. This phenomenon will be discussed later in more details.

3.2 Channel Parameters

In general the time varying fading channel model is too complex for the understanding and performance analysis of wireless channels. Fortunately, the *wide-sense stationary uncorrelated scattering (WSSUS)* model adequately approximate many practical wireless channels [62, 63]. In this WSSUS model, the time-varying fading process is assumed to be a wide-sense stationary random process and the signal copies from the scatterings by different objects are assumed to be independent. Consider Fig. 3-2, where $s(t)$ is a transmitted signal through a channel whose impulse response $h(\tau, t)$, and $s_h(t)$ is the received signal which involves fading effects, and $r(t)$ is the received signal of both AWGN and fading effects.

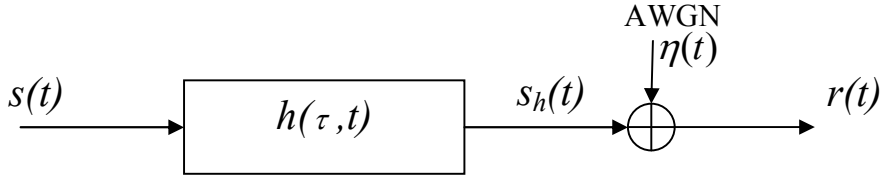


Figure 3-2: Channel model.

The WSSUS assumption may be characterized by the uncorrelated scattering auto-correlation function

$$R_{hh}(\tau_1, \tau_2; \Delta t) = \frac{1}{2} E[h^*(\tau_1; t)h(\tau_2; t + \Delta t)], \quad (3.3)$$

then *average power of the channel as a function of time delay τ* can be achieved when we let $\Delta t = 0$ (which is called *multipath intensity profile* or *delay power spectrum*)

$$R_{hh}(\tau) = R_{hh}(\tau; 0), \quad (3.4)$$

besides, *the spaced frequency, spaced time correlation function* of the channel, which provide us a measure of frequency coherence of the channel. i.e.,

$$R_{hh}(f_1, f_2; \Delta t) = \frac{1}{2} E[H^*(f_1; t)H(f_2; t + \Delta t)]. \quad (3.5)$$

Furthermore, we define the Doppler power spectrum by setting the $\Delta f = 0$, which is considered as a Fourier transform of the $R_{hh}(\Delta f; \Delta t)$ with respect to the time difference as:

$$\Psi_{hh}(\lambda) = \int_{-\infty}^{\infty} R_{hh}(0; \Delta t) e^{-j2\pi\lambda\Delta t} d\Delta t. \quad (3.6)$$

And so, we can define the following parameters, which are often used to characterize this WSSUS fading channel:

- *Multipath spread* T_m [63]

It is defined as the range of values over which the delay power spectrum $R_{hh}(\tau)$ is nonzero. For urban environments, T_m can [64] range from 0.5 μs to 5 μs .

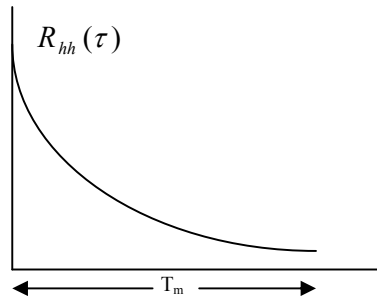


Figure 3-3: Illustrate multipath spread concept.

- *Doppler spread* B_d

Defined for range of values over which the Doppler power spectrum $\Psi_{hh}(\lambda)$ is nonzero. Indeed, the value of the Doppler spread B_d provides a measure of how rapidly the channel impulse response varies in time. The larger the value of B_d , the more rapidly the channel impulse response is changing with time.

- *Coherence time* $(\Delta t)_c$

For a time-varying channel, the channel impulse response varies with time. Defining a *coherence time*, denoted by $(\Delta t)_c$, which gives a measure of the time duration over which the channel impulse response is essentially invariant (or highly correlated). In reality, the coherence time is also considered as another measurement referred to Doppler spread as:

$$(\Delta t)_c \approx \frac{1}{B_d} \quad (3.7)$$

- *Coherence bandwidth* $(\Delta f)_c$

Considering a fading channel, signals with different frequency contents can undergo different degrees of fading. Defining *coherence bandwidth*, denoted by $(\Delta f)_c$, which gives an idea of measuring the width of the frequency band in which fading is highly correlated. Moreover, the $(\Delta f)_c$ is related to T_m by [63]:

$$(\Delta f)_c \approx \frac{1}{T_m} \tag{3.8}$$

Based on these channel parameters, we may characterize the time varying fading channels as in the following subsection. Other important channel parameters could be considered from statistics; like mean, and variance of a channel. Nevertheless, for purpose of channel modeling the previous were considered.

3.3 Channel Classifications And Models

3.3.1 Frequency Non-selective versus Frequency Selective:

If the bandwidth of the transmitted signal is small compared with $(\Delta f)_c$, then all frequency components of the signal would roughly undergo the same degree of fading. Hence, the channel is classified as *frequency non-selective* (also called *flat fading*). We notice that because of the reciprocal relationship between $(\Delta f)_c$ and T_m , also the one between bandwidth and symbol duration T_s , in a frequency non-selective channel, the symbol duration is large compared with T_m . In this case, delays between different paths are relatively small with respect to the symbol duration. We can assume that we would receive only one copy of the signal, whose gain and phase are actually determined by the superposition of all those copies that come within T_m . Flat fading is simply could be roughly represented as in Fig. 3-4, where f_c is the carrier frequency.

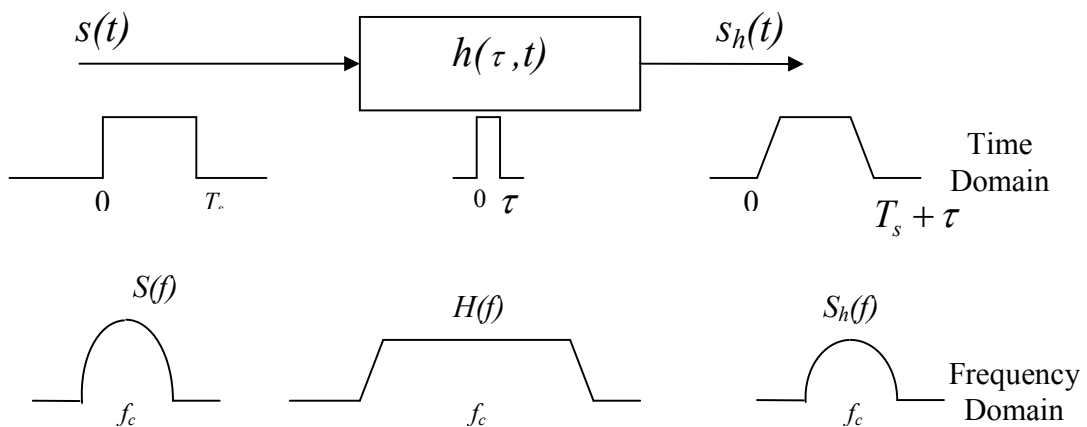


Figure 3-4: Flat fading characteristics.

On the other hand, if the bandwidth of the transmitted signal is large compared with $(\Delta f)_c$, then different frequency components of the signal (that differ by more than $(\Delta f)_c$) would undergo different degrees of fading. So the channel is classified as *frequency selective*. Due to the reciprocal relationships, the symbol duration is small compared with T_m . Delays between different paths can be relatively large with respect to the symbol duration. We then assume that we would receive multiple copies of the signal. Unlike Fig. 3-4 the spectrum of the transmitted signal, $S(f)$, has a bandwidth that is greater than the coherence bandwidth $(\Delta f)_c$. The frequency selective fading channels are also known as wideband channels since the bandwidth of the transmitted signal $s(t)$ is wider than the bandwidth of the channel impulse response.

3.3.2 Slow Fading versus Fast Fading:

If the symbol duration is small compared with $(\Delta t)_c$ then the channel is classified as *slow fading*. Slow fading channels are very often modeled as *time-invariant* channels over a number of symbol intervals. Moreover, the channel parameters, which are slow varying, may be estimated with different estimation techniques.

On the other hand, if $(\Delta t)_c$ is close to or smaller than the symbol duration, the channel is considered to be *fast fading* (also known as *time selective fading*). In general, it is difficult to estimate the channel parameters in a fast fading channel.

We notice that the above classifications of a fading channel depend on the properties of the transmitted signal. The two ways of classifications give rise to four different types of channel as:

- *Frequency non-selective slow fading*
- *Frequency selective slow fading*
- *Frequency non-selective fast fading*
- *Frequency selective fast fading*

If a channel is frequency non-selective slow fading (also known as *non-dispersive*), then the relationships

$$T_m < T_s \text{ and } T_s < (\Delta t)_c$$

must be satisfied, where T_s is the symbol duration, which is equal to reciprocal of the symbol bandwidth W_s . Therefore,

$$T_m < (\Delta t)_c \text{ or } T_m B_d < 1.$$

The product $T_m B_d$ is called the *spread factor* of the physical channel. If $T_m B_d < 1$, the physical channel is referred as *underspread*. While if $T_m B_d > 1$, the physical channel is

referred as *overspread*. Therefore, if a channel is classified as frequency non-selective slow fading, the physical channel must be under-spread. For simplicity, we summarize these categories in TABLE 3-1 [63].

TABLE 3-1: DECISION CRITERIA FOR THE TYPES OF CHANNEL MODEL TO USE.

	$T > (\Delta t)_c$	$T < (\Delta t)_c$
$W > B_d$	Frequency Selective Fast Fading	Frequency Selective Slow Fading
$W < B_d$	Frequency Non-selective Fast Fading	Frequency Non-selective Slow Fading

Based on the previous classifications, we can develop mathematical models for the different kinds of fading channels to facilitate the performance analysis of communication systems in fading environments. The followings are common fading channel models:

3.3.3 Frequency Non-selective Fading Channel Model:

First, let us consider frequency non-selective fading channels. Suppose that the signal $s(t)$ is sent. Frequency non-selectiveness implies that we can assume only one copy of the signal is received

$$r(t) = h(t)s(t). \quad (3.9)$$

In (3.9), the complex gain imposed by the fading channel is represented by $h(t) = \alpha(t)e^{j\theta(t)}$, where $\alpha(t)$ and $\theta(t)$ are the overall (real) gain and the overall phase shift resulting, actually, from the superposition of many copies with different gains and phase shifts. In general, $\alpha(t)$ and $\theta(t)$ are modeled as WSS random processes.

For a slow fading channel, $\alpha(t)$ and $\theta(t)$ can be assumed to be invariant over an observation period less than $(\Delta t)_c$. Therefore, they can be simply replaced by random variables. Denoting the corresponding random variables by α and θ , we have $h(t) = h = \alpha e^{j\theta}$. Since the gains $\alpha \cos(\theta)$ and $\alpha \sin(\theta)$ on the in-phase and the quadrature channels result from the superposition of large number of contributions, they can be modeled as Gaussian random variables. Very often, they are modeled as i.i.d zero mean Gaussian random variables. Thus, the complex gain h is a zero-mean symmetric complex Gaussian random variable. This also implies that α is a Rayleigh distributed and θ is uniformly distributed on $[0, 2\pi)$. The resulting model is called a frequency non-selective slow *Rayleigh fading* channel. In reality, this model is accurate when there is no direct-line-of-sight (LOS) path between the transmitter and the receiver. Figure 3-5 shows α probability density function (pdf), which is expressed in a mathematical form as:

$$f(\alpha) = \frac{2\alpha}{\sigma^2} e^{-\frac{\alpha^2}{\sigma^2}}, \alpha \geq 0, \quad (3.10)$$

where $\sigma^2 = E[\alpha^2]$.

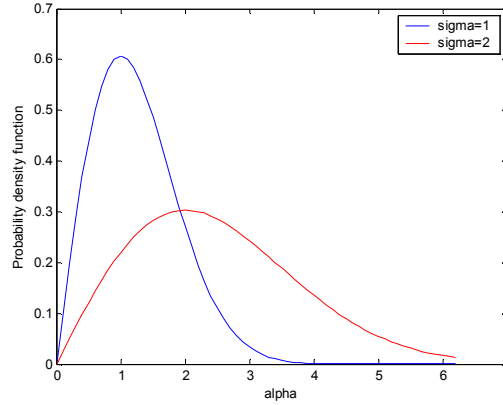


Figure 3-5: Probability density function of Rayleigh distribution.

Furthermore, the Rayleigh fading channel envelope with respect to time, its peaks, deep fades, and variance, are shown in Fig. 3-6.

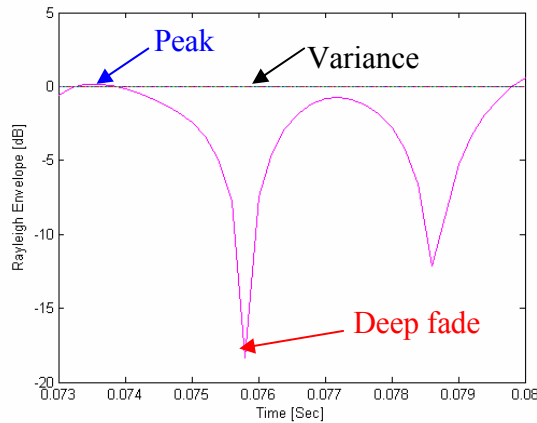


Figure 3-6: Rayleigh fading channel envelope.

For a fast fading channel, the characterizations of the random processes $\alpha(t)$ and $\theta(t)$ depend on the Doppler power spectrum which, in turn, depends on the physical channel environment, such as the heights of the transmitter and receiver antenna, the polarization of the radio wave, the speed of the mobile, and the speed and geometry of the scatters. By considering the received signal at a mobile unit for special case where a vertical monopole antenna is employed at the mobile unit with a ring of scatters, the WSS process $h(t)$ is modeled [65] as a zero-mean complex Gaussian process, as will be discussed later.

3.3.4 Frequency Selective Fading Channel Model:

In a frequency selective fading channel, many distinct copies of the transmitted signal are received at the receiver. For the slow fading case, the received signal can be expressed as

$$r(t) = \sum_{l=1}^L h_l s(t - \tau_l), \quad (3.11)$$

where $h_l = \alpha_l e^{j\theta_l}$ for $l = 1, 2, \dots, L$, are the complex gains for the received paths. In (3.11), the number of distinct paths L , the gain of each distinct path α_l , the phase shift of each distinct path θ_l , and the relative delay of each distinct path τ_l are all random variables. In the fast fading channel case, all these random variables become random processes.

3.4 Diversity Techniques for Multipath Fading Channels

In a frequency selective fading channel, we obtain L independent copies of the desired signal from L different paths. We may use diversity techniques to improve the system performance in these fading paths. The idea is that while some copies may undergo deep fades, others may not. After there, the L independently faded copies are “optimally” combined to give a statistic for decision like a Maximal Ratio Combiner MRC. Hence, it might be still to obtain enough energy to make the correct decision on the transmitted symbol. There are several different kinds of diversity which are commonly employed in wireless communication systems. Among of existing is a frequency diversity technique.

Frequency diversity technique

It is a process based on modulating the information signal through L different carriers. Each carrier should be separated from the others by at least the coherence bandwidth $(\Delta f)_c$ so that different copies of the signal undergo independent fading. In reality, frequency diversity can be used to combat frequency selective fast fading into frequency non-selective fast fading, by considering the received signal of the time-varying frequency non-selective fading along each carrier, over the m^{th} one as [61, 63]:

$$r_m(t) = s_m(t)h_m(t) + \eta_m(t). \quad (3.12)$$

Where $r_m(t)$ is the m^{th} carrier received signal, $s_m(t)$ is the m^{th} transmitted signal, $h_m(t)$ is the m^{th} fading channel, and $\eta_m(t)$ is AWGN.

3.5 Jakes Model

The Jakes fading model is a deterministic method for simulating time-correlated Rayleigh fading waveforms [66], which is commonly used to characterize flat fading narrowband channels. This model assumes a receiver has an omni-directional antenna, so that the power spectral density $\psi_{hh}(\theta)$ arriving at the receiver as a function of the uniform distributed

angle θ . Furthermore, the scatters present in the communication channel are fixed so that they do not introduce further Doppler effects.

Lets start with reformulate the fading channel equation as follows:

$$h(t, \tau) = h(t)\delta(\tau - \tau_0) \quad (3.13)$$

where τ_0 represents the delay. Let \mathbf{v} denotes the velocity vector of the receiver and γ is the angle between the direction of the velocity vector and the Line-Of-Sight (LOS) between transmitter and receiver, the relationship between the Doppler frequency shift f_k and the angle θ is

$$f_k = \frac{v}{\lambda} \cos(\theta_k - \gamma), \quad (3.14)$$

and so the Doppler shift can be represented as

$$f(\theta) = \frac{v}{\lambda} \cos(\theta - \gamma), \quad (3.15)$$

where v is the modulus of the vector \mathbf{v} . This relationship allows us to rewrite the received power spectral distribution as a function of the Doppler shift as follows:

$$\psi_{hh}(f) = \sum_{i=1}^L \psi_{hh}(\theta_i(f)) \left| \frac{\partial \theta(\nu)}{\partial f} \right|_{\theta=\theta_i(f)}, \quad (3.16)$$

where $\theta_i(\nu) = \gamma \pm \cos^{-1}(\lambda \nu / f)$ denotes the i^{th} inverse solution of (3.14). In the interval $(-\pi, \pi]$, there are two inverse solutions. Thus, the power spectral density, as a function of f is

$$\psi_{hh}(f) = \frac{\psi_{hh}(0)}{\pi} \frac{1}{\sqrt{f_d^2 - f^2}}, \quad f \in [-f_d, f_d] \quad (3.17)$$

where $f_d = \frac{v}{\lambda}$. Starting from $\psi_{hh}(f)$, we can compute the correlation of the transfer function as the inverse Fourier transform of $\psi_{hh}(f)$ and the result is known in closed form

$$R_{hh}(\Delta t, 0) = \psi_{hh}(0) J_0(2\pi f_d \Delta t), \quad (3.18)$$

where J_0 is the zeroth order Bessel function of the first kind [66], It is clear the variance of autocorrelation can be achieved by substituting a zero value as $R_{hh}(0,0) = \psi_{hh}(0)$ which is denoted as σ_h . Figure 3-7 shows the uniform PSD of the Jakes model, with twins pairs at maximum Doppler frequency f_d . Hence, the discrete unity ACF can be achieved by replacing $nT_b = \Delta t$ i.e.

$$R_{hh}(n) = J_0(2\pi f_d T_b |n|). \quad (3.19)$$

Figure 3-8 shows the unity zeroth order Bessel function of the first kind; likes the ACF for the Jakes model.

3.6 AWGN Channel Model

From Fig. 3-2, we find in addition to fading effects, the channel is disturbed by noise, here we consider the zero-mean Additive White Gaussian Noise (AWGN) $\eta_m(t)$ over each carrier, where $\{\eta_m(t)\}_{m=1,\dots,M}$ are assumed to be mutually independent and identically distributed with variance σ_η^2 is added to the fading effects.

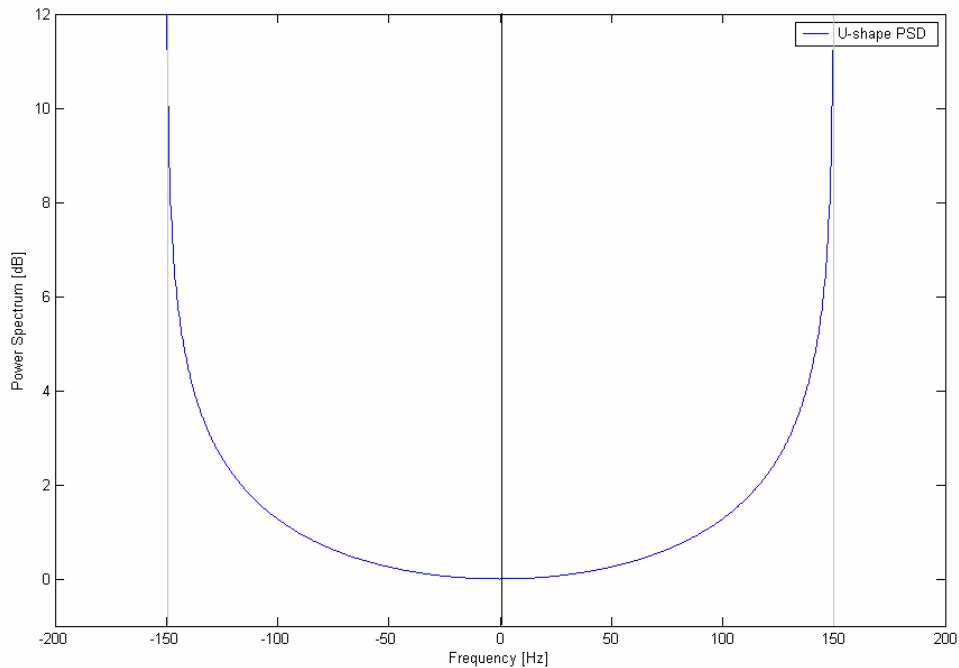


Figure 3-7: PSD of the Jakes model.

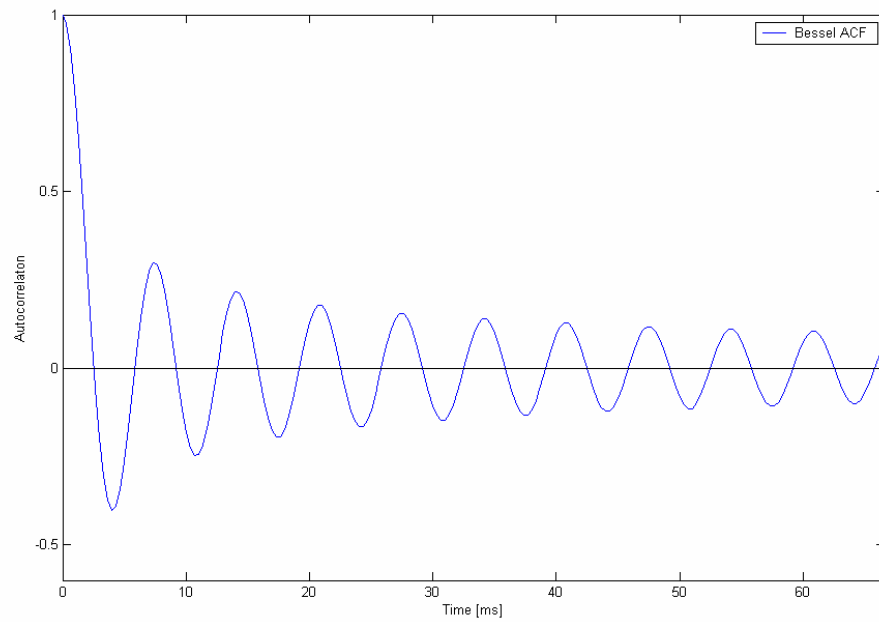


Figure 3-8: Normalized ACF of Jakes model.

Chapter 4

Receiver Design

4.1 Introduction

In taking the design of a basestation system for DS-CDMA, the transmitter operates bit synchronously as it broadcasts to all users simultaneously. When orthogonal codes are used, the mobile terminals linear correlated filters perform well in decoding the signal sent by advantage of this orthogonality. This orthogonality gives performance as if there is only one user in the system where is no interference from others or single user performance under ideal conditions and no multipaths.

In contrast on the uplink from mobile to base station, the wireless system synchronization is difficult to be maintained in order to the mobility of each user and needs tight closed loop timing control between the base station and the mobile. If this timing control is not maintained then the orthogonal properties of the spreading codes is lost and performance is severely degraded. In reality, multipath effects are common in the mobile radio channels which destroy this orthogonal property due to the path delays between received signals. Under this scenario randomly selected codes can be a better choice to model channel conditions as they provide an average interference level which is noise like for a large enough number of users [36]. Thus, considering this scenario is very important for the DS-CDMA systems as be considered in this report. It is well known that if a signal is corrupted by Additive White Gaussian Noise (AWGN) the filter with impulse response matched to the signal maximizes the signal to noise ratio [63]. However, with multiple users cross-correlation noise or Multiple Access Interference (MAI) occurs the correlator or Match Filter (MF) is no longer the optimal detector. Furthermore, in the near-far problem, which is referred to users' power effects on the desired one, also, the correlator filter considers random power effects on the intended. Hence, a multiuser filter has to be considered instead. The decorrelator filter based receiver treats both the MAI, and near-far problems as will be discussed in more details. Indeed, the DS-CDMA suffers from the near-far problem and the cross-correlation between users (MAI) problem.

In this chapter we present structures of both conventional correlator filter, and decorrelator filter based receivers. Next we present simulation results of near-far and MAI problems for both receivers. Finally, we offer our conclusions on the receivers.

4.2 Conventional MC-DS-CDMA Receiver

From the preceding chapter we can represent the m^{th} synchronous received signal from the multi fading-AWGN channel in the complex form as

$$r_m(t) = \sum_{n=-\infty}^{\infty} \sum_{k=1}^K h_m(n) \sqrt{E_{b_k}} b_k(n) c_k(t - nT_b) e^{j2\pi f_m t} + \eta_m(t). \quad (4.1)$$

Considering the conventional receiver structure of a correlator along each carrier followed by MRC [39] as the Fig. 4-1.

Converting the serial modulated signal to parallel, then despreading using chip waveform $c(t)$, followed the m^{th} carrier has an output for the user 1 as an example :

$$z_m = \int_0^{T_b} r_m(t)c(t)e^{-j2\pi f_m t} dt \quad (4.2)$$

which can be represented in a vector form as follows:

$$z_m = \mathbf{s}_1^T \mathbf{x}_m \quad (4.3)$$

where $\mathbf{x}_m = [x_m(0) \ x_m(1) \ \dots \ x_m(N-1)]$, and $\mathbf{s}_1 = [s_1(0) \ s_1(1) \ \dots \ s_1(N-1)]^T$ is the normalized spreading code of the first user (desired user).

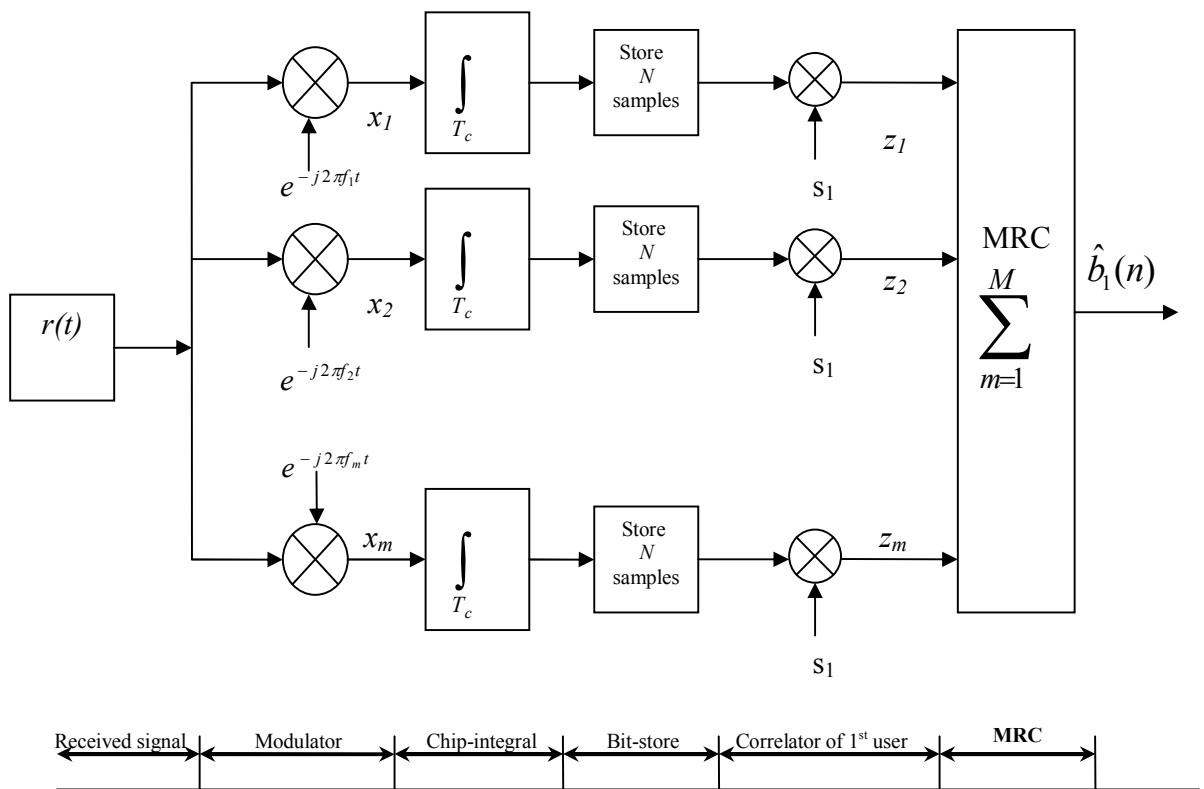


Figure 4-1: Correlator receiver; consisting of a correlator along each carrier followed by MRC.

By replacing the paralleled received signal with the data sequences from (4. 1) in (4. 3) we get

$$z_m = \underbrace{\sum_{n=-\infty}^{\infty} h_m(n) \sqrt{E_{b_1}} b_1(n) \mathbf{s}_1^T \mathbf{s}_1}_{\text{term1}} + \underbrace{\sum_{n=-\infty}^{\infty} \sum_{k=2}^K h_m(n) \sqrt{E_{b_k}} b_k(n) \mathbf{s}_k^T \mathbf{s}_1}_{\text{cross-correlation(MAI)}} + \mathbf{Z}_m. \quad (4. 4)$$

Where and $\mathbf{z}_m(n)$ is the AWGN vector with zero mean and σ_z^2 is the variance of the received noise multiplied by the vector \mathbf{s}_1 . Due to the central limit theorem, the second term with noise distribution becomes closer and closer to a Gaussian law as the system size increases without bound [67]. Hence, the conventional receiver ignores the MAI and treats it as noise, therefore for random spreading codes, on average, as the number of users increase the MAI increases, which limits the number of users that can share the same bandwidth. As can be seen from (4. 4), the second term is the summation of the cross-correlations between users, multiplied by the other users data bit $b_k(n)$ with the fading channel effects. For equal power users the magnitude of the interfering term is therefore dependent on

- the sign of the data of the other users
- the cross-correlation of the spreading codes to the user of interests spreading code
- the number of interfering users

As the number of users increases the magnitude of this MAI term will increase and could impair receiver performance. The cross-correlation of the spreading codes will determine the amount of interference, and the timing synchronization will also determine the cross-correlation properties between the users. If the other users' codes are orthogonal to the spreading code of interest then the interference from the other users will be zero. If however the codes are not orthogonal to the spreading code of our interest then the correlator filter output includes the energy collected from the cross-correlation of the spreading code of the user of interests with each interfering spreading code.

Finally, applying the MRC with using perfect channel knowledge we get:

$$\hat{b}_1 = \text{sgn} \left(\text{Re} \left[\sum_{m=1}^M h_m^*(n) z_m(n) \right] \right) \quad (4. 5)$$

4.3 Decorrelator Detector Based Receiver

The decorrelator [68] inverts the channel correlation for leaving the received signal without interference but by doing so increases the noise component. The decorrelator advantage is that no knowledge of the received powers is required, and its performance is independent of the interfering users' power. Through this receiver the received signal in (4. 1) is processed firstly by demodulator over the m^{th} carrier in order to achieve the baseband data signal, then a chip-match filter is processed, which consists of an integrator with a chip duration T_c , the

output samples are then stored during one bit interval, resulting in a $N \times 1$ vector. After that stage, the received vector at the m^{th} carrier is processed by the near-far resisting decorrelating detector [36]. Finally, the MRC is applied to optimize retrieving data sequences as in the [40], this receiver structure is shown in Fig. 4-2. For the purpose of writing mathematical formulations let us pass through the figure stages step by step until the final stage as the following:

- the received signal is demodulated by the m^{th} carrier along each path. Thus, a one has the m^{th} received signal formulas as

$$x_m(n) = r_m(t) e^{-j2\pi f_m t}. \quad (4.6)$$

This formula can be replaced by data sequences from (4.1) with involving effects of the superposition for the attenuated signal due to the fading suppression and delaying chip correlator filtering effects, we can represent this demodulated received signal from (4.6) for the K users as the following manner

$$x_m(t) = \sum_{n=-\infty}^{\infty} \sum_{k=1}^K h_m(n) \sqrt{E_{b_k}} b_k(n) c_k(t - nT_b) + \eta_m(t). \quad (4.7)$$

For simplicity we can represent the $N \times 1$ vector of the previous samples for K users in $\mathbf{x}_m(n)$ as

$$\mathbf{x}_m(n) = \sum_{k=1}^K h_m \sqrt{E_{b_k}} b_k(n) \mathbf{s}_k + \boldsymbol{\eta}_m(n). \quad (4.8)$$

Where $\mathbf{s}_k = [s_k(0) \ s_k(1) \ \dots \ s_k(N-1)]^T$ denotes the normalized spreading sequences vector of k^{th} user and $\boldsymbol{\eta}_m(n)$ is the AWGN vector with zero mean and covariance $\sigma_\eta^2 \mathbf{I}_N$.

According to [69], decorrelator filtering can be used successfully to suppress the MAI, which consists of a weighting factors w in order to eliminate the MAI. For the user 1 as an example we choose this w as the following

$$\mathbf{w}_1 = \sum_{k=1}^K [\mathbf{R}^{-1}]_{1k} \mathbf{s}_k, \quad (4.9)$$

where $\mathbf{R} = [\mathbf{s}_1 \ \mathbf{s}_2 \ \dots \ \mathbf{s}_K]^T [\mathbf{s}_1 \ \mathbf{s}_2 \ \dots \ \mathbf{s}_K]$ is the normalized cross-correlation, and $[\mathbf{R}^{-1}]_{ij}$ denotes the $(i, j)^{\text{th}}$ element of the inverse for the normalized crosscorrelation. Thus, the output of the decorrelator filtering (observed equation) for the associated 1st user is given by

$$y_m(n) = \mathbf{w}_1^T \mathbf{x}_m(n) = \sqrt{E_{b_1}} b_1(n) h_m(n) + \xi_m(n), \quad (4.10)$$

where $\xi_m(n)$ is zero mean Gaussian noise with variance $\sigma_\xi^2 = \sigma_\eta^2 [\mathbf{R}^{-1}]_{11}$.

Concerning to the observed equation we note that the decorrelator successfully eliminate the MAI, and near-far problems as be seen from the equation (4. 10), we just have the data bit sequence, and fading effects, and its independent of cross-correlation of the other users rather than the correlator filter based receiver. Indeed, this detector doesn't need to estimate the users amplitude, which are considered as an independent. Unfortunately, the main drawback for this based receiver is more complex computations is needed than the conventional correlator one, due to increasing number of users leads to more computations is required dealing with correlation inverse matrix of the spreading codes.

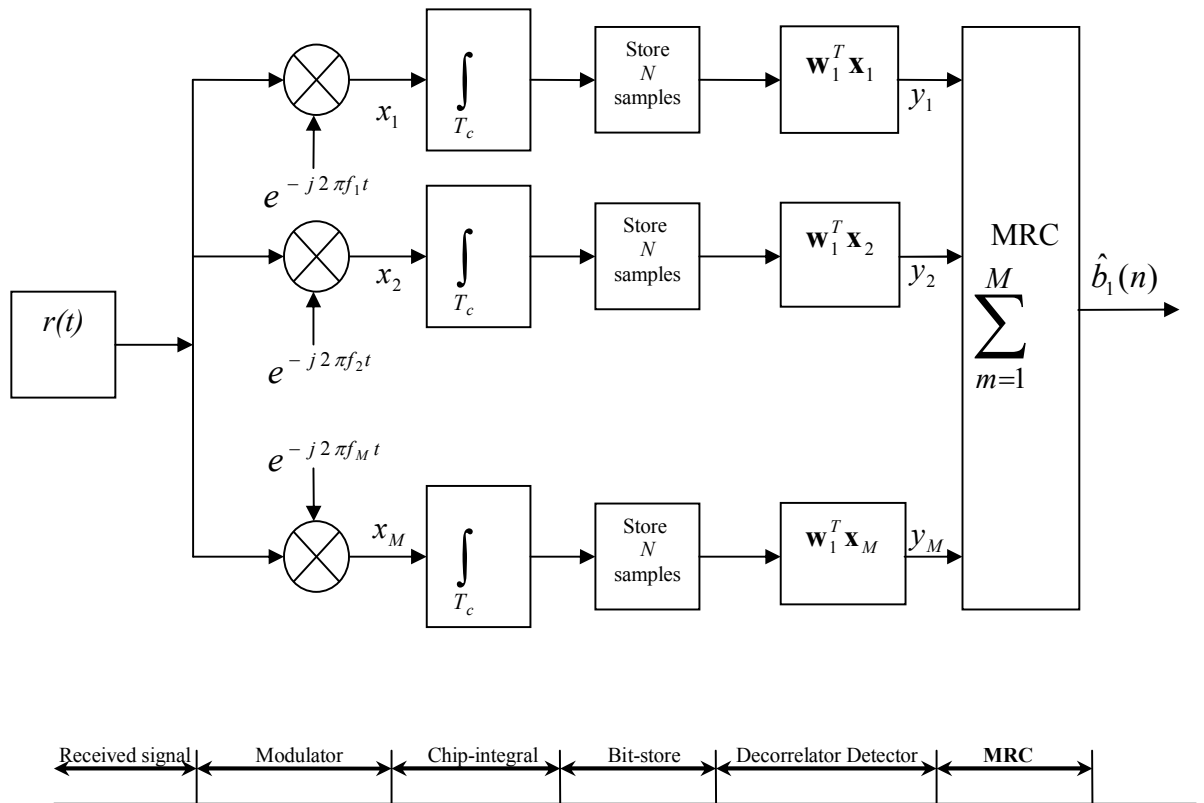


Figure 4-2: Decorrelator receiver; consisting a decorrelator along each carrier followed by MRC.

Finally, we may consider a known channel for comparative studying using the Maximum ratio combiner to determine the data symbol for the associated 1st user in presenting the observed data in (4. 10), as follows

$$\hat{b}_1(n) = \text{sgn} \left(\text{Re} \left[\sum_{m=1}^M h_m^*(n) y_m(n) \right] \right). \quad (4. 11)$$

4.4 Simulation Results

In this section, computer simulation results are provided to illustrate the BER performance of the MC-DS-CDMA system using the conventional correlator filter based receiver, and the decorrelator filter based receiver, under fading channel, each using a gold code of length $N=31$. In addition, the fading processes $\{h_m(n)\}_{m=1,\dots,M}$ are generated according to the modified Jakes model [66], with 16 distinct oscillators. They are normalized to have a unit variance, i.e. $\sigma_h^2 = 1$. The average SNR per carrier for the desired user is defined by

$$\text{SNR} = 10 \log_{10} (E_{b_i} \sigma_h^2 / \sigma_\eta^2). \quad (4.12)$$

The bit energy of the desired user is set to $E_{b_i} = 1$ and the noise is generated according to the SNR. Figure 4-3 illustrates the idea of near-far problem, which shows the BER performance of the both based receivers of 10 users with different power scenarios. As appeared the correlator based receiver may work as well as the decorrelator one in absence of near far problems. However, as this problem takes place more and more the correlator suffers from higher BER than the decorrelator while increasing SNR, which refers to MAI problems between users. In other words, the decorrelator filter based receiver resists the near-far problem, particularly, for higher SNR values, while the correlator filter based receiver is less resisting. For the purpose of studying the effect of number of users on the both receivers we investigate Fig. 4-4, which shows the BER performance versus number of users at different SNR values, in presence of near-far problems for single carrier DS-CDMA. As can be seen the decorrelator filter based receiver is not affected deeply with raising the number of users rather than the correlated one which diverges for worse BER performance, it is clear here that the MAI serve more in presence of near-far problems. That is equivalent to say, presenting both near-far and MAI problems means a more degradation for the correlator's one. Thus, the decorrelator can be considered to be a appealing with raising number of users without suffering from the cross-correlation between users (MAI) and power differences (near-far) rather than the matched correlator receiver. In addition, increasing number of carriers a more diversity gain improvement can be achieved for both receivers as shown in Fig. 4-5.

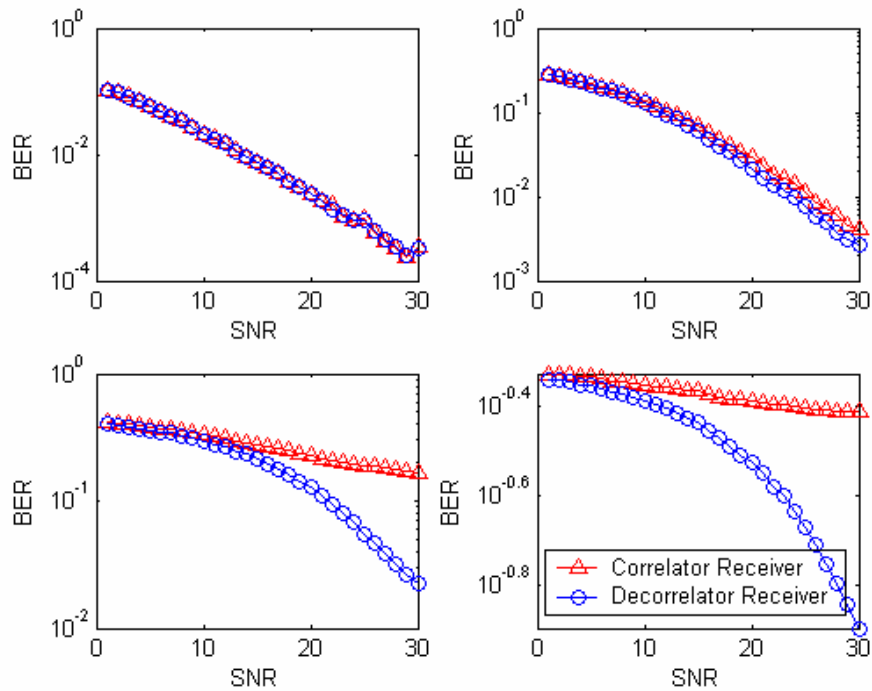


Figure 4-3: The BER performance vs the SNR, $K=10$, 31 spreading codes, and different power users scenarios for single carrier. The upper left with equal power, right $10 \cdot \text{power1}$, lower left $100 \cdot \text{power1}$, lower right $1000 \cdot \text{power1}$.

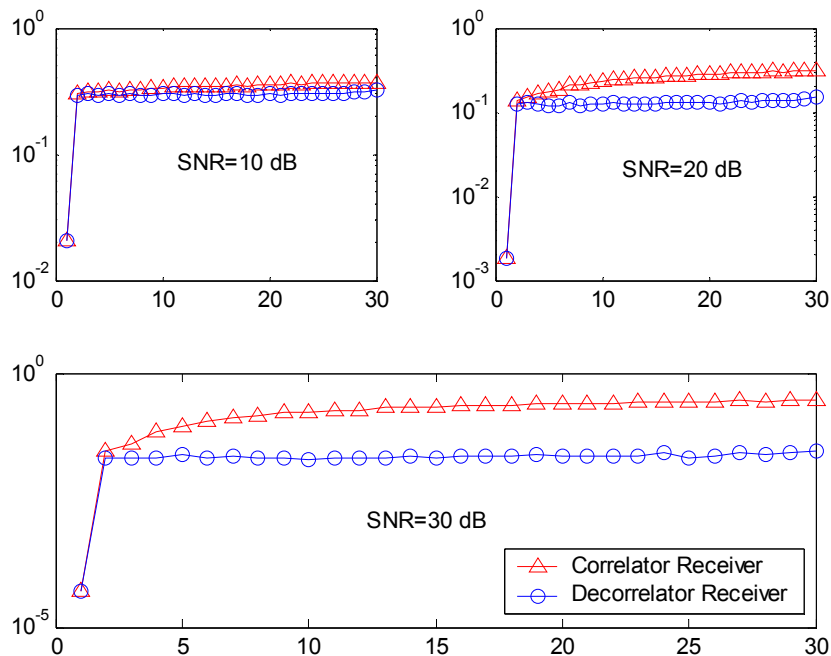


Figure 4-4: BER performance versus number of users, with near-far problem scenario, at different SNR, with 31 spreading gold sequence, for single carrier.

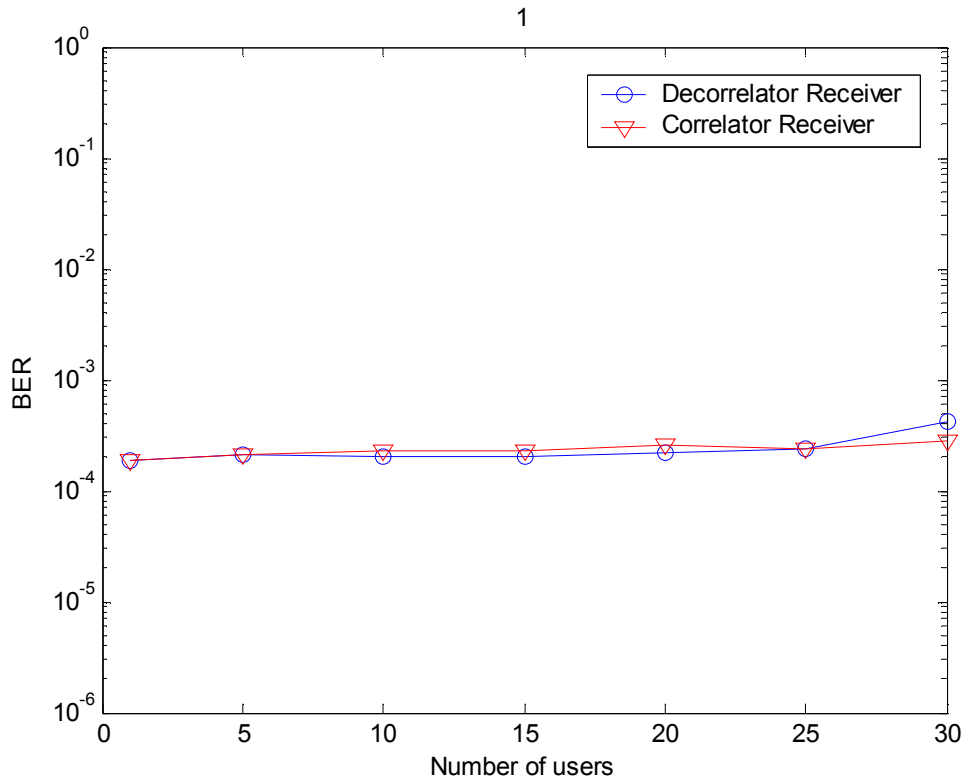


Figure 4-5: BER performance versus number of users, without near-far problems, at SNR=15 dB, with N=31 spreading gold sequence, for 2 carriers.

4.5 Conclusion

The conventional MC-DS-CDMA correlator receiver, which consists of a correlator along each carrier followed by a maximal ratio combiner (MRC), doesn't suppress the MAI, and so far it doesn't resist near-far scenarios. In addition, this receiver is not appealing to increasing number of users, with using quasi-orthogonal spreading codes, or the transmission through fading channels.

On the other hand, the decorrelator receiver, which consists of a chip-match filter over T_c interval, followed by a resistant near-far decorrelating detector and MRC, suppresses the MAI perfectly, even if near-far problems exist. In addition, this receiver is more appealing for increasing number of users than the correlator one, which can be considered as a single user receiver.

Increasing number of carriers, more diversity gain improvements can be achieved. Thus, considering the decorrelator receiver structure is very important to be investigated for MC-DS-CDMA systems rather than the correlator one.

Chapter 5

Channel Estimation

The design of receivers usually requires channel state information to achieve optimal diversity combining and coherent symbol detection. Indeed, channel estimation can be performed in two different ways [44]:

- Training sequence aided techniques.
- Blind techniques.

In this chapter, we consider the adaptive estimation of time-varying MC-DS-CDMA mobile Rayleigh fading channels using training sequence aided techniques based on:

- Kalman filtering. Particularly, we propose to investigate the relevance of high order AR models in the Kalman filter based channel estimator.
- Least Mean Square (LMS) based channel estimator
- Recursive Least Square (RLS) based channel estimator

This chapter is organized as follows. Section 5.1 provides literature survey and backgrounds about existing channel estimation techniques. The autoregressive modeling of Rayleigh fading channels is investigated in Section 5.2. In Section 5.3, we introduce Kalman filtering based channel estimator and compare it with those based on LMS and RLS filters in Sections 5.4, and 5.5 respectively. Finally, we discuss the results and provide our comments in Section 5.6.

5.1 Introduction

From the previous chapter, the conventional MC-DS-CDMA receiver [39], which consists of a correlator along each carrier followed by MRC, assumes that the channel fading processes are perfectly known. Unfortunately, the fading processes are usually unknown and, hence, should be estimated. The time variations of fading channels are typically modeled as stochastic processes using WSSUS models with U-shaped band-limited Doppler power spectra, and a zeroth order Bessel function of the first kind and ACF according to the Jakes model [65].

This key feature about channel dynamics is not exploited when directly estimating the fading processes by means of a recursive least square solution as in [63], or Least Mean Square (LMS) and Recursive Least Square (RLS) algorithms, like in [38], where independent MMSE filters are designed separately for each carrier, to be combined jointly for detecting optimization, with providing a mechanism to track the channel fading parameters in a time-varying channel.

Alternatively, when an Autoregressive (AR) model is used to describe the time evolution of the fading process, Kalman filtering can be carried out and is shown to provide superior

performance over the model-independent LMS and RLS based channel estimators [63]. In [70] a Kalman filter is found to be used for tracking fading channels. Nevertheless, the AR model parameters are unknown and, hence, must be determined. In addition, the selection of the AR model order must be investigated.

The AR parameters can be estimated from the received noisy signal. Among the existing methods, Tsatsanis *et al.* [71] have proposed to estimate the AR parameters from channel covariance estimates by means of a standard Yule-Walker estimator. Their work can be summarized in the following Algorithm

- Collect the noisy observations corresponding to the transmitted training sequences.
- Estimate the AR parameters by using a YW estimator applied to an estimate of the channel covariance matrix.
- As the AR parameters are estimated, Kalman filtering algorithm can be carried out.

However, this method results in biased estimates, where the estimated AR parameters are far from the true values.

In [45], the parameters of the AR model are estimated by means of an Expectation Maximization (EM) algorithm involving a Kalman smoothing, as follows:

The parameter matrices of the AR model are estimated via the method of expectation maximization (EM) with two algorithms.

- The first algorithm, using results from Kalman smoothing, provides a closed-form solution to the maximization problem in the iterative EM procedure.
- A new proposed algorithm with only forward-time recursions that approximates the iterative EM solution for slowly changing Doppler spreads.

Nevertheless, only first order AR model is considered for the Kalman filter based estimator.

Recently, in [40], the authors have proposed a two-cross-coupled Kalman filter based structure for the joint estimation of MC-DS-CDMA fading channels and their corresponding AR parameters using decision directed techniques as follows:

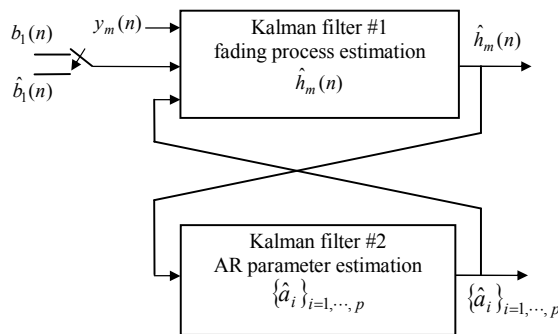


Figure 5-1: Coupled Kalman filter [40].

- One Kalman filter is used to estimate the fading process along each carrier.
- The second one makes it possible to estimate the corresponding AR parameters from the estimated fading process. Indeed, the estimated fading process is expressed as a linear function of the AR parameters which then defines the observation equation of the second filter.

This estimator is shown to provide significant results over the model-independent LMS or RLS based estimators, especially for channels with high Doppler rates. Nevertheless, only second order AR model is used for the sake of simplicity.

On the other hand, several authors (e.g., [70], [72- 74]) have expressed the AR parameters by first fitting the AR process autocorrelation function to the Jakes one, which is determined by using known Doppler rates or mobile speeds, and then solving the resulting Yule-Walker Equations (YWE). As one finds in [70] a second-order AR model is investigated for their proposed receiver structure. Furthermore, a study of decision-directed Kalman channel estimators over flat Rayleigh fading channels in [72] is done. While in [73] a robust Kalman filtering algorithm is used to estimate the channel responses for the adaptation of the proposed Decision-feedback equalizer (DFE) receiver under the situation of partially known channel statistics. The proposed receiver involves feedback filters for estimating channel responses, and its error covariance. However, only low order AR models are considered and they are not well suited to approximate a band-limited spectrum.

In addition, due to the band-limited nature of Jakes Doppler spectrum, severely ill-conditioned YWE are unavoidable for all but very small AR model orders. To solve the ill-conditioning problem, Baddour *et al.* [75] have suggested adding a very small positive bias to the main diagonal of the autocorrelation matrix in the YWE. This removes the band-limitation of the Jakes Doppler spectrum and enables them to use very high order AR models to accurately simulate and estimate Rayleigh fading channels.

Channel Estimation Techniques

Once a model has been established, its parameters have to be continuously estimated to track the channel changes. If the receiver has a-priori knowledge of the transmitted information over the channel, it can utilize this knowledge to obtain more accurate estimation of the channel impulse response. This method is simply called *Training sequence based Channel estimation*. , in other words, known symbols are transmitted specifically to aid the receiver's channel estimation algorithms. It has the advantage of being used in any radio communications system quite easily. Even though this is the most popular method in use today, it still has its drawbacks. One of the main drawbacks is that it is wasteful of bandwidth, due to overhead frames. Precious bits in a frame that might have been otherwise used to transport information are stuffed with training sequences for channel estimation. In addition, it suffers from the reception operation, which needs receipt of the whole frame that the channel estimate can be extracted from the embedded training sequence, where most communication systems send information at lumped frames. Moreover, for fast fading channels we interest in the coherence time of the channel which might be shorter than the frame time. Two common categories are existed in this technique:

- *Data Aided:* In the DA channel estimators utilize the filter output samples for which the data is known. This can be accomplished by transmitting a separate channel sounding reference signal (pilot signal) from which the channel is estimated [76]. Another way of implementing DA channel estimation is to utilize known pilot symbols time division multiplexed in the transmitted data stream [77]. The channel needs to be interpolated between the pilot symbol intervals.
- *Decision Directed:* The DD channel estimators utilize the decisions of the receiver to remove the effect of data modulation [78]. The DD channel estimation often applies prediction of the complex channel coefficients, since only the past decisions are available for channel estimator [78]. By using tentative decisions smoother type channel estimation filters can also be applied [79].

Non Data Aided (Blind Techniques), on the other hand, NDA channel estimators estimate the channel without utilizing data (training sequences), i.e., the receiver must determine the channel without the aid of known symbols. In reality, recently, this technique has been considered widely by researchers [80] with certain underlying mathematical information about the kind of data being transmitted. These methods might be bandwidth efficient due to no need for overhead frames. Unfortunately, it has some drawbacks. They are notoriously slow to converge. These methods are extremely computationally intensive and hence their application to fast or relatively fast fading channels has gained very little attention [81]. They also do not have the portability of training sequence-based methods, and more complexity. It is important to indicate that a one algorithm works for a particular system may not work with another due to the fact of sending different types of information over the channel.

5.2 Autoregressive Model

5.2.1 Autoregressive Model Background:

The autoregressive (AR) model of an order p can be written as $AR(p)$, i.e. time of a stationary random process X_t is regressed on the past values of itself as

$$X_t = \alpha_1 X_{t-1} + \dots + \alpha_{t-p} X_{t-p} + Z_t, \quad (5.1)$$

where Z_t is a purely random process with zero mean i.e. $E(Z_t) = 0$, and variance σ_Z^2 . The parameters $\alpha_1, \dots, \alpha_p$ are called the *AR coefficients*.

Yule-Walker equation

For the general case $AR(p)$, we can multiply (5.1) by X_{t-k} and take the expectation value to produce the *Yule-Walker equation* as

$$\gamma(-k) = \alpha_1 \gamma(-k+1) + \dots + \alpha_p \gamma(-k+p), \quad \forall k \quad (5.2)$$

where $\gamma(k)$ is the autocovariance function at lag k , that $\gamma(k) = Cov(X_t, X_{t+k})$, and $Cov(X, Y) = E((X - \mu_x)(Y - \mu_y)^*)$.

From the autocovariance definition, $\gamma(-k) = \gamma(k)$. Thus, if the random process is considered an ergodic, then a one can replace $\gamma(k)$ by the estimates in (5. 2). The estimated $\gamma(k)$ is calculated as

$$\hat{\gamma}(k) = \frac{1}{N} \sum_{t=1}^{N-k} (x_t - \bar{x})(x_{t+k} - \bar{x}), \quad (5. 3)$$

where $\bar{x} = \frac{1}{N} \sum_{t=1}^N x_t$. By substituting (5. 3) into (5. 2), the estimates of AR coefficients $\hat{\alpha}_1, \dots, \hat{\alpha}_p$ can be solved, such that, multiply (5. 1) with X_t

$$X_t^2 = \alpha_1 X_{t-1} X_t + \dots + \alpha_p X_{t-p} X_t + Z_t X_t, \quad (5. 4)$$

then take the expectation value

$$\sigma_x^2 = \gamma(0) = \alpha_1 \gamma(1) + \dots + \alpha_p \gamma(p) + \sigma_z^2, \quad (5. 5)$$

and therefore $\hat{\sigma}_z^2$ can be obtained by replacing α_k and $\gamma(k)$ with the estimates of $\hat{\alpha}_k$ and $\hat{\gamma}(k)$, and vice versa.

AR Spectrum

Wiener-Khintchine theorem: For any stationary stochastic process with an autocovariance function $\gamma(k)$, there exists a function $p(f)$ such that,

$$\gamma(k) = \int e^{2\pi i k f} p(f) df. \quad (5. 6)$$

The function $p(f)$ is the *spectral density function*, or simply the *spectrum*. The quantity $p(f)df$ represents the contribution to variance of components within frequencies in the range $(f, f + df)$. Furthermore, the inverse of the relation is

$$p(f) = \sum_{k=-\infty}^{\infty} \gamma(k) e^{-j2\pi k f} = \gamma(0) + 2 \sum_{k=1}^{\infty} \gamma(k) \cos(2\pi k f) \quad (5. 7)$$

For AR(1), the spectrum is

$$p(f) = \frac{\sigma_z^2}{|1 - \alpha e^{-2\pi j f}|^2} = \frac{\sigma_z^2}{1 - 2\alpha \cos(2\pi f) + \alpha^2} \quad (5.8)$$

For the general case AR(p) the spectrum is

$$p(f) = \frac{\sigma_z^2}{|1 - \alpha e^{-2\pi j f} - \dots - \alpha e^{-2\pi j p f}|^2} \quad (5.9)$$

5.2.2 Autoregressive Modeling of Rayleigh Fading Channels:

From the previous chapter we have the observed equation of the decorrelator filter based receiver as

$$y_m(n) = \mathbf{w}_1^T \mathbf{x}_m(n) = \sqrt{E_{b_1}} b_1(n) h_m(n) + \xi_m(n). \quad (5.10)$$

The stochastic characteristics of the m^{th} carrier fading process $h_m(n)$ mainly depend on the maximum Doppler frequency

$$f_d = v f_c / c, \quad (5.11)$$

where v is the mobile speed, f_c is the central carrier frequency and c is the light speed.

According to [65], the theoretical normalized Power Spectral Density (PSD) associated with either the in-phase or quadrature portion of the fading process $h_m(n)$ is band-limited and U-shaped. Moreover, it exhibits two peaks at $\pm f_d$ as follows:

$$\Psi_{hh}(f) = \begin{cases} \frac{1}{\pi f_d \sqrt{1 - (f/f_d)^2}}, & |f| \leq f_d \\ 0, & \text{else where} \end{cases}. \quad (5.12)$$

Thus, the corresponding normalized discrete-time Autocorrelation Function (ACF) satisfies

$$R_{hh}(n) = J_0(2\pi f_d T_b |n|), \quad (5.13)$$

where $J_0(\cdot)$ is the zero-order Bessel function of the first kind and $f_d T_b$ denotes the Doppler rate.

In reality, exact AR model is impossible for fitting the Jakes one. However, we may get a sophisticated AR model replicate the previous PSD, and ACF by raising AR model order up to p^{th} order, which we have to find as a best-fit. Since a p^{th} order AR process, denoted by

AR(p), may exhibit up to p peaks in the frequency domain, the fading process along the m^{th} carrier can be modeled as

$$h_m(n) = -\sum_{i=1}^p a_i h_m(n-i) + u_m(n), \quad (5.14)$$

where $\{a_i\}_{i=1,\dots,p}$ are the AR model parameters and $u_m(n)$ denotes the zero-mean complex white Gaussian driving process with equal variances σ_u^2 along all carriers.

Although it has a rational power spectral density

$$\psi_{hh}(f) = \frac{\sigma_u^2}{\left|1 + \sum_{i=1}^p a_i e^{-j2\pi fi}\right|^2}, \quad (5.15)$$

it can closely approximate to the U-shape jakes one. Indeed, the relationship between the AR parameters and the Jakes model ACF $R_{hh}(n)$ can be held from (5.14), by multiplying both sides with $h_m(n)$ as:

$$R_{hh}(n) = \begin{cases} -\sum_{i=1}^p a_i R_{hh}(n-i), & n \geq 1 \\ -\sum_{i=1}^p a_i R_{hh}(-i) + \sigma_u^2, & n = 0 \end{cases}. \quad (5.16)$$

Equation (5.16) can be represented in a matrix form for $n = 1, \dots, p$ as follows:

$$\underbrace{\begin{bmatrix} R_{hh}(0) & R_{hh}(-1) & \cdots & R_{hh}(-p+1) \\ R_{hh}(1) & R_{hh}(0) & \cdots & R_{hh}(-p+2) \\ \vdots & \vdots & \ddots & \vdots \\ R_{hh}(p-1) & R_{hh}(p-2) & \cdots & R_{hh}(0) \end{bmatrix}}_{\mathbf{R}_{hh}} \underbrace{\begin{bmatrix} a_1 \\ a_2 \\ \vdots \\ a_p \end{bmatrix}}_{\mathbf{a}} = - \underbrace{\begin{bmatrix} R_{hh}(1) \\ R_{hh}(2) \\ \vdots \\ R_{hh}(p) \end{bmatrix}}_{\mathbf{v}}. \quad (5.17)$$

In addition, the variance of the driving process can be expressed as

$$\sigma_u^2 = R_{hh}(0) + \sum_{i=1}^p a_i R_{hh}(-i) \quad (5.18)$$

Given $R_{hh}(n)$ in (5.13), the AR parameters can be determined by solving the set of p YWE in (5.17). Since \mathbf{R}_{hh} is an autocorrelation matrix, which is positive semi-definite, nonsingular for all except of purely harmonic lower p order or fewer sinusoids. Hence, its

inverse exists and a unique solution for AR parameters can be calculated by $\mathbf{a} = -\mathbf{R}_{hh}^{-1}\mathbf{v}$. Unfortunately, due to the band-limited nature of the Doppler fading processes, \mathbf{R}_{hh} will become nearly singular when the driving process variance σ_u^2 gets very small which is the case when increasing the AR model order. Indeed, the YWE will suffer from ill-conditioning starting from very small AR model orders. For this reason and for simplicity purposes, previous studies (e.g., [70], [72-74]) have focused only on low order AR models. These ill conditions can be measured by [82, p.354]

$$|R_{hh}| = \prod_{i=0}^{p-1} \sigma_i^2, \quad (5.19)$$

where $|R_{hh}|$ is the determinant of R_{hh} , and σ_i^2 is the driving noise variance to an AR(i), while the values of σ_i^2 is very small the R_{hh} is nearly singular i.e., its determinant approaches to zero, and significant errors in determining AR parameters can't be avoided. Deeply, the stability and accuracy of AR models of bandlimited processes are suffering as σ_i^2 is smaller. A lower bound on MMSE is known from prediction theory to be given by the infinite prediction memory case, in which case the asymptotic σ_i^2 can be expressed via kolmogoroff-Szego formula [83, p.491]

$$\lim_{p \rightarrow -\infty} \sigma_p^2 = \exp \left[\frac{1}{2\pi} \int_{-\pi}^{\pi} \ln \psi_{hh}(e^{j\omega}) d\omega \right], \quad (5.20)$$

where $\omega = 2\pi f$ and $\psi_{hh}(j\omega) = \sum_{i=-\infty}^{\infty} R_{hh}(i) e^{-ji\omega}$ the desired power spectrum of the process.

A more important consideration of stability investigation for the fast σ_p^2 converges to its zero asymptotic value by [84], where a study of the behavior of linear prediction errors as the predictor order increases was performed. The MMSE of one-step-ahead linear prediction was observed to decrease *exponentially* to zero with increasing model order for many processes with bandlimited spectra. However, from their study, lower order models result in a poor match to the desired bandlimited ACF.

From the preceding discussion, solving YWE it doesn't seem possible to be estimated in stable AR parameters of large orders accurately, with using finite word length computations' AR models. To solve the ill-conditioning problem, Baddour *et al.* [75] have suggested a simple heuristic approach to improve the conditioning of \mathbf{R}_{hh} by adding a very small positive bias ε to its main diagonal. This means that the fading process is modeled by an AR process disturbed by an additive white noise. Thus, the first $p+1$ autocorrelation lags of the resulting AR(p) process will satisfy:

$$\hat{R}_{hh}(n) = \begin{cases} R_{hh}(0) + \varepsilon, & n = 0 \\ R_{hh}(n), & n = 1, 2, \dots, p \end{cases} \quad (5.21)$$

with the lower bound

$$\lim_{p \rightarrow -\infty} \sigma_p^2 = \exp \left\{ \frac{1}{2\pi} \int_{-\pi}^{\pi} \ln [\psi_{hh}(e^{j\omega}) + \varepsilon] d\omega \right\} > 0. \quad (5.22)$$

This scenario is obvious when we illustrate the driving process variances of AR model orders with different Doppler rates as in Fig. 5-2.

It was demonstrated in [75] that the value of the added bias ε that results in the most accurate AR parameters computation depends mainly on the Doppler rate $f_d T_b$. Two methods were proposed by [75] for achieving a stationary driving process based on a time varying IIR filters. For the purpose of minimizing *Quantitative Measures* [85], they present a typical values of ε , which represents a tradeoff between the improved condition number of \mathbf{R}_{hh} and the bias introduced in the model, are given in TABLE 5-1.

As the ill-conditioning problem can be solved by the above approach, dealing with high order AR models will become possible.

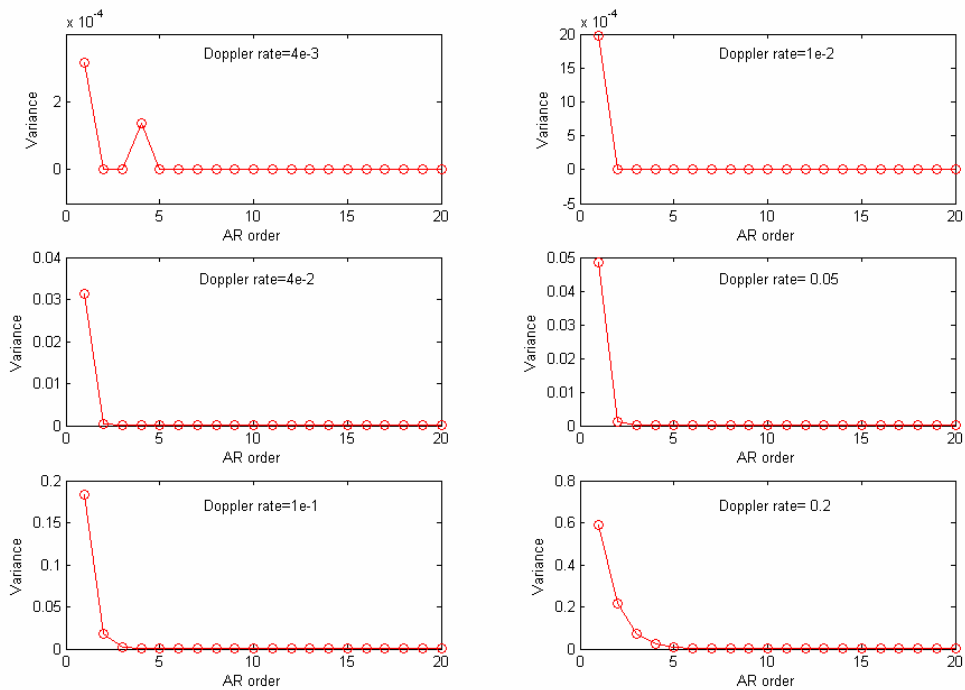


Figure 5-2: Driving process variance versus the model order with different Doppler rate scenarios.

TABLE 5-1: TYPICAL VALUES OF THE ADDED BIAS \mathcal{E} FOR DIFFERENT DOPPLER RATES.

Doppler rate $f_d T_b$	Added bias \mathcal{E}
0.001	10^{-5}
0.005	10^{-6}
0.01	10^{-7}
0.05	10^{-8}
0.1	10^{-9}
0.2	10^{-9}

Low AR model orders fitting Jakes model

Consider Fig. 5-3, where the first, and second orders AR model ACF fitting the Bessel Jakes one, as can be seen each of the first and second orders, doesn't fit well the Bessel ACF. Although the second AR model order has a better approximation to the Jakes ACF, but it stills far from the fitting.

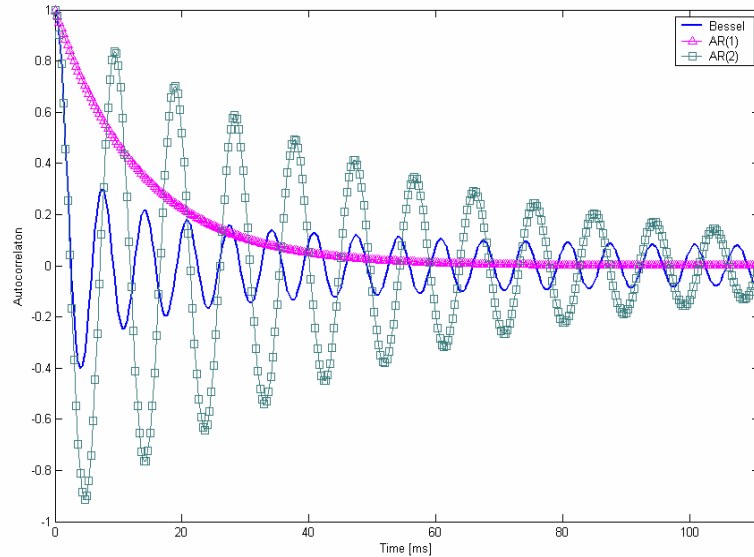


Figure 5-3: Autocorrelation function of the Jakes model and that of the fitted AR (p) process with $p=1, 2$, $f_d = 150\text{ Hz}$ and $f_d T_b = 0.05$.

Furthermore, Fig. 5-4 represents small AR model orders- first and second- PSD fitting the U-shape of the Jakes one, which confirms the low orders could not approximate well the Raleigh fading channels.

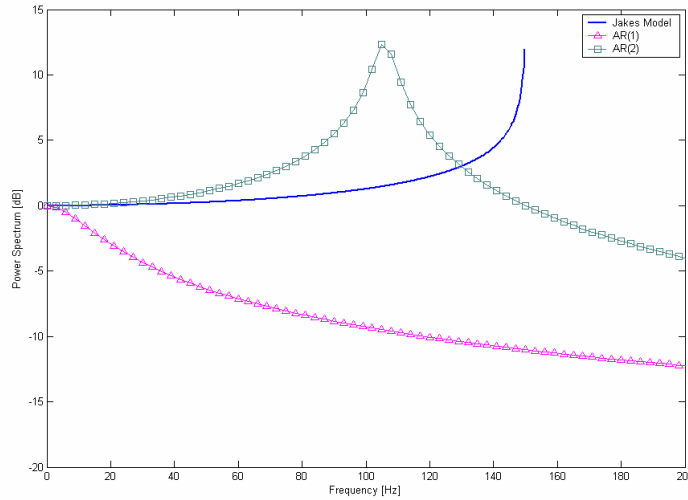


Figure 5-4: Power spectral density of the Jakes model and that of the fitted AR(p) process with $p=1, 2$, $f_d = 150\text{Hz}$ and $f_d T_b = 0.05$.

High order AR model fitting Jakes model

Consider Fig. 5-5 which shows high AR model orders ACF fitting the Bessel of 50, 100, and 200 AR model orders. As can be noticed, increasing an AR model order more and more a better approximation to the Jakes ACF. This is also could be seen from the Jakes U-shape fitted by high orders AR models PSD of the corresponding ACF orders in the Fig. 5-5. Thus, increasing the AR model order will lead to a better fit between the statistics of the resulting AR process and the realistic Jakes channel.

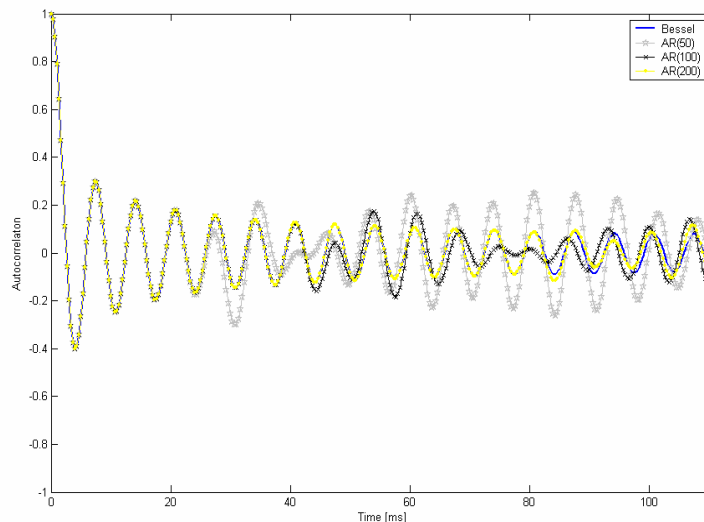


Figure 5-5: Autocorrelation function of the Jakes model and that of the fitted AR (p) process with $p=50, 100$, and 200 , $f_d = 150\text{Hz}$ and $f_d T_b = 0.05$.

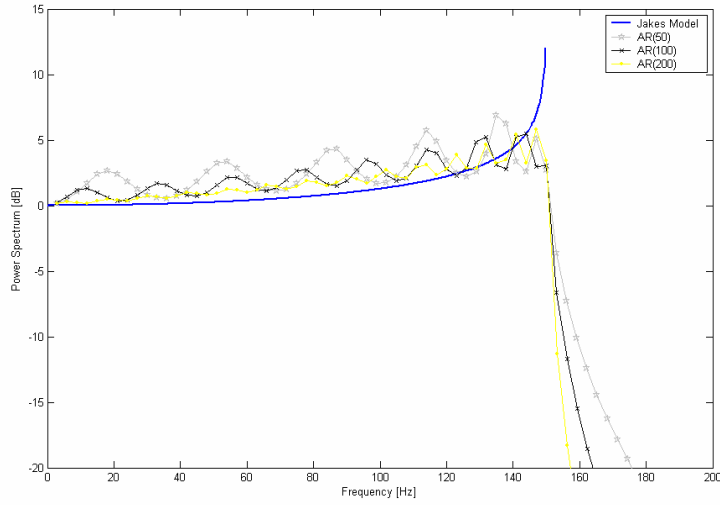


Figure 5-6: Power spectral density of the Jakes model and that of the fitted AR(p) process with $p=50$, 100 and 200. $f_d = 150\text{Hz}$ and $f_d T_b = 0.05$.

For the purpose of our AR model orders studying, consider Fig. 5-7 and Fig. 5-8, where we, respectively, present the ACF and the PSD of the Jakes model fitted by AR process one, whose order is 1, 2, 5, 20, and 100, a one may conclude to use higher AR model orders.

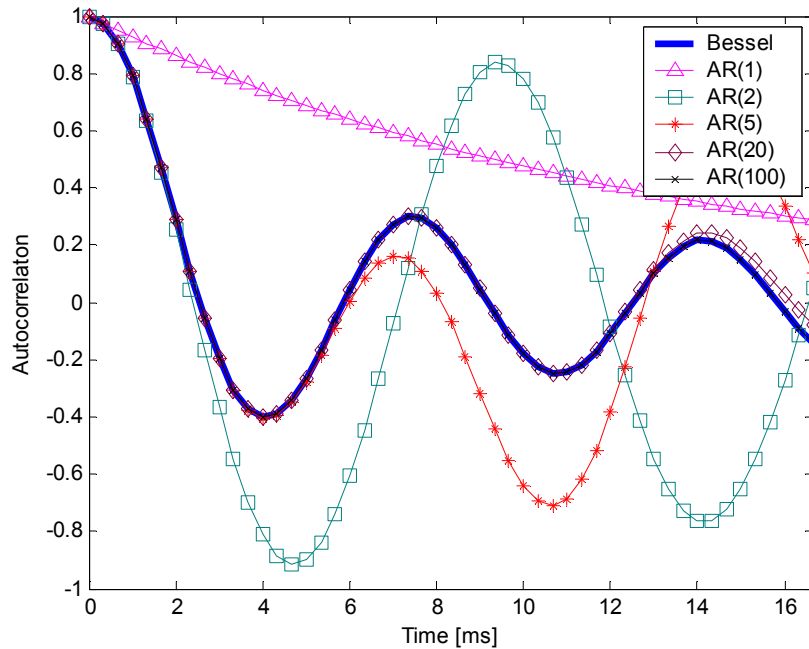


Figure 5-7: Autocorrelation function of the Jakes model and that of the fitted AR (p) process with $p=1$, 2, 5, 20, and 100. $f_d = 150\text{Hz}$ and $f_d T_b = 0.05$.

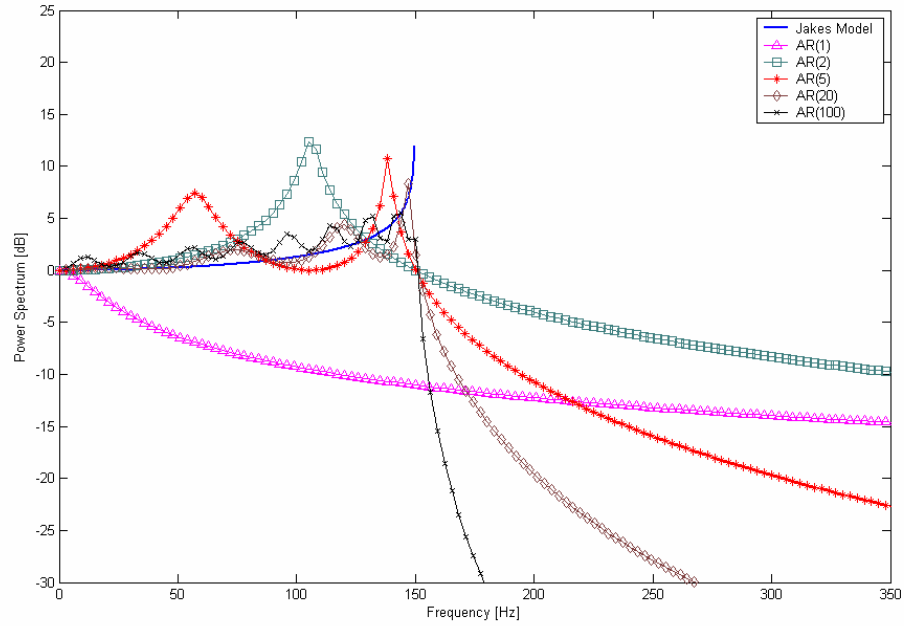


Figure 5-8: Power spectral density of the Jakes model and that of the fitted AR(p) process with p=1, 2, 5, 20 and 100. $f_d = 150\text{Hz}$ and $f_d T_b = 0.05$.

However, the higher the AR model order, the higher the computational cost. Indeed, the complexity is of $O(p^3)$ as will be seen later, this also could be noticed in Fig. 5-9, where a typical experiments using time tracking simulation is roughly established in the unity simulated time diagram on Pentium IV processor, which shows more increasing computational costs as AR model orders raising. Thus, a compromise has to be found.

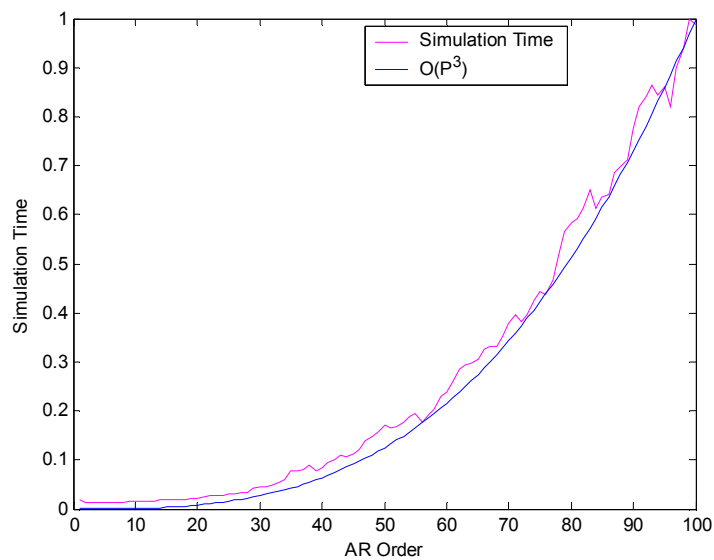


Figure 5-9: Simulation time with AR model.

Moreover, TABLE 5-2 shows a typical AR(5) parameters of a fading channel with $f_c = 1800\text{MHz}$, $T_b = 100\mu\text{s}$ and various mobile speeds, as can be seen the AR(5) parameters are associated to Doppler rates (mobile speed for particular carrier frequency, and symbol rate).

TABLE 5-2: THE FADING PROCESS AR(5) PARAMETERS FOR $f_c = 1800\text{MHz}$, $T_b = 100\mu\text{s}$ AND VARIOUS MOBILE VELOCITIES.

Mobile velocity (Km/hr)	15	30	45	60	75	90
Doppler frequency f_d (Hz)	25	50	75	100	125	150
Doppler rate $f_d T_s$	0.0025	0.005	0.0075	0.01	0.0125	0.015
a_1	-0.79761	-1.0978	-1.4814	-1.7923	-1.8278	-1.9012
a_2	-0.49616	-0.35024	-0.15788	0.013402	0.075537	0.22188
a_3	-0.19728	0.09892	0.48294	0.78391	0.79141	0.79326
a_4	0.09896	0.24934	0.44077	0.56975	0.5147	0.3698
a_5	0.39252	0.10103	-0.28319	-0.57463	-0.55372	-0.48371
σ_p^2	2.1016e-005	3.1434e-006	4.4858e-006	5.6578e-007	6.1036e-007	7.1219e-007

5.3 Kalman Filtering

An adaptive filter is a filter containing coefficients that are updated by some type of adaptive algorithm to improve or somehow optimize the filter's response to a desired performance criterion [86]. Hence, a number of recent research interest in the adaptive algorithms, i.e., [87] offer a complexity study of Normalized Least Mean Square (NLMS), and Block Recursive Least Mean Square (BRLS). While in [88] a studying of a generalization NLMS algorithm is investigated. In addition, a convergence studying of Affine Projection Algorithms (APA) is considered in [89]. Also, a deep working of a variable step size NLMS and APA is studied in [90]. Furthermore, [91] introduce a compromising of complexity and performance of modern adaptive receivers. In general, adaptive filters consist of two basic parts: the filter which applies the required processing on the incoming signal which is to be filtered, and an adaptive algorithm, which adjusts the coefficients of that filter to somehow improve its performance. One of famous adaptive filters is known as a Kalman filter that estimates the states of a stochastic system.

5.3.1 Kalman Filter Background:

Consider system and measurement vector models, which are known collectively as the state space models:

$$\mathbf{x}(k) = \mathbf{A}\mathbf{x}(k-1) + \mathbf{W}(k-1) \quad (5.23)$$

$$\mathbf{y}(k) = \mathbf{C}\mathbf{x}(k-1) + \mathbf{V}(k) \quad (5.24)$$

where \mathbf{A} denotes the state transition matrix, which relates the various states of the system model at different times to each other, while $\mathbf{W}(k)$, and $\mathbf{V}(k)$ represent the system noise matrix and measurement noise matrix, respectively. The Kalman recursive algorithm is summarized in the equations listed in TABLE 5-3, where $\mathbf{R}(k)$, $\mathbf{Q}(k)$ represent the measurement noise covariance matrix and the system noise covariance matrix, respectively that are defined as:

$$\mathbf{R}(k) = E[\mathbf{V}(k)\mathbf{V}^{*T}], \quad (5.25)$$

$$\mathbf{Q}(k) = E[\mathbf{W}(k)\mathbf{W}^{*T}], \quad (5.26)$$

where bold face letter denotes a matrix. The superscripts \mathbf{T} , -1 , and $*$ represent the transpose, the inverse, and the conjugate of a matrix, respectively.

TABLE 5-3: MULTI-DIMENSIONAL KALMAN RECURSIVE EQUATIONS.

Recursive estimator:	$\hat{\mathbf{x}}(k) = \mathbf{A}\hat{\mathbf{x}}(k-1) + \mathbf{K}(k)[\mathbf{y}(k) - \mathbf{C}\mathbf{A}\hat{\mathbf{x}}(k-1)]$
Estimator gain:	$\mathbf{K}(k) = \mathbf{P}\mathbf{C}^H(k, k-1)[\mathbf{R}(k) + \mathbf{C}\mathbf{P}(k, k-1)\mathbf{C}^H]^{-1}$ where $\mathbf{P}(k, k-1) = \mathbf{A}\mathbf{P}(k-1)\mathbf{A}^H + \mathbf{Q}(k-1)$
Error covariance matrix:	$\mathbf{P}(k) = \mathbf{P}(k, k-1) - \mathbf{K}(k)\mathbf{C}\mathbf{P}(k, k-1)$

Furthermore, the variables descriptions, and their dimensions are presented in TABLE 5-4, where M represents the number of measured samples in the observed vector $\mathbf{y}(k)$, N denotes to the number of estimated samples in the vector $\hat{\mathbf{x}}(k)$. Physically, the dimensions M and N represented the number of measurement signals used to generate the mean square error and the number of parameters to be estimated, respectively.

TABLE 5-4: SUMMARY OF THE KALMAN VECTOR AND MATRIX VARIABLES.

DESCRIPTION	VARIABLE	MATRIX DIMENSION (<i>Row</i> \times <i>Column</i>)
Measurement Vector	$\mathbf{y}(k)$	$M \times 1$
Estimated Parameter Vector	$\hat{\mathbf{x}}(k)$	$N \times 1$
State Transition Matrix	\mathbf{A}	$N \times N$
Kalman Gain Matrix	$\mathbf{K}(k)$	$N \times M$
Measurement Matrix	\mathbf{C}	$M \times N$
Predicted State Error Covariance Matrix	$\mathbf{P}(k, k-1)$	$N \times N$
Measurement Noise Covariance Matrix	$\mathbf{R}(k)$	$M \times M$
System Noise Covariance Matrix	$\mathbf{Q}(k)$	$N \times N$
State Error Covariance Matrix	$\mathbf{P}(k)$	$N \times N$

Kalman Complexity

The complexity or the number of operations required by the KF algorithm is summarized in TABLE 5-5, where the number of complex operations for each of the KF equations is calculated by considering, the multiplication of two complex matrices of size $M \times N$ and $N \times P$ requires an MNP complex operations for each of additions and multiplications, furthermore, the addition of two $M \times N$ complex matrices requires MN additions [92].

TABLE 5-5: COMPLEXITY CALCULATION OF THE KALMAN ALGORITHM PER ITERATION BASED ON THE KALMAN RECURSIVE EQUATIONS LISTED IN TABLE 5-3.

Kalman Recursive Operations from Table	Addition/ Subtraction	Multiplication
Kalman recursive estimator:		
$\mathbf{A}\hat{\mathbf{x}}(k-1)$	N^2	N^2
$\mathbf{C}\mathbf{A}\hat{\mathbf{x}}(k-1)$	MN	MN
$[\mathbf{y}(k) - \mathbf{C}\mathbf{A}\hat{\mathbf{x}}(k-1)]$	M	–
$\mathbf{K}(k)[\mathbf{y}(k) - \mathbf{C}\mathbf{A}\hat{\mathbf{x}}(k-1)]$	MN	MN
$\mathbf{A}\hat{\mathbf{x}}(k-1) + \mathbf{K}(k)[\mathbf{y}(k) - \mathbf{C}\mathbf{A}\hat{\mathbf{x}}(k-1)]$	N	–
Kalman gain:		
$\mathbf{P}(k, k-1)\mathbf{C}^H$	MN^2	MN^2
$\mathbf{C}\mathbf{P}(k, k-1)\mathbf{C}^H$	NM^2	NM^2
$\mathbf{R}(k) + \mathbf{C}\mathbf{P}(k, k-1)\mathbf{C}^H$	M^2	–
$[\mathbf{R}(k) + \mathbf{C}\mathbf{P}(k, k-1)\mathbf{C}^H]^{-1}$	M^3	M^3
$\mathbf{P}(k, k-1)\mathbf{C}^H [\mathbf{R}(k) + \mathbf{C}\mathbf{P}(k, k-1)\mathbf{C}^H]^{-1}$	M^2N	M^2N
Predictor state error matrix:		
$\mathbf{P}(k-1)\mathbf{A}^H$	N^3	N^3
$\mathbf{A}\mathbf{P}(k-1)\mathbf{A}^H$	N^3	N^3
$\mathbf{A}\mathbf{P}(k-1)\mathbf{A}^H + \mathbf{Q}(k-1)$	N^2	–
State Error Matrix:		
$\mathbf{C}\mathbf{P}(k, k-1)$	MN^2	MN^2
$\mathbf{K}(k)\mathbf{C}\mathbf{P}(k, k-1)$	MN^2	MN^2
$\mathbf{P}(k, k-1) - \mathbf{K}(k)\mathbf{C}\mathbf{P}(k, k-1)$	N^2	–
Total complexity	$2N^3 + N^2(3M+3) + N(2M^2+2M+1) + M^3 + M^2 + M$	$2N^3 + N^2(1+3M) + N(2M^2+2M) + M^3$

The complexity here is calculated by assigning $M = 1$, which implied that the mean square error is calculated on a symbol by symbol basis. Consequently, based on the last line of the total complexity of the Kalman algorithm per iteration can be written as:

- Number of complex additions or subtractions = $2N^3 + 6N^2 + 5N + 3$
- Number of complex multiplications or divisions = $2N^3 + 4N^2 + 4N + 1$

Calculating the complexity has been assumed that the inversion of the unit matrix $[\mathbf{R}(k) + \mathbf{C}\mathbf{P}(k, k-1)\mathbf{C}^H]^{-1}$ is the same complexity of the Gauss-Jordan elimination process [93], namely M^3 complex additions and M^3 complex multiplications.

Figure 5-9 clarifies the Kalman recursive algorithm idea, where the Kalman gain, update estimates, and covariance, are in the TABLE 5-3, in addition, the project stage for the next coming iteration as obvious in the figure.

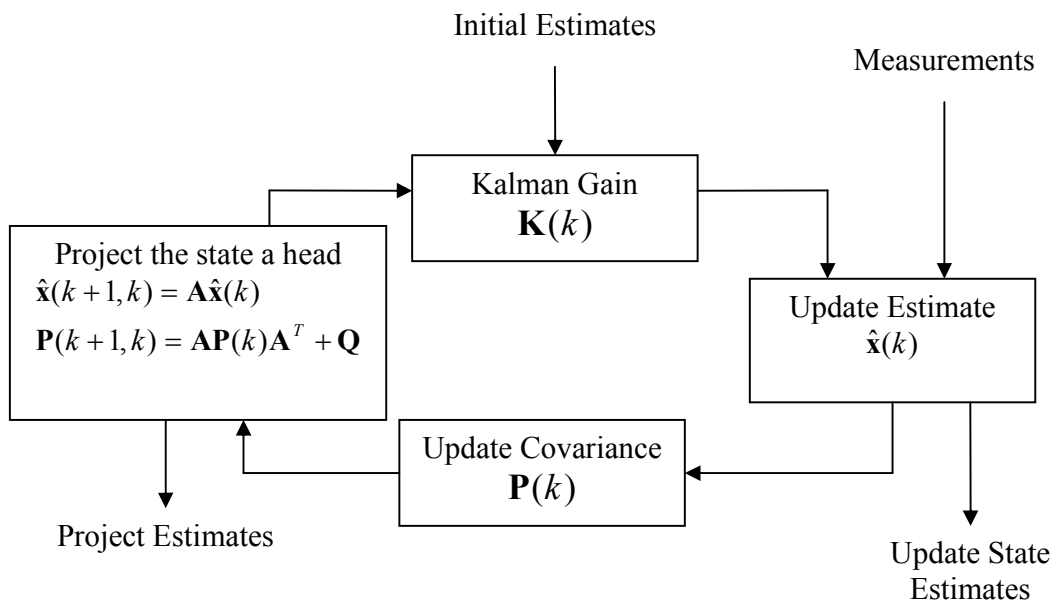


Figure 5-10: Recursive Kalman algorithm.

5.3.2 Kalman Filtering Based Channel Estimation:

Since our purpose is to estimate the m^{th} carrier fading sequence $h_m(n)$ modeled by a p^{th} order AR process as in (5. 14), the $p \times 1$ state vector is defined as follows:

$$\mathbf{h}(n) = [h(n) \quad h(n-1) \quad \cdots \quad h(n-p+1)]^T. \quad (5. 27)$$

Here we will drop the carrier subscript, for the sake of simplicity and clarity of presentation,. Thus, the resulting state space representation of the m^{th} carrier fading channel (4. 10) and (5. 14) is given by:

$$\mathbf{h}(n+1) = \mathbf{\Phi}\mathbf{h}(n) + \mathbf{g}u(n), \quad (5. 28)$$

$$y(n) = \mathbf{b}^T(n)\mathbf{h}(n) + \xi(n), \quad (5. 29)$$

where the state transition matrix Φ , the input vector \mathbf{g} and the observation vector $\mathbf{b}(n)$ are respectively defined as follows:

$$\Phi = \begin{bmatrix} -a_1 & -a_2 & \cdots & -a_p \\ 1 & 0 & \cdots & 0 \\ & \ddots & & \vdots \\ 0 & \cdots & 1 & 0 \end{bmatrix}, \quad (5.30)$$

$$\mathbf{g} = [1 \ 0 \ \cdots \ 0]^T, \text{ and } \mathbf{b}(n) = \sqrt{E_{b_1}} b_1(n) [1 \ 0 \ \cdots \ 0]^T$$

Given the above state space representation of the system, Kalman filtering can be carried out to provide the estimation $\hat{\mathbf{h}}(n+1/n)$ of the state vector $\mathbf{h}(n+1)$ given the set of observations $\{y(i)\}_{i=1, \dots, n}$ as listed below:

The so-called innovation process $\alpha(n)$ is first obtained:

$$\alpha(n) = y(n) - \mathbf{b}^T(n) \hat{\mathbf{h}}(n/n-1). \quad (5.31)$$

Its variance is then defined:

$$C(n) = E[\alpha(n)\alpha^*(n)] = \mathbf{b}^T(n) \mathbf{P}(n/n-1) \mathbf{b}(n) + \sigma_{\xi}^2, \quad (5.32)$$

where $\mathbf{P}(n/n-1)$ denotes the so-called error covariance matrix.

The Kalman gain is calculated in the following manner:

$$\mathbf{K}(n) = \Phi \mathbf{P}(n/n-1) \mathbf{b}(n) C^{-1}(n). \quad (5.33)$$

The estimation of the state vector $\hat{\mathbf{h}}(n+1/n)$ and the fading process $\hat{h}(n+1/n)$ are respectively given by:

$$\hat{\mathbf{h}}(n+1/n) = \Phi \hat{\mathbf{h}}(n/n-1) + \mathbf{K}(n) \alpha(n), \quad (5.34)$$

$$\hat{h}(n+1/n) = \mathbf{g}^T \hat{\mathbf{h}}(n+1/n), \quad (5.35)$$

The error covariance matrix is updated as follows:

$$\mathbf{P}(n/n) = \mathbf{P}(n/n-1) - \mathbf{P}(n/n-1) \mathbf{b}(n) C^{-1}(n) \mathbf{b}^T(n) \mathbf{P}(n/n-1), \quad (5.36)$$

and

$$\mathbf{P}(n+1/n) = \Phi \mathbf{P}(n/n) \Phi^H + \mathbf{g} \sigma_u^2 \mathbf{g}^T, \quad (5.37)$$

Finally, we apply the MRC to retrieve the data sequence as the following manner:

$$\hat{b}_1(n) = \text{sgn}\left(\text{Re}\left[\sum_{m=1}^M \hat{h}_m^*(n)y_m(n)\right]\right) \quad (5.38)$$

It should be noted that, the state vector and the error covariance matrix are initially assigned to zero vector identity matrix respectively, i.e. $\hat{\mathbf{h}}(0/-1)=\mathbf{0}$ and $\mathbf{P}(0/-1)=\mathbf{I}_p$. The above Kalman filtering algorithm requires a training period during which $b_1(n)$ is known at the receiver to adjust to the channel. Once in the so-called decision-directed mode, the detected symbol $\hat{b}_1(n)$ defined in (5.38) will be used instead [46]. Figure 5-11 shows the observed received signals from the decorrelator proceed via the feedback Kalman channel estimator, followed by the MRC.

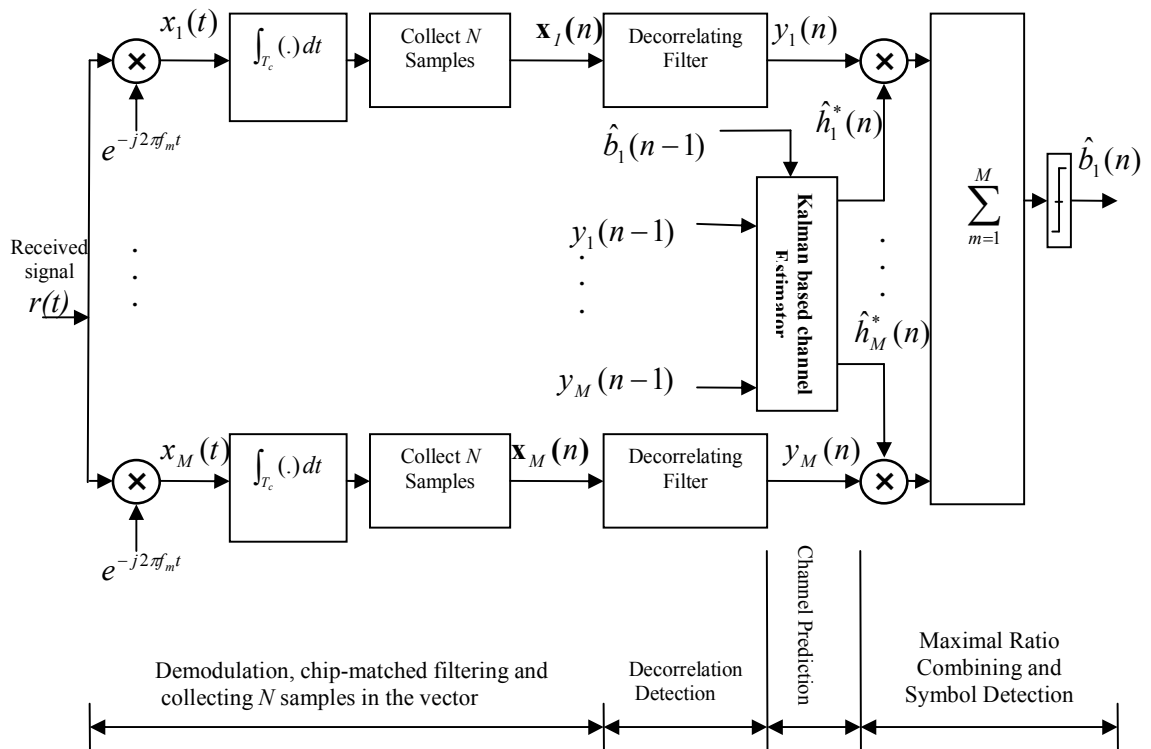


Figure 5-11: Kalman filtering channel estimator.

5.4 LMS Channel Estimator

Figure 5-12 shows the illustrated LMS channel estimator feedback to detect observed signals from the decorrelator. Given the available observation $y_m(n)$ from the decorrelator,

and the unit energy training sequence $b_1(n)$ (i.e., $E_{b_1} = 1$), the LMS filter can be carried out to adaptively estimate the fading process over the m^{th} carrier $h_m(n)$ by minimizing the Mean Square Error (MSE) criteria $E[|y_m(n) - b_1(n)h_m(n)|^2]$, as follows:

$$\hat{h}_m(n+1) = \hat{h}_m(n) + \mu[y_m(n) - b_1(n)\hat{h}_m(n)]b_1^*(n) \quad (5.39)$$

where $\mu > 0$ is the step size.

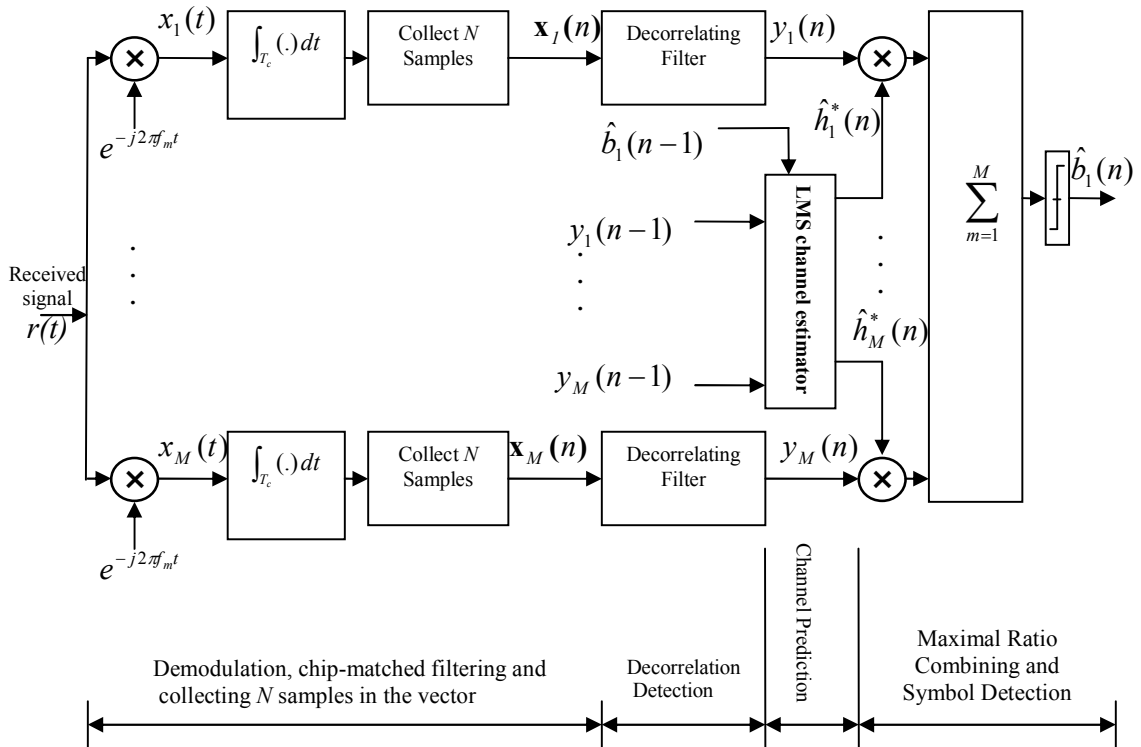


Figure 5-12: LMS filter channel estimator.

Applying the Maximum ratio combining we determine the data symbol for the 1st user, as

$$\hat{b}_1(n) = \text{sgn}\left(\text{Re}\left[\sum_{m=1}^M \hat{h}_m^*(n)y_m(n)\right]\right). \quad (5.40)$$

5.5 RLS Channel Estimator

The RLS channel estimator is presented in Fig. 5-13. This estimator calculates the estimates of the channel by minimizing the cost function

$$\sum_{i=0}^n \lambda^{n-i} |y_m(i) - b_1(i)h_m(i)|^2 \quad (5.41)$$

where $0 < \lambda < 1$ is the forgetting factor, and the new fading channel estimate at $n + 1$ using information available up to time n in training mode as

$$\hat{h}_m(n+1) = \hat{h}_m(n) + [y_m(n) - b_1(n)\hat{h}_m(n)]K_m^*(n), \quad (5.42)$$

where $K_m(n)$ gain is given by

$$K_m(n) = [\lambda + P_m(n)b_1^2(n)]^{-1} P_m(n)b_1(n), \quad (5.43)$$

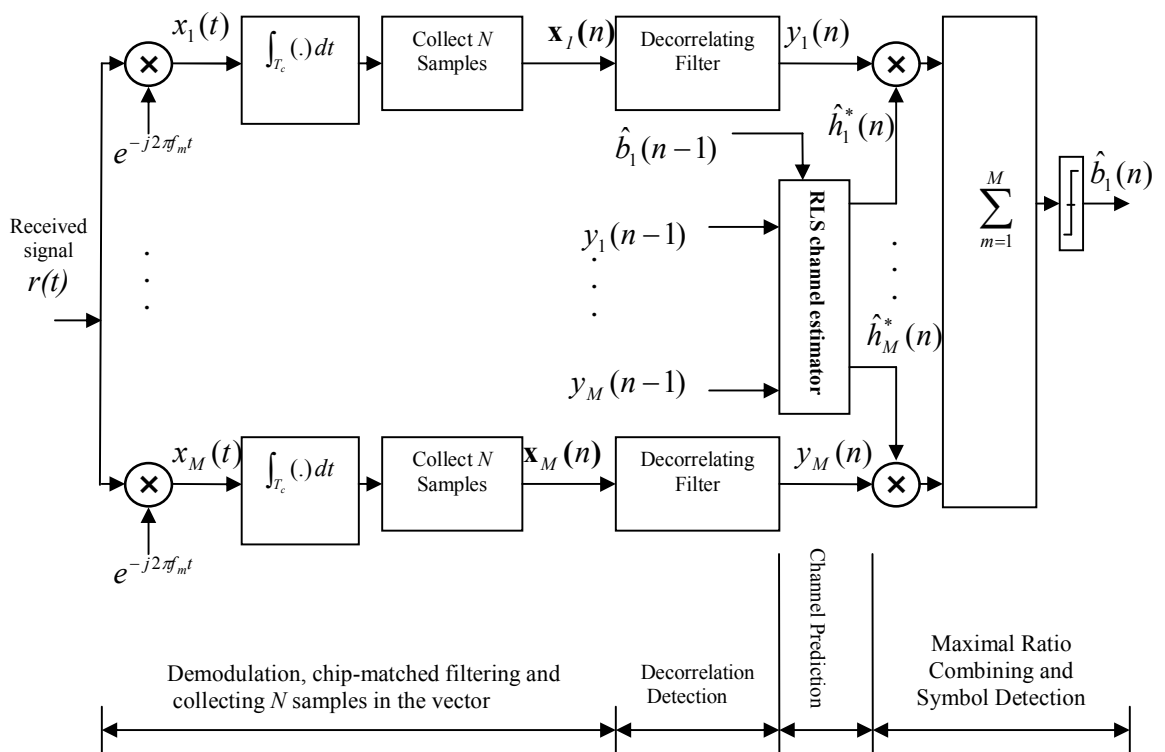


Figure 5-13: RLS filter channel estimator.

and $P_m(n)$ is updated recursively as

$$P_m(n+1) = \lambda^{-1}[1 - K_m(n)b_1^*(n)]P_m(n). \quad (5.44)$$

By using the Maximum ratio combining in order to determine the data symbol for the 1st user, we get:

$$\hat{b}_1(n) = \text{sgn}\left(\text{Re}\left[\sum_{m=1}^M \hat{h}_m^*(n)y_m(n)\right]\right). \quad (5.45)$$

It is worth here to denote that, the LMS and RLS channel estimators as in the previous equations don't need priori statistics of a Rayleigh fading channel like the Kalman channel estimator. Furthermore, the Kalman estimator is a faster convergence algorithm than the both. However, it suffers from higher computational costs [47], especially, for high order AR models.

5.6 Simulation Results

5.6.1 Simulation Protocols:

In this section, computer simulation results are provided to illustrate the Bit Error Rate (BER) performance of the MC-DS-CDMA system using Kalman channel estimator with high order AR models, under different fading rate scenarios. In addition, the performance of the Kalman estimator is compared with the standard LMS and RLS based ones. We consider a system of $K=10$ multiple-access active users, each using a gold code of length $N=31$. In addition, the fading processes $\{h_m(n)\}_{m=1,\dots,M}$ are generated according to the modified Jakes model [66] with 16 distinct oscillators. They are normalized to have a unit variance, i.e. $\sigma_h^2 = 1$. The average Signal-to-Noise Ratio (SNR) per carrier for the desired user is defined by:

$$\text{SNR} = 10 \log_{10} (E_{b_i} \sigma_h^2 / \sigma_\eta^2). \quad (5.46)$$

The bit energy of the desired user is set to $E_{b_i} = 1$ and the noise is generated according to the SNR. Moreover, the value of the added bias ε is chosen as in TABLE 5-1 for AR models whose order is larger than 4.

Furthermore, the difference of squared BER vs SNR performance to reflect accuracy is calculated in the cost function

$$\text{Cost} = \sum_{i=1}^{\text{Max}(\text{SNR})} (\text{BER}(\text{AR}) - \text{BER}(\text{Decorrelator}))^2. \quad (5.47)$$

While, the difference of the squared BER vs Doppler rate is done just by replacing summing over Doppler rate points.

5.6.2 Results And Comments:

According to Fig. 5-14, which illustrate the BER performance of the MC-DS-CDMA system versus SNR, the Kalman filter based channel estimator results in much lower BER than the LMS and RLS based ones which tend to an error floor at high SNR. Therefore, exploiting the channel statistics by using AR models in the proposed channel estimator results in significant performance improvement over the model-independent LMS and RLS based estimators. In addition, increasing the AR model order will improve the BER performance of the system with the amount of improvement decreases as the AR model order increases. Furthermore, a significant frequency diversity gain is obtained when

increasing the number of carriers from $M=1$ to $M=3$. In Fig. 5-15, the effects of different fading rates on the BER performance with the various channel estimators are illustrated. For low Doppler rates i.e., $f_d T_b < 0.01$, comparable BER performances can be noticed for the various estimators. However, for high Doppler rates i.e., $f_d T_b > 0.01$, the Kalman estimator performs much better than the others especially for high order AR models. Therefore, the Kalman estimator is appealing for high Doppler rate environments.

For the purpose of finding the most possible AR model order, consider Fig. 5-16, which illustrates roughly a measure of accuracy- normalized squared BER performance differences with respect to the known fading channels from the decorrelator- for the both SNR and Doppler rates previous scenarios, and computational costs. With assuming the largest achievable AR model order is 20, a one can assume an AR model order between 4 and 8 are acceptable, that trade-off between the accuracy for the SNR, Doppler rate scenarios, and computational costs. Figure 5-17 assumes that an AR(100) model order is the most difficult one to be obtained, a one can assume to choose AR model order between 5 and 20. Indeed, it is not easy to consider an AR(100) to be achievable.

Figure 5-18 shows the estimated envelope and phase of the fading process along the first carrier using the Kalman filter based estimator with AR(5) model, the LMS estimator and the RLS estimator. From this figure one can notice that the Kalman filter based estimator provides much better estimation than the LMS and RLS estimators. Based on and the various tests we have carried out, a 5th order AR model can provide a trade-off between the accuracy of the model and the computational complexity $O(p^3)$ of the Kalman estimation algorithm.

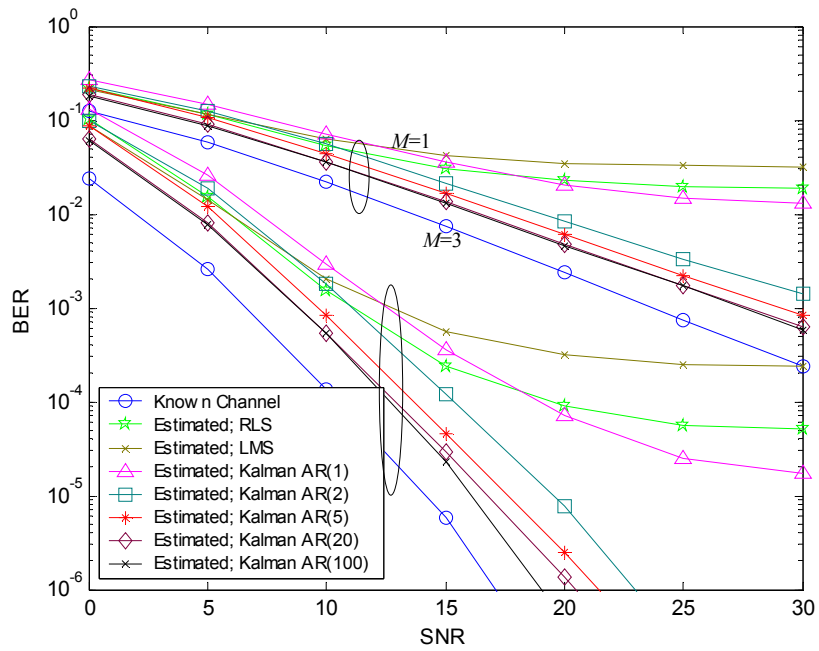


Figure 5-14: BER performance vs SNR of the MC-DS-CDMA system with the various channel estimators for number of carriers $M=1$ and $M=3$, $f_d T_b = 0.05$ [47].

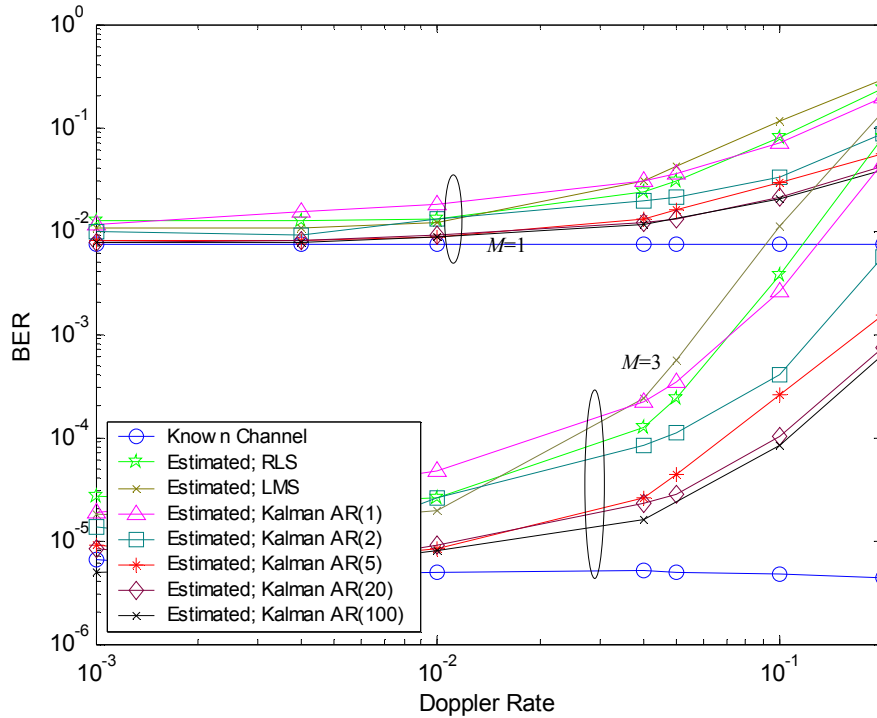


Figure 5-15: BER performance of the MC-DS-CDMA system with the various channel estimators versus the Doppler rate for number of carriers $M=1$ and $M=3$, SNR=15 dB [47].

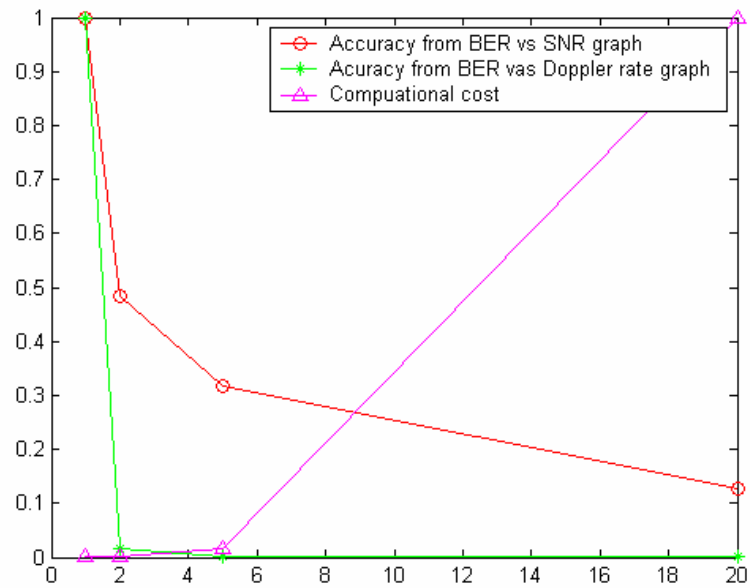


Figure 5-16: Accuracy of square (BER) vs AR model orders, max of p is 20.

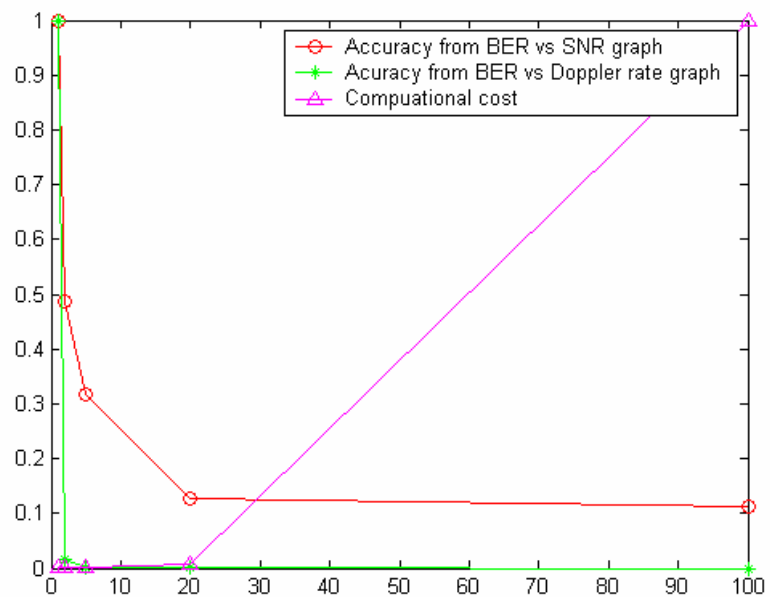


Figure 5-17: Accuracy of square (BER) vs AR model orders, max of p is 100.

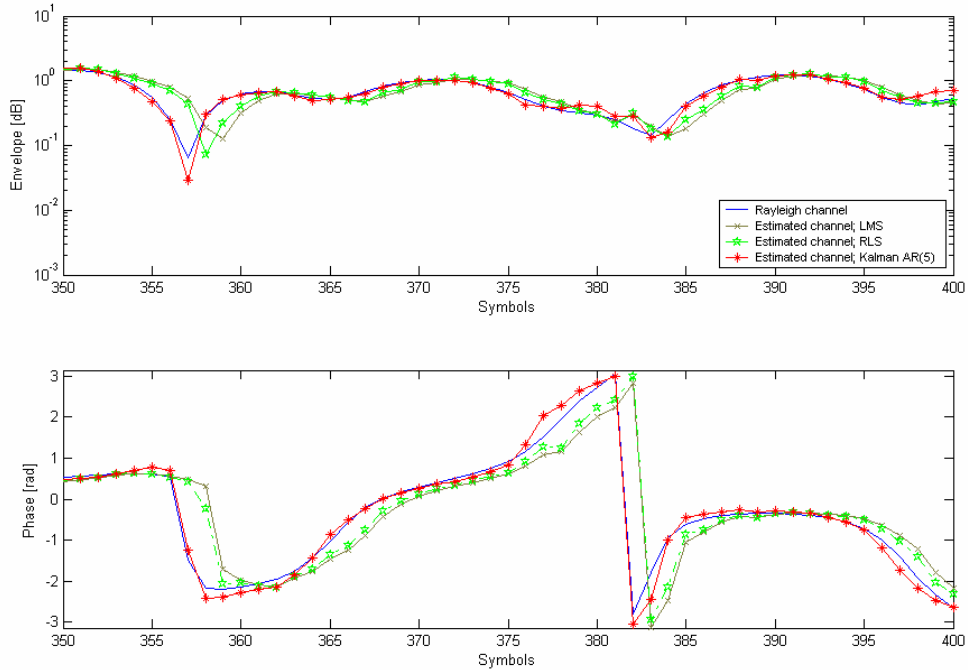


Figure 5-18: Envelope and phase of the estimated fading process along the first carrier with the various channel estimators. SNR=20 dB and $f_d T_b = 0.05$ [46].

5.7 Conclusion

The estimation of rapidly time-varying MC-DS-CDMA fading channels based on Kalman, LMS, and RLS filters is considered. In addition, the relevance of high order AR models using the Kalman filter based channel estimator is investigated. According to our simulations, Kalman filter based channel estimator is appealing to compact fading effects efficiently, especially, for high order AR models. In addition, it is much better than LMS and RLS, particularly, for high SNR, and Doppler rates. Furthermore, an AR(5) model can be recommended since it provides a trade-off between the accuracy of the model and the computational cost.

Chapter 6

Conclusions and Future Works

This thesis focuses primarily on the estimation of time-varying MC-DS-CDMA fading channels based on Kalman filtering with high order AR models. The MC-DS-CDMA mobile wireless systems combine the advantages of both multicarrier modulation and DS-CDMA. Among them, high bandwidth efficiency, high system capacity, fading resilience, and high immunity to narrow band interference can be pointed out. We consider a MC-DS-CDMA receiver structure that can serve well in rapidly time-varying fading channels, suppress the MAI, and resist the near-far problems, with optimal combining coherent detection. It consists of:

- A decorrelator multiuser detector
- A Kalman filter based channel estimator
- A maximal ratio combiner

In addition, we investigate the relevance of high order AR models in the Kalman filtering based channel estimator for compacting time-varying fading channels. Furthermore, a comparative study between the Kalman filter based channel estimator and the existing LMS and RLS channel estimators is carried out. Our conclusions are the following:

- Exploiting channel statistics by using an AR model in the Kalman filter based channel estimator provides much better BER performance than the model-independent LMS and RLS channel estimators.
- Higher AR model order in Kalman filter yields more improvement in BER performance.
- The Kalman filter based channel estimator in high SNR scenarios has much better BER performance than the LMS and RLS based ones, especially for high AR model orders.
- The LMS and RLS based estimators suffer from higher Doppler rates than Kalman channel estimator.
- An AR(5) model can provide a trade-off between the computational costs, the accuracy of the AR model and the subsequent BER.

While completing this work a number of research topics were raised for the estimation of time-varying fading channels. The following suggestion for future work can be pointed out:

- 1- Although we consider only synchronous MC-DS-CDMA systems, one can extend the proposed approach to the asynchronous MC-DS-CDMA systems.
- 2- The relevance of the Kalman filter based channel estimation with high order AR models can be investigated for other systems than MC-DS-CDMA such as OFDM and MC-CDMA.

- 3- As the estimation of fading channels based on Kalman filtering requires restrictive Gaussian assumptions about the additive noise and driving process variances, an alternative approach is to consider the relevance of H_∞ (H-infinity) filtering with high order AR models.
- 4- The Kalman filter based channel estimator uses a decision directed approach to separate channel estimation from symbol detection. As an alternative, a non-linear approach such as Particle filtering can be considered to jointly estimate the fading process and the transmitted data symbols.

References

- [1] Leff B. (Feb. 1994): "Making sense of wireless standard and system designs". Microwaves & RF, pp. 113-118.
- [2] Hanzo L. (Jul. 1998): "Bandwidth-Efficient Wireless Multimedia Communications". Proceedings of The IEEE, Vol. 86, NO. 7.
- [3] Billström O. Cederquist L., Ewerbring M., Sandegren G. and Uddenfeldt J. (Mar. 2006): "Fifty years with mobile phones From novelty to no. 1 consumer product". Ericsson Review, NO.3.
- [4] Kinoshita K., and Nakagawa M. (1996): "Japanese Cellular Standard", The Mobile Communication Handbook. J.D Gipson (ed.). Boca Raton, FL: CRC Press, pp. 449-461.
- [5] Telecommunications Industry Association (1989): "Dual-mode Subscriber Equipment-Network Equipment Compatibility Specification, Interim Standard IS-54".
- [6] Prasad R. (1996): CDMA for Wireless Personal Communications, Artech House, Inc.
- [7] Ojanpera T., and Prasad R., (eds.) (1998): Wideband CDMA for Third Generation Mobile Communication. Norwood, MA: Artech House.
- [8] Rappaport T. S., (1996): Wireless Communications Principles & Practice. IEEE Press. New York, Prentice Hall, pp. 399-422.
- [9] Bell T., Adam J., and Lowe S. (Jan. 1996): "Communications". IEEE Spectrum, pp. 30-41.
- [10] Kohonen J. (2003): Introduction to 3G Mobile Communications. Boston London: Artech House.
- [11] Ohmori S., Yamao Y., and Nakajima N. (Dec. 2000) "The Future Generation of Mobile Communications Based on Broad Access Technologies". IEEE Communication Magazine. Vol. 38, NO. 12, pp. 134-142.
- [12] Lawrey E., (Oct. 1997): "The suitability of OFDM as a modulation technique for wireless telecommunications, with a CDMA comparison". Australia. (<http://www.skydsp.com/publications/4thyrthesis/index.htm#Table%20of%20Contents>) (8.5.2007)
- [13] Steele R., Ed. (1992): Mobile Radio Communications. New York: IEEE Press/Pentech.
- [14] Gibbson J. D.(1996): The Mobile Communications Handbook. New York: IEEE Press/CRC Press.
- [15] (Feb. 1995): "Special issue on the European path toward UMTS". IEEE Personal Communication Magazine, Vol. 2, NO. 1.
- [16] Hanzo L. and Stefanov J. (1992): The pan-European digital cellular mobile radio system-known as GSM. Mobile Radio Communication. R. Steele, Ed. London: Pentech, ch. 8, pp. 677-773.
- [17] Telecommunications Industry Association. (1989): Dual-mode Subscriber Equipment-Network Equipment Compatibility Specification, Interim Standard IS-54.
- [18] Ojanpera T. (1996): Overview of research activities for third generation mobile communications. In Digital Beamforming in Wireless Communication. J. Litva and T. K.-Y. Lo, Eds. Norwood, MA: Artech House, pp. 415-446.
- [19] Pehkonen K., Holma H., Keskitalo I., Nikula E., and Nestman T. (Sept. 1997): A performance analysis of TDMA and CDMA based air interface solutions for UMTS high bit rate services. In Proc. PIMRC'97. Helsinki, pp. 22-26. 48.
- [20] Pajukoski K. and Savisalo J. (Sept. 1997): Wideband CDMA test system. In Proc. PIMRC'97, Helsinki, pp. 669-673.
- [21] Klein A., Pirhonen R., Skold J., and Suoranta R. (Sept. 1997): FRAMES Multiple access mode 1-Wideband TDMA with and without spreading. In Proc. PIMRC'97, Helsinki. pp. 37-41.
- [22] Baier P. W., Jung P., and Klein A. (Feb. 1996): "Taking the challenge of multiple access for third-generation cellular mobile radio systems-A European view". IEEE Communication Magazine. Vol. 34, NO. 2, pp. 82-89.
- [23] Engstroem B. and Oesterberg C. (1994): A system for test of multi-access methods based on OFDM. In Proc. VTC'94, Stockholm, Sweden, pp. 1843-1847.
- [24] Baier P. W., Blanz J., and Schmalenberger R. (1996): Fundamentals of smart antennas for mobile radio applications. In Digital Beamforming in Wireless Communication. J. Litva and T. K.-Y. Lo, Eds. Norwood, MA: Artech House, pp. 345-376.
- [25] Adachi F. *et al.* (Sept. 1996): Coherent DS-SS—Promising multiple access for wireless multimedia mobile communications. In Proc. IEEE ISSSTA'96. Mainz, Germany, pp. 351-358.
- [26] Intermec 2003 (Jul. 2003): "Taking it to the Streets: A Guide to Wide Area Wireless for the Non-Technical Business Professional". (http://epsfiles.intermec.com/eps_files/eps_wp/TakingItToTheStreets_wp_web.pdf) (05.05.2007).

References

- [27] European Commission (Aug. 1994): "Advanced communications technologies and services (ACTS) workplan". DGXIII-B-RA946043-WP.
- [28] 3rd Generation Mobile System Group. URL: <http://www.3gpp.org> (01-05-2007).
- [29] Swales S., Beach M. (Apr. 1994): "Third Generation Wireless Networks". University of Bristol, Future Communication Systems course.
- [30] Molisch A. (Sep. 2005): *Wireless Communication*. John Wiley & Sons, Ltd.
- [31] OFDM as a modulation technique for wireless communications, with a CDMA comparison. (URL: <http://www.skydsp.com/publications/4thyrthesis>) (08-07-2006).
- [32] Mohr W. (Aug. 2002): "Heterogeneous Networks to Support User Needs with Major Challenges for New Wideband Access Systems" *Wireless Personal Communication*. (Kluwer), Vol. 22, NO. 2, pp. 109-137.
- [33] Nakagawa H. (Sep. 6-7, 2002): "Vision in WP8F and Activity in Japan for Future Mobile Communication System". In Strategic Workshop 2002 Unified Global Infrastructure, Prague, Czech Republic.
- [34] Jamallpour A., Wada T., and Yamazato T. (Feb. 2005): "A Tutorial on Multiple Access Technologies for Beyond 3G Mobile Networks". *IEEE Communication Magazine*. Vol. 43, NO. 2.
- [35] Proglor M., Evci C., and Umehira M. (Sept. 1999): "Air interface access schemes for broadband mobile systems". *IEEE Communication Magazine*. pp. 106-15.
- [36] Verdu S. (2003): *Multuser Detection*. Cambridge. U.K., Cambridge University press.
- [37] Prasad R. and Hara S. (Dec. 1997): "Overview of Multicarrier CDMA". *IEEE Communication Magazine*. pp. 126-33.
- [38] Miller S. and Rainbolt B. (Nov. 2000): "MMSE detection of multicarrier CDMA". *IEEE Journal Select. Areas Communication*. Vol. 18, pp. 2356-2362.
- [39] Kondo S. and Milstein L. (Feb. 1996): "Performance of multicarrier DS-CDMA systems". *IEEE Transactions Communication*. Vol. 44, pp. 238-246.
- [40] Jamoos A., Labarre D., Grivel E. and Najim M. (Sept. 4-8 2005): Two cross coupled Kalman filters for joint estimation of MC-DS-CDMA fading channels and their corresponding autoregressive parameters. In Proc. EUSIPCO'05. Antalya.
- [41] Jamoos A., Grivel E. and Najim M. (Sep. 5-8, 2004): Designing Adaptive Filters-Based MMSE Receivers for Asynchronous Multicarrier DS-CDMA Systems. In proceedings IEEE PIMRC'04. pp.2930-2934, Barcelona, Spain.
- [42] Jamoos A., Grivel E. and Abdel Nour H. (May. 26-28, 2005): Kalman Filtering based Channel Prediction and Decorrelation Multiuser Detection for MC-DS-CDMA Systems. In Proc. of the 8th Cost 276 workshop, Norway.
- [43] Jamoos A., Grivel E. and Najim M. (Mar. 18-23, 2005): Blind Adaptive Multi-User Detection for Multi-Carrier DS-CDMA Systems in Frequency Selective Fading Channels. In proceedings IEEE ICASSP'05. pp. 925-928, Philadelphia, USA.
- [44] Tugnait J. K., Tong L., and Ding Z. (May. 2000): "Single-user channel estimation and equalization". *IEEE Signal Processing Magazine*. Vol. 17, NO. 3, pp. 17-28.
- [45] Gao W., Tsai S. and Lehnert J. S. (Feb. 2003): "Diversity combining for DS/SS systems with time-varying, correlated fading branches". *IEEE Transactions Communication*. Vol. 51, NO. 2, pp. 284-295.
- [46] Hassasneh W., Jamoos A., Grivel E., and Abdel Nour H. (Sept. 19-21 2006): Estimation of MC-DS-CDMA Fading Channels Based on Kalman Filtering with High Order Autoregressive Models. In Proc. MCWC'06. Amman.
- [47] Hassasneh W., Jamoos A., and Abdel Nour H. (Dec.19-21 2006): Adaptive Channel Estimation for Multi-carrier DS-CDMA Mobile Communication Systems. In Proc. ACIT2K. Al Yarmouk.
- [48] Yang S. (1998): *CDMA RF System Engineering*. Artech House, Boston London.
- [49] Glisic S. G. (2004): *Advanced Wireless Communications - 4G Technologies*. Wiley.
- [50] Schulze H., and Luders (2005): *Theory and Applications of OFDM and CDMA- wideband Wireless Communications*. John Wiley & Sons Ltd.
- [51] Jamalipour A., Wada T., and Yamazato T. (Feb. 2005): "A Tutorial on Multiple Access Technologies for Beyond 3G Mobile Networks". *IEEE Communication Magazine*.
- [52] Telecomm. Industry Association (TIA) (1993): *Mobile station - Base station compatibility standard for dual-mode wideband spread spectrum cellular system*, EIA/TIA Interim Standard IS-95. Washington, DC.

References

- [53] Viterbi A. J. (1995): CDMA: Principles of Spread Spectrum Communication. Addison-Wesley Publishing Company.
- [54] Pickholtz R. L., Milstein L. B., and Schilling D. L. (May. 1991): "Spread spectrum for mobile communications". IEEE Transactions on Vehicular Technology. Vol. 40, pp. 313-322.
- [55] Zigangirov K. (2004): Theory of Code Division Multiple Access Communication. Canada.
- [56] Mandyam G., and Lai J. (2002): Third-generation CDMA systems for enhanced data services. Prentice-Hall. First edition, USA.
- [57] Yang L. and Hanzo L. (Oct. 2003): "Multicarrier DS-CDMA: A Multiple Access Scheme for Ubiquitous Broadband Wireless Communications". IEEE Communication Magazine. Vol. 41, NO. pp. 116-24, 10.
- [58] Suwa S., Atarashi H., and Sawahashi M. (Sept. 2002): "Performance Comparison between MC-DS-CDMA and MC-CDMA for Reverse Link Broadband Packet Wireless Access". Proc. VTC-2002 Fall, Vancouver, Canada, pp. 2076-80.
- [59] Paulraj A. J. and Ng B. C. (Feb. 1998): "Space-time modems for wireless personal communications". IEEE Personal Communication Vol. 5, NO. 1, pp. 36-48.
- [60] Viterbi A. J., Viterbi A. M., and Zehavi E. (Apr. 1993): "Performance of power-controlled wideband terrestrial digital communication". IEEE Transactions on Vehicular Technology. Vol. 41, NO. 4, pp. 559-569.
- [61] Rappaport S. T. (1996): Wireless Communications. Prentice-Hall. First edition, USA.
- [62] Peterson R. L., Ziemer R. E., and Borth D. E. (1995): Introduction to Spread Spectrum Communications. Prentice Hall, Inc.
- [63] Proakis J. G. (1995): Digital Communications. New York: McGraw-Hill.
- [64] Lee W. C. Y. (1989): Mobile Cellular Telecommunication Systems. McGraw-Hill, Inc.
- [65] Dent P., Bottomley G. and Croft T. (Jun. 1993): "Jakes fading model revisited". IEE Electronics Letters. Vol. 29, NO. 13, pp.1162-1163.
- [66] Barbarossa S. (Mar. 2005): Multiantenna Wireless Communication Systems. Artech House. First edition, Italy.
- [67] Guo D., Verdu S., and Rasmussen L. (Dec. 2002): "Asymptotic Normality of Linear Multiuser Receiver Outputs". IEEE Transactions on Information Theory. Vol. 48, NO. 12.
- [68] Lupas R. and Verdu S. (Jan. 1989): "Linear multiuser detectors for synchronous code-division multiple-access channels". IEEE Transactions Information Theory. Vol. 35, pp. 123-136.
- [69] Hara S. and Parsad R. (Dec. 1997): "Overview of multicarrier CDMA". IEEE Communication Magazine. pp. 126-133.
- [70] Komninakis C., Fragouli C., Sayed A., and Wesel R. (May 2002): "Multi-input multi-output fading channel tracking and equalization using Kalman estimation". IEEE Transactions On Signal Processing. Vol. 50, NO.5, pp. 1065-1076.
- [71] Tsatsanis M., Giannakis G., and Zhou G. (Sept. 1996): "Estimation and equalization of fading channels with random coefficients". Signal Processing. Vol. 53, pp. 211-229.
- [72] Wu H., and Duel-Hallen A. (May. 2000): "Multiuser detectors with disjoint Kalman channel estimators for synchronous CDMA mobile radio channels". IEEE Transactions On Communication. Vol. 48, NO. 5, pp. 752-756.
- [73] Chen L., and Chen B. (Jul. 2001): "A robust adaptive DFE receiver for DS-CDMA systems under multipath fading channels". IEEE Transactions Signal Processing. Vol. 49, pp. 1523-1532.
- [74] Lindbom L., Ahlen A., Sternad M., and Falkenstrom M. (Jan. 2002): "Tracking of time-varying mobile radio channels. II. A case study". IEEE Transactions On Communication. Vol. 50, NO. 1, pp. 156-167.
- [75] Baddour K., and Beaulieu N. (Jul. 2005): "Autoregressive modeling for fading channel simulation". IEEE Transactions On Wireless Communication. Vol. 4, NO. 4, pp. 1650-1662.
- [76] Li H., and Cavers J. (1991): "An adaptive filtering technique for pilot-aided transmission systems". IEEE Transactions on Vehicular Technology. Vol. 40, NO.3, pp. 532-545.
- [77] Fechtel S., and Meyr H. (1994): "Optimal parametric feed forward estimation of frequency-selective fading radio channels". IEEE Transactions on Communication. Vol. 42, NO. 21314, pp. 1639-1650.
- [78] Kam P., and Teh C. (1987): "The Adaptive diversity reception over a slow nonselective fading channel". IEEE Transactions on Communication. Vol. 35, No. 5, pp. 572-574.
- [79] Liu Y., and Bloestein S. (1995): "Identification of frequency non-selective fading channels using decision feedback and adaptive linear prediction". IEEE Transactions on Communication. Vol. 43, NO. 2/3/4, pp. 1484-1492.

References

- [80] Xu G., Liu H., Tong L., and Kailath T. (1995): "A least-squares approach to blind channel identification". IEEE Transactions on Signal Processing. Vol. 43, NO. 12, pp. 2982-2993.
- [81] Tsatsanis M. (1995): "Time-varying system identification and channel equalization using wavelets and higher-order statistics". Digital Signal Processing Techniques and Applications. ed., C.T Leondes, Academic Press, Vol. 68, pp. 333-394.
- [82] Giordano A., and Hsu F. (1985): Least Square Estimation with Applications to Digital Signal Processing. New York: Wiley.
- [83] Papoulis A. (1991): Probability, Random Variables, and Stochastic Processes. New York: McGraw-Hill.
- [84] Colman G., Blostein S., and Beaulieu N. (1997): An ARMA multipath fading simulator. In Wireless Personal Communication.: Improving Capacity, Services and Reliability, Boston, MA: Kluwer,.
- [85] Young D., and Beaulieu N. (Jan. 2003): "Power margin quality measures for correlated random varieties derived from the normal distribution". IEEE Transactions Information Theory. Vol. 49, NO. 1, pp. 241–252.
- [86] Simon H. (2002): Adaptive Filter Theory. Prentice-Hall. Fourth edition, USA.
- [87] Montazeri M. and Duhamel P., (Feb. 1995): "A Set of Algorithms Linking NLMS and Block RLS Algorithms U". IEEE Transactions on Signal Processing, Vol. 43, No. 2.
- [88] Morgan D. and Kratzer, S., (Aug. 1996): "On a Class of Computationally Efficient, Rapidly Converging, Generalized NLMS Algorithms". IEEE Signal Processing Letters, Vol. 3, No. 8.
- [89] Sankaran S. and Beex A., (April 2000): "Convergence Behavior of Affine Projection Algorithms". IEEE Transactions On Signal Processing, Vol. 48, No. 4.
- [90] Shin H., Sayed A., and Song W., (Feb. 2004): "Variable Step-Size NLMS and Affine Projection Algorithms". IEEE Signal Processing Letters, Vol. 11, No. 2.
- [91] Soni R., Gallivan K., and Jenkins W.,(Feb. 2004): "Low-Complexity Data Reusing Methods in Adaptive Filtering," IEEE Transactions On Signal Processing, Vol. 52, No. 2.
- [92] Hanzo L., Wong C., and Yee M., (2002): Adaptive Wireless Transceivers, John Wiley & Sons, Ltd, England.
- [93] Press W., Teukolsky S., Vetterling W., and Flannery B., (1992): "Minimization or Maximization of Functions". In Numerical Recipes in C, ch. 10, pp. 394-455, Cambridge: Cambridge University Press.

Estimation of MC-DS-CDMA Fading Channels Based on Kalman Filtering with High Order Autoregressive Models

Walid Hassasneh¹, Ali Jamoos², Eric Grivel² and Hanna Abdel Nour¹

¹Department of Electronics Engineering, Al-Quds University, P.O. Box 20002, Jerusalem, Palestine

²Equipe Signal & Image, UMR 5131 LAPS, 351 Cours de la libération, 33405 Talence Cedex, France

Email: walid_hassasneh@yahoo.com; ali.jamoos@laps.u-bordeaux1.fr; egrivel@u-bordeaux1.fr; habdalnour@eng.alquds.edu

Abstract—This paper deals with the estimation of rapidly time-varying Rayleigh fading channels in synchronous multi-carrier direct-sequence code division multiple access (MC-DS-CDMA) systems. When the fading channel is approximated by an autoregressive (AR) process, it can be estimated by means of Kalman filtering for instance. Nevertheless, this requires the a priori estimation of the AR parameters. One standard solution consists in first fitting the AR process autocorrelation function to the Jakes one and then solving the resulting Yule-Walker equations (YWE). However, due to the band-limited nature of the Jakes Doppler spectrum, severely ill-conditioned YWE are unavoidable for all but very small AR model orders. Therefore, previous studies focused only on 1st and 2nd order AR models. To overcome the ill-conditioning problem, a very small positive bias can be added to the main diagonal of the autocorrelation matrix in the YWE. Even if the resulting process is not band-limited and corresponds to an AR process+noise model, the approximation can be of interest. Indeed, according to our simulation results, high-order AR models+noise yield significant results in terms of spectrum approximation and bit error rate (BER). However, to reduce the computational cost, a 5th order AR model can be considered.

Index Terms—Autoregressive processes, Rayleigh fading channels, Jakes model, Kalman filters, MC-DS-CDMA.

I. INTRODUCTION

For the last decade, there has been a great deal of interest in multi-carrier direct-sequence code division multiple access (MC-DS-CDMA) systems [1] due to their potentials for high data rate transmission, high bandwidth efficiency, fading resilience and interference suppression capability. Indeed, MC-DS-CDMA has been adopted as an option for the down-link transmission in the CDMA2000 third generation cellular standard [2].

Receiver design usually requires channel state information to achieve optimal diversity combining and coherent symbol detection. When considering the conventional MC-DS-CDMA receiver [3], which consists of a correlator along each carrier followed by a maximal ratio combiner (MRC), the channel fading processes are assumed to be perfectly known at the receiver. However, the fading processes are usually unknown and, hence, must be estimated. In that case, training sequence/pilot aided techniques and blind techniques [4] are two basic families for channel estimation. In this paper, we will focus our attention on training based channel estimation because blind techniques require longer observation window and have higher complexity than training based techniques.

The time-varying fading channels are typically modeled as stochastic processes with band-limited Doppler power spectra according to the Jakes model [5]. This information about channel dynamics cannot be however exploited when directly

estimating the fading processes by means of a recursive least square solution as in [6], or a least mean square (LMS) and recursive least square (RLS) algorithms as in [7]. Alternatively, Kalman filtering combined with an autoregressive (AR) model to describe the time evolution of the fading processes is shown to provide superior bit error rate (BER) performance over the model-independent LMS and RLS based channel estimators [7] [8]. Nevertheless, the AR model parameters are unknown and, hence, must be estimated. In addition, the selection of the AR model order must be investigated.

On the one hand, the AR parameters can be estimated from the received noisy signal. Among the existing methods, Tsatsanis *et al.* [9] have proposed to estimate the AR parameters from estimates of the channel data covariance function, by means of a standard Yule-Walker estimator. However, this method results in biased AR parameters estimates. In [10], the AR model parameters are estimated by using an expectation maximization (EM) algorithm involving a Kalman smoothing. Nevertheless, only 1st order AR model is considered. Recently, in [11], the authors have proposed a two-cross-coupled Kalman filter based structure for the joint estimation of MC-DS-CDMA fading channels and their corresponding AR parameters. One Kalman filter is used to estimate the fading process along each carrier while the second one makes it possible to estimate the corresponding AR parameters from the estimated fading process. This estimator is shown to outperform the model-independent LMS or RLS based estimators, especially for channels with high Doppler rates. Nevertheless, only 2nd order AR model is used for the sake of simplicity.

On the other hand, several authors (e.g., [8] [12] [13] [14]) have expressed the AR parameters by first fitting the AR process autocorrelation function to the Jakes one and then solving the resulting Yule-Walker equations (YWE). However, only low-order AR models are studied, but are not well suited to approximate a band-limited spectrum. Increasing the order could provide better approximation, but severely ill-conditioned YWE are unavoidable in that case. To overcome this problem, Baddour *et al.* [15] in the framework of channel simulation have suggested adding a very small positive bias ε to the main diagonal of the autocorrelation matrix in the YWE. Hence, this procedure consists in modeling the channel by a sum of an AR process whose order is very high and a zero-mean white noise with variance ε .

In this paper, we consider the estimation of rapidly time-varying MC-DS-CDMA Rayleigh fading channels based on Kalman filtering. More particularly, we propose to investigate the relevance of high-order AR models in the Kalman filter based channel estimator.

The remainder of the paper is organized as follows. In section II, we recall the synchronous MC-DS-CDMA system model and the receiver structure presented in [11]. The estimation of the fading channels based on Kalman filtering with high-order AR models is introduced in section III. Simulation results are reported in section IV for a DS-CDMA system based on one or more carriers.

II. MC-DS-CDMA SYSTEM MODEL

A down-link synchronous MC-DS-CDMA system with binary phase shift keying (BPSK) modulation is considered based on M carriers and involving K users. The transmitted signal at the m^{th} carrier can be expressed as follows:

$$S_m(t) = \text{Re} \left[\sum_{n=-\infty}^{+\infty} \sum_{k=1}^K \sqrt{E_{b_k}} b_k(n) c_k(t - nT_b) e^{j2\pi f_m t} \right] \quad (1)$$

where E_{b_k} is the bit energy of the k^{th} user, $b_k(n) \in \{-1, 1\}$ is the n^{th} data bit of the k^{th} user, T_b is the bit duration and f_m is the m^{th} carrier frequency. Furthermore, the spreading waveform of the k^{th} user is given by:

$$c_k(t) = \sum_{i=0}^{N-1} s_k(i) \psi(t - iT_c) \quad (2)$$

where T_c denotes the chip duration, $N = T_b/T_c$ is the processing gain, $s_k(i) \in \{\pm 1/\sqrt{N}\}$ with $i = 0, 1, \dots, N-1$ is the normalized spreading sequence and $\psi(t)$ is the chip pulse shape, assigned to 1 over the interval $[0, T_c]$ and 0 otherwise. The MC-DS-CDMA signal is assumed to be transmitted over a rapidly time-varying frequency-selective Rayleigh fading channel. By suitably choosing the number M of carriers, the carrier spacing and the bandwidth of the chip pulse shape $\psi(t)$ [3], each carrier can be assumed to undergo independent frequency non-selective flat fading. Thus, the system will provide a frequency diversity gain equal to the number of carriers.

In addition to the fading, the transmitted signal at the m^{th} carrier is disturbed by a zero-mean additive white Gaussian noise (AWGN) process $\eta_m(t)$. The noise processes $\{\eta_m(t)\}_{m=1, \dots, M}$ are assumed to be mutually independent and identically distributed, with equal variance σ_η^2 . Therefore, the continuous time received signal at the m^{th} carrier in its complex analytic form is given by:

$$r_m(t) = \sum_{n=-\infty}^{+\infty} \sum_{k=1}^K \sqrt{E_{b_k}} b_k(n) c_k(t - nT_b) h_m(n) e^{j2\pi f_m t} + \eta_m(t) \quad (3)$$

where the fading processes $\{h_m(n) = \beta_m(n) e^{j\theta_m(n)}\}_{m=1, \dots, M}$ are mutually independent and identically distributed complex Gaussian random processes. Indeed, $h_m(n)$ is zero-mean with a uniformly distributed phase $\theta_m(n)$ on $[0, 2\pi[$ and a Rayleigh distributed envelop $\beta_m(n)$. The variances of $\{h_m(n)\}_{m=1, \dots, M}$ are all assumed equal to σ_h^2 .

To retrieve the desired symbol sequence $b_1(n)$ of the first user, from the received signals $\{r_m(t)\}_{m=1, \dots, M}$, we use the

receiver structure presented in [11].

Let us recall the main steps of this receiver:

- First, the demodulated signal over the m^{th} carrier is processed with a chip-matched filter, which consists of an integrator with duration T_c . The samples are then stored during one bit interval, resulting in the following $N \times 1$ vector:

$$\mathbf{x}_m(n) = \sum_{k=1}^K \sqrt{E_{b_k}} b_k(n) h_m(n) \mathbf{s}_k + \boldsymbol{\eta}_m(n) \quad (4)$$

where $\mathbf{s}_k = [s_k(0) \ s_k(1) \ \dots \ s_k(N-1)]^T$ denotes the normalized spreading vector related to the k^{th} user and $\boldsymbol{\eta}_m(n)$ is an $N \times 1$ vector of AWGN samples.

- At that stage, the received vector at the m^{th} carrier is processed by the near-far resistant decorrelating detector [16], which can be written in the following form for user 1:

$$\mathbf{w}_1 = \sum_{k=1}^K [\mathbf{R}^{-1}]_{1k} \mathbf{s}_k \quad (5)$$

where $\mathbf{R} = [\mathbf{s}_1 \ \mathbf{s}_2 \ \dots \ \mathbf{s}_K]^T [\mathbf{s}_1 \ \mathbf{s}_2 \ \dots \ \mathbf{s}_K]$ is the normalized cross correlation matrix of the spreading vectors and $[\mathbf{R}^{-1}]_{ij}$

denotes the $(i, j)^{\text{th}}$ element of the inverse of the matrix \mathbf{R} .

This decorrelating detector is designed to eliminate the multiple access interference caused by other users and yields the following observation:

$$y_m(n) = \mathbf{w}_1^T \mathbf{x}_m(n) = \sqrt{E_{b_1}} b_1(n) h_m(n) + \xi_m(n) \quad (6)$$

where $\xi_m(n)$ is a zero-mean Gaussian noise with variance $\sigma_\xi^2 = \sigma_\eta^2 [\mathbf{R}^{-1}]_{11}$.

- The observations $\{y_m(n)\}_{m=1, \dots, M}$ are combined by using a MRC [17]. This results in the following decision about the desired user data symbol:

$$\hat{b}_1(n) = \text{sgn} \left(\text{Re} \left(\sum_{m=1}^M h_m^*(n) y_m(n) \right) \right) \quad (7)$$

Since the fading processes $\{h_m(n)\}_{m=1, \dots, M}$ are unknown, we propose to investigate their estimations based on Kalman filtering with high-order AR models in the next section.

III. KALMAN FILTERING BASED CHANNEL ESTIMATION

AR Modeling of Rayleigh Fading Channels

The stochastic characteristics of the m^{th} carrier fading process $h_m(n)$ depend on the maximum Doppler frequency:

$$f_d = v f_c / c \quad (8)$$

where v is the mobile speed, f_c is the central carrier frequency and c is the light speed.

According to [5], the theoretical power spectral density (PSD) associated with either the in-phase or quadrature portion of the fading process $h_m(n)$ is band-limited and U-shaped. Moreover, it exhibits two peaks at $\pm f_d$ as follows:

$$\Psi_{hh}(f) = \begin{cases} \frac{1}{\pi f_d \sqrt{1-(f/f_d)^2}}, & |f| \leq f_d \\ 0, & \text{elsewhere} \end{cases} \quad (9)$$

The corresponding normalized discrete-time autocorrelation function (ACF) hence satisfies:

$$R_{hh}(n) = J_0(2\pi f_d T_b |n|) \quad (10)$$

where $J_0(\cdot)$ is the zero-order Bessel function of the first kind and $f_d T_b$ denotes the Doppler rate.

Since a p^{th} order AR process, denoted by $\text{AR}(p)$, may exhibit up to p peaks in the frequency domain, the fading process along the m^{th} carrier can be modeled as follows:

$$h_m(n) = -\sum_{i=1}^p a_i h_m(n-i) + u_m(n) \quad (11)$$

where $\{a_i\}_{i=1, \dots, p}$ are the AR model parameters and $u_m(n)$ denotes the zero-mean complex white Gaussian driving process with equal variance σ_u^2 along all carriers.

The relationship between the AR parameters and the fading process ACF $R_{hh}(n)$ is given by:

$$R_{hh}(n) = -\sum_{i=1}^p a_i R_{hh}(n-i) \quad n \geq 1 \quad (12)$$

Equation (12) can be represented in a matrix form for $n=1, \dots, p$ as follows:

$$\underbrace{\begin{bmatrix} R_{hh}(0) & R_{hh}(-1) & \cdots & R_{hh}(-p+1) \\ R_{hh}(1) & R_{hh}(0) & \cdots & R_{hh}(-p+2) \\ \vdots & \vdots & \ddots & \vdots \\ R_{hh}(p-1) & R_{hh}(p-2) & \cdots & R_{hh}(0) \end{bmatrix}}_{\mathbf{R}_{hh}} \underbrace{\begin{bmatrix} a_1 \\ a_2 \\ \vdots \\ a_p \end{bmatrix}}_{\mathbf{a}} = \underbrace{\begin{bmatrix} R_{hh}(1) \\ R_{hh}(2) \\ \vdots \\ R_{hh}(p) \end{bmatrix}}_{\mathbf{v}} \quad (13)$$

Moreover, using (11), the variance of the driving process can be expressed as follows:

$$\sigma_u^2 = R_{hh}(0) + \sum_{i=1}^p a_i R_{hh}(-i) \quad (14)$$

Given $R_{hh}(n)$ in (10), the AR parameters can be obtained by solving the YWE, i.e. $\mathbf{a} = -\mathbf{R}_{hh}^{-1} \mathbf{v}$, where \mathbf{R}_{hh}^{-1} denotes the inverse of the fading process autocorrelation matrix.

Nevertheless, when solving the YWE, one has to pay attention to the condition number of the autocorrelation matrix \mathbf{R}_{hh} as it will determine the accuracy of the solution. Indeed, due to the band-limited nature of the Doppler fading process spectrum, the YWE suffers from ill-conditioning for all but very small AR model orders. For this reason and for the sake of simplicity, previous studies (e.g., [8] [12] [13] [14]) focused only on low-order AR models. As mentioned in section I, Baddour *et al.* [15] suggested a simple heuristic approach to reduce the condition number of \mathbf{R}_{hh} , by adding a very small positive bias ε to its main diagonal. Thus, the first $p+1$ autocorrelation lags of the resulting $\text{AR}(p)$ process satisfy:

$$\hat{R}_{hh}(n) = \begin{cases} R_{hh}(0) + \varepsilon, & n = 0 \\ R_{hh}(n), & n = 1, 2, \dots, p \end{cases} \quad (15)$$

It was demonstrated in [15] that the value of the added bias ε mainly depends on the Doppler rate $f_d T_b$. Typical values of ε , which represent a trade-off between the improved condition number of \mathbf{R}_{hh} and the bias introduced in the model, are given in Table I. These values are obtained empirically and are recommended for model orders up to 1000.

TABLE I
TYPICAL VALUES OF THE ADDED BIAS ε FOR VARIOUS DOPPLER RATES.

Doppler rate $f_d T_b$	Added bias ε
0.001	10^{-5}
0.005	10^{-6}
0.01	10^{-7}
0.05	10^{-8}
0.1	10^{-9}
0.2	10^{-9}

As the ill-conditioning problem can be “solved” by the above approach, dealing with high-order AR models becomes possible: indeed, as illustrated in Fig. 1, the higher the order, the better the approximation of the true Rayleigh channel PSD. Looking at the ACF for order equal to 1, 2, 5 and 20 (see Fig. 2) can be an alternative to see the relevance of high-order AR process+noise for Rayleigh channel modeling. However, the higher the AR model order, the higher the computational cost. Thus, a compromise has to be found.

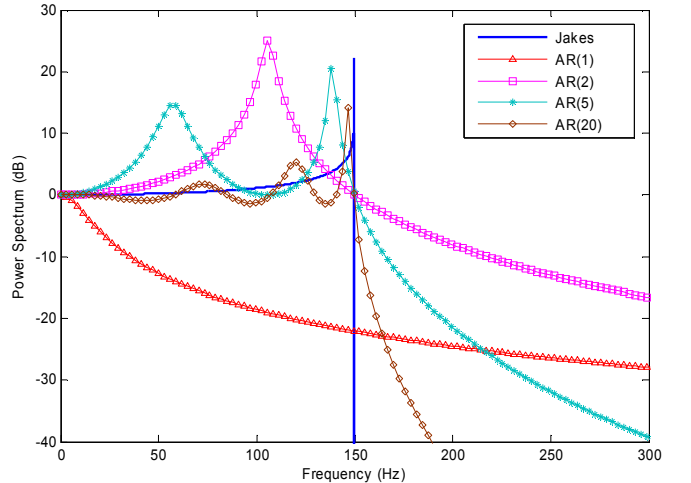


Fig. 1. Power spectral density of the Jakes model and that of the fitted $\text{AR}(p)$ process with $p=1, 2, 5$, and 20 . $f_d = 150\text{Hz}$ and $f_d T_b = 0.05$.

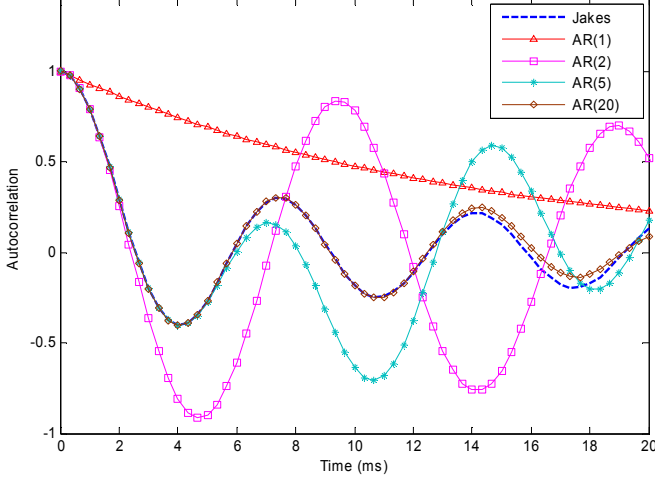


Fig. 2. Autocorrelation function of the Jakes model and that of the fitted AR (p) process with $p=1, 2, 5,$ and 20 . $f_d = 150\text{Hz}$ and $f_d T_b = 0.05$.

Estimation of the Fading Processes

Since our purpose is to estimate the m^{th} carrier fading sequence $h_m(n)$ modeled by a p^{th} order AR process as in (11), the $p \times 1$ state vector is defined as follows:

$$\mathbf{h}(n) = [h(n) \quad h(n-1) \quad \cdots \quad h(n-p+1)]^T \quad (16)$$

It should be noted that, for the sake of simplicity and clarity of presentation, the carrier subscript is dropped.

Thus, the resulting state space representation of the m^{th} carrier fading channel system (6) and (11) is given by:

$$\mathbf{h}(n+1) = \mathbf{\Phi} \mathbf{h}(n) + \mathbf{g} u(n) \quad (17)$$

$$y(n) = \mathbf{b}^T(n) \mathbf{h}(n) + \xi(n) \quad (18)$$

where the transition matrix $\mathbf{\Phi}$, the input vector \mathbf{g} and the observation vector $\mathbf{b}(n)$ are respectively defined as follows:

$$\mathbf{\Phi} = \begin{bmatrix} -a_1 & -a_2 & \cdots & -a_p \\ 1 & 0 & \cdots & 0 \\ & \ddots & & \vdots \\ 0 & \cdots & 1 & 0 \end{bmatrix}, \quad (19)$$

$$\mathbf{g} = [1 \quad 0 \quad \cdots \quad 0]^T, \quad \text{and} \quad \mathbf{b}(n) = \sqrt{E_{b_1}} b_1(n) [1 \quad 0 \quad \cdots \quad 0]^T$$

Given the above state space representation of the system, Kalman filtering can be carried out to provide the estimation $\hat{\mathbf{h}}(n+1/n)$ of the state vector $\mathbf{h}(n+1)$ given the set of observations $\{y(i)\}_{i=1, \dots, n}$ as listed below:

The so-called innovation process $\alpha(n)$ is first obtained:

$$\alpha(n) = y(n) - \mathbf{b}^T(n) \hat{\mathbf{h}}(n/n-1) \quad (20)$$

Its variance is then defined:

$$C(n) = E[\alpha(n) \alpha^*(n)] = \mathbf{b}^T(n) \mathbf{P}(n/n-1) \mathbf{b}(n) + \sigma_\xi^2 \quad (21)$$

where $\mathbf{P}(n/n-1)$ denotes the so-called a priori error covariance matrix at time n .

The Kalman gain is calculated in the following manner:

$$\mathbf{K}(n) = \mathbf{\Phi} \mathbf{P}(n/n-1) \mathbf{b}(n) C^{-1}(n) \quad (22)$$

The estimation of the state vector $\hat{\mathbf{h}}(n+1/n)$ and the fading process $\hat{h}(n+1/n)$ are respectively given by:

$$\hat{\mathbf{h}}(n+1/n) = \mathbf{\Phi} \hat{\mathbf{h}}(n/n-1) + \mathbf{K}(n) \alpha(n) \quad (23)$$

$$\hat{h}(n+1/n) = \mathbf{g}^T \hat{\mathbf{h}}(n+1/n) \quad (24)$$

The error covariance matrix \mathbf{P} is updated as follows:

$$\mathbf{P}(n/n) = \mathbf{P}(n/n-1) - \mathbf{P}(n/n-1) \mathbf{b}(n) C^{-1}(n) \mathbf{b}^T(n) \mathbf{P}(n/n-1) \quad (25)$$

$$\mathbf{P}(n+1/n) = \mathbf{\Phi} \mathbf{P}(n/n) \mathbf{\Phi}^H + \mathbf{g} \sigma_u^2 \mathbf{g}^T \quad (26)$$

It should be noted that the state vector and the error covariance matrix are initially assigned to zero vector and identity matrix respectively, i.e. $\hat{\mathbf{h}}(0/-1) = \mathbf{0}$ and $\mathbf{P}(0/-1) = \mathbf{I}_p$.

Like most adaptive algorithms, the above Kalman filtering algorithm requires a training period during which $b_1(n)$ is known at the receiver to adjust to the channel. Once in the so-called decision-directed mode, the detected symbol $\hat{b}_1(n)$ defined in (7) will be used instead.

It should be noted that the computational cost $O(p^3)$ of the above Kalman estimation algorithm increases much when the AR model order increases.

IV. SIMULATION RESULTS

A. Simulation Protocols

In this section, computer simulation results are provided to illustrate the BER performance of the MC-DS-CDMA system using Kalman channel estimator with high-order AR models, under realistic Jakes model with various fading rate scenarios. In addition, the performance of the Kalman estimator is compared with the standard LMS and RLS based ones.

We consider a system of $K=10$ multiple-access active users, each using a gold code of length $N=31$. Here, moderate values for the number of carriers (i.e. $M=1$ and $M=3$) are used as adopted by the third generation CDMA2000 standard [2]. In addition, the fading processes $\{h_m(n)\}_{m=1, \dots, M}$ are generated according to the modified Jakes model [18] and they are normalized to have a unit variance, i.e. $\sigma_h^2 = 1$. The average SNR per carrier for the desired user is defined by:

$$\text{SNR} = 10 \log_{10}(E_{b_1} \sigma_h^2 / \sigma_\eta^2) \quad (27)$$

The bit energy of the desired user is set to $E_{b_1} = 1$ and the noise is generated according to the SNR.

Moreover, the value of the added bias ε is chosen as in Table I for AR models whose order is larger than 4.

B. Results, Comments and Conclusion

Fig. 3 shows the estimated envelope and phase of the fading process along the first carrier using the Kalman filter based estimator with AR(5) model, the LMS estimator and the RLS estimator. From this figure, one can notice that the Kalman filter based estimator provides much better estimation than the LMS and RLS based ones.

According to Fig. 4, which illustrates the BER performance of the MC-DS-CDMA system versus SNR, the Kalman filter based channel estimator results in much lower BER than the LMS and RLS based ones which tend to an error floor at high SNR. Therefore, exploiting the channel statistics by using AR models in the proposed channel estimator results in significant performance improvement over the model-independent LMS and RLS based estimators. In addition, increasing the AR model order will improve the BER performance of the system.

Furthermore, a significant frequency diversity gain is obtained when increasing the number of carriers from $M=1$ to $M=3$.

In Fig. 5, the effects of different fading rates on the BER performance with the various channel estimators are illustrated. For low Doppler rates $f_d T_b < 0.01$, comparable BER performances can be noticed for the various estimators. However, for high Doppler rates $f_d T_b > 0.01$, the Kalman estimator performs much better than the others especially for high-order AR models.

Based on Fig. 4 and Fig. 5, an AR(20) model is preferable as it always yields lower BER than an AR(5) model. Nevertheless, to reduce the computational cost $O(p^3)$ of the estimation algorithm, an AR(5) model is recommended, especially for low Doppler rate scenarios.

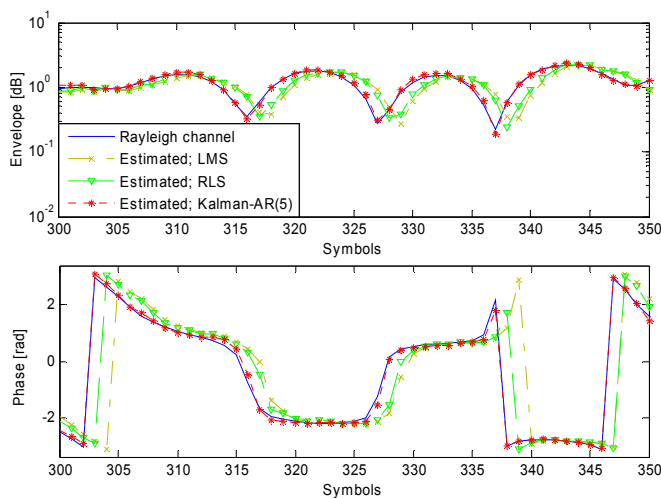


Fig. 3. Envelope and Phase of the estimated fading process along the first carrier with the various channel estimators. SNR=20 dB and $f_d T_b = 0.05$.

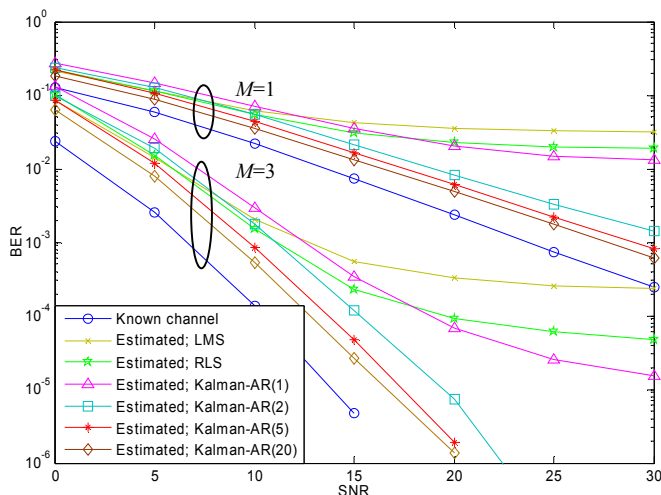


Fig. 4. BER performance of the MC-DS-CDMA system with the various channel estimators for number of carriers $M=1$ and $M=3$. $f_d T_b = 0.05$.

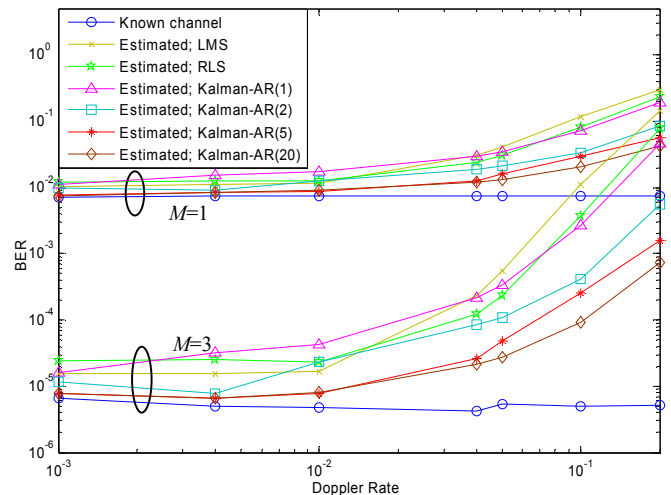


Fig. 5. BER performance of the MC-DS-CDMA system with the various channel estimators versus the Doppler rate for number of carriers $M=1$ and $M=3$. SNR=15 dB.

REFERENCES

- [1] L. Hanzo, L. Yang, E. Kuan and K. Yen, Single and Multi-carrier DS-SS, Multiuser Detection, Space Time Spreading, Synchronization and Standard, Wiley & Sons, Ltd., 2003.
- [2] CDMA2000, Physical layer standard for cdma2000 spread spectrum systems. 2001.
- [3] S. Kondo and L. Milstein, "Performance of multicarrier DS-SS systems," IEEE Trans. Commun., vol. 44, pp. 238-246, February 1996.
- [4] J. K. Tugnait, Lang Tong and Zhi Ding, "Single-user channel estimation and equalization," IEEE Signal Processing Magazine, vol. 17, no. 3, pp. 17-28, May 2000.
- [5] W. C. Jakes, Microwave Mobile Communications. New York: Wiley, 1974.
- [6] S. Miller and B. Rainbolt, "MMSE detection of multicarrier CDMA," IEEE Journal Select. Areas Commun., vol. 18, pp. 2356-2362, Nov. 2000.
- [7] D. N. Kalofonos, M. Stojanovic and J. G. Proakis, "Performance of adaptive MC-SS detectors in rapidly fading Rayleigh channels," IEEE Trans. On Wireless Commun., vol. 2, no. 2, pp. 229-239, March 2003.
- [8] C. Kominakis, C. Fragouli, A. H. Sayed and R. D. Wesel, "Multi-input multi-output fading channel tracking and equalization using Kalman estimation," IEEE Trans. On Signal Processing, vol. 50, no.5, pp. 1065-1076, May 2002.
- [9] M. Tsatsanis, G. B. Giannakis and G. Zhou, "Estimation and equalization of fading channels with random coefficients," Signal Process., vol. 53, pp. 211-229, Sept. 1996.
- [10] W. Gao, S. Tsai and J. S. Lehnert "Diversity combining for DS/SS systems with time-varying, correlated fading branches" IEEE Trans. Commun., vol. 51, no. 2, pp. 284-295, Feb. 2003.
- [11] A. Jamoos, D. Labarre, E. Grivel and M. Najim, "Two cross coupled Kalman filters for joint estimation of MC-DS-SS fading channels and their corresponding autoregressive parameters," in Proc. EUSIPCO'05, Antalya, 4-8 Sept. 2005.
- [12] H. Y. Wu and A. Duel-Hallen, "Multiuser detectors with disjoint Kalman channel estimators for synchronous CDMA mobile radio channels," IEEE Trans. Commun., vol. 48, no. 5, pp. 752-756, May 2000.
- [13] L. M. Chen and B. S. Chen, "A robust adaptive DFE receiver for DS-SS systems under multipath fading channels," IEEE Trans. Signal Process., vol. 49, pp. 1523-1532, July 2001.
- [14] L. Lindbom, A. Ahlen, M. Sternad and M. Falkenstrom, "Tracking of time-varying mobile radio channels. II. A case study," IEEE Trans. On Communications, vol. 50, no. 1, pp. 156-167, Jan. 2002.
- [15] K. E. Baddour and N. C. Beaulieu, "Autoregressive modeling for fading channel simulation," IEEE Trans. On Wireless Commun., vol. 4, no. 4, pp. 1650-1662, July 2005.
- [16] S. Verdú, Multiuser Detection. Cambridge, U.K., Cambridge University press, 1998.
- [17] J. G. Proakis, Digital Communications. New York: McGraw-Hill, 1995.
- [18] P. Dent, G. Bottomley and T. Croft, "Jakes fading model revisited," IEE Electronics Letters, vol. 29, no. 13, pp.1162-1163, June 1993.

ADAPTIVE CHANNEL ESTIMATION FOR MULTI-CARRIER DS-CDMA MOBILE COMMUNICATION SYSTEMS

Walid Hassasneh¹, Ali Jamoos², Eric Grivel² and Hanna Abdel Nour¹

¹Department of Electronics Engineering, Al-Quds University, P.O. Box 20002, Jerusalem, Palestine

²Equipe Signal & Image, UMR 5131 LAPS, 351 Cours de la libération, 33405 Talence Cedex, France
Email: walid_hassasneh@yahoo.com; ali.jamoos@laps.u-bordeaux1.fr; egrivel@u-bordeaux1.fr; habdalnour@eng.alquds.edu

ABSTRACT

In this paper, we investigate the adaptive estimation of time-varying Rayleigh fading channels in Multi-Carrier Direct-Sequence Code Division Multiple Access (MC-DS-CDMA) mobile communication systems. When the fading channel is modeled by an Autoregressive (AR) process, it can be adaptively estimated by means of Kalman filtering. Nevertheless, this requires the a priori estimation of the AR parameters. Based on the well-known Jakes model, the AR parameters can be obtained by first fitting the AR process autocorrelation function to the Jakes one and then solving the resulting Yule-Walker Equations (YWE). However, due to the band-limited nature of the Jakes Doppler spectrum, severely ill-conditioned YWE are unavoidable for all but very small AR model orders. For this reason and for the sake of simplicity, previous studies focused only on first and second order AR models. To solve the ill-conditioning problem, a very small positive bias is added to the main diagonal of the autocorrelation matrix in the YWE. This removes the band-limitation of the original spectrum and, hence, enables us to investigate the relevance of high order AR models. Simulation results show that a fifth order AR model can provide a trade-off between the accuracy of the model and the computational cost.

Keywords: MC-DS-CDMA, fading channels, adaptive Kalman filters, autoregressive processes, Jakes model.

1. INTRODUCTION

In recent years, there has been a great deal of interest in Multi-Carrier Direct-Sequence Code Division Multiple Access (MC-DS-CDMA) mobile wireless communication systems [1] due to their potentials for high data rate transmission, high bandwidth efficiency, fading resilience and interference suppression capability. Indeed, MC-DS-CDMA has been adopted as an option for the down-link transmission in the CDMA2000 third generation cellular standard [2].

The design of receivers usually requires channel state information to achieve optimal diversity combining and coherent symbol detection. The conventional MC-DS-CDMA receiver [3], which consists of a correlator along each carrier followed by a Maximal Ratio Combiner

(MRC), assumes that the channel fading processes are perfectly known at the receiver. However, the fading processes are usually unknown and, hence, should be estimated. There are two basic categories of channel estimation techniques: Training sequence aided techniques and blind techniques [4]. Compared with the training based techniques, blind techniques require longer observation window and have higher complexity. Thus, we will focus our attention on training based adaptive channel estimation in this paper.

The time variations of fading channels are typically modeled as stochastic processes with U-shaped band-limited Doppler power spectra according to the Jakes model [5]. However, this key feature about channel dynamics is not exploited when directly estimating the fading processes by means of a recursive least square solution as in [6], or Least Mean Square (LMS) and Recursive Least Square (RLS) algorithms as in [7]. Alternatively, when an Autoregressive (AR) model is used to describe the time evolution of the fading process, Kalman filtering can be carried out and is shown to provide superior performance over the model-independent LMS and RLS based channel estimators [7] [8]. Nevertheless, the AR model parameters are unknown and, hence, must be determined. In addition, the selection of the AR model order must be investigated.

On the one hand, the AR parameters can be estimated from the received noisy signal. Among the existing methods, Tsatsanis *et al.* [9] have proposed to estimate the AR parameters from channel covariance estimates by means of a standard Yule-Walker estimator. However, this method results in biased estimates. In [10], the parameters of the AR model are estimated by means of an Expectation Maximization (EM) algorithm involving a Kalman smoothing. Nevertheless, only first order AR model is considered. Recently, in [11], the authors have proposed a two-cross-coupled Kalman filter based structure for the joint estimation of MC-DS-CDMA fading channels and their corresponding AR parameters. One Kalman filter is used to estimate the fading process along each carrier while the second one makes it possible to estimate the corresponding AR parameters from the estimated fading process. This estimator is shown to provide significant results over the model-independent LMS or RLS based estimators, especially for channels with high Doppler rates. Nevertheless, only second order AR model is used for the sake of simplicity.

On the other hand, several authors (e.g., [8][12][13][14]) have expressed the AR parameters by first fitting the AR process autocorrelation function to the Jakes one and then solving the resulting Yule-Walker Equations (YWE). However, only low order AR models are considered and they are not well suited to approximate a band-limited spectrum. In addition, due to the band-limited nature of Jakes Doppler spectrum, severely ill-conditioned YWE are unavoidable for all but very small AR model orders. To solve the ill-conditioning problem, Baddour *et al.* [15] have suggested adding a very small positive bias to the main diagonal of the autocorrelation matrix in the YWE. This removes the band-limitation of the Jakes Doppler spectrum and enables them to use very high order AR models to accurately simulate Rayleigh fading channel.

In this paper, we consider the adaptive estimation of time-varying MC-DS-CDMA mobile Rayleigh fading channels based on Kalman filtering. Particularly, we propose to investigate the relevance of high order AR models in the Kalman filter based channel estimator.

The remainder of the paper is organized as follows. In section 2, we recall the synchronous MC-DS-CDMA system model and the receiver structure proposed by one of the authors in [11]. The adaptive estimation of the fading channels is introduced in section 3. Simulation results are reported in section 4 and conclusions are given in section 5.

2. MC-DS-CDMA SYSTEM DESCRIPTION

Let us consider a down-link synchronous MC-DS-CDMA system with Binary Phase Shift Keying (BPSK) modulation based on M carriers and involving K users. The transmitted signal at the m^{th} carrier can be expressed as follows:

$$S_m(t) = \text{Re} \left[\sum_{n=-\infty}^{+\infty} \sum_{k=1}^K \sqrt{E_{b_k}} b_k(n) c_k(t - nT_b) e^{j2\pi f_m t} \right] \quad (1)$$

where E_{b_k} is the bit energy of the k^{th} user, $b_k(n) \in \{-1, 1\}$ is the n^{th} data bit of the k^{th} user, T_b is the bit duration and f_m is the m^{th} carrier frequency. Furthermore, the spreading waveform of the k^{th} user is given by:

$$c_k(t) = \sum_{i=0}^{N-1} s_k(i) \psi(t - iT_c) \quad (2)$$

where T_c is the chip duration, $N = T_b/T_c$ is the processing gain, $s_k(i) \in \{\pm 1/\sqrt{N}\}$ with $i = 0, 1, \dots, N-1$ is the normalized spreading sequence and $\psi(t)$ is the chip pulse shape, assigned to 1 over the interval $[0, T_c]$ and 0 otherwise.

The MC-DS-CDMA signal is assumed to be transmitted over a rapidly time-varying frequency-selective Rayleigh fading channel. By suitably choosing the number M of carriers, the carrier spacing and the bandwidth of the chip pulse shape $\psi(t)$ [3], each carrier can be assumed to undergo independent frequency non-selective flat fading. Thus, the system will provide a frequency diversity gain equal to the number of carriers.

In addition to the fading, the transmitted signal at the m^{th} carrier is corrupted by a zero-mean Additive White Gaussian

Noise (AWGN) process $\eta_m(t)$. The noise processes $\{\eta_m(t)\}_{m=1, \dots, M}$ are assumed to be mutually independent and identically distributed, with equal variance σ_η^2 . Therefore, the continuous time received signal at the m^{th} carrier in its complex analytic form is given by:

$$r_m(t) = \sum_{n=-\infty}^{+\infty} \sum_{k=1}^K \sqrt{E_{b_k}} b_k(n) c_k(t - nT_b) h_m(n) e^{j2\pi f_m t} + \eta_m(t) \quad (3)$$

where the fading processes $\{h_m(n) = \beta_m(n) e^{j\theta_m(n)}\}_{m=1, \dots, M}$ are mutually independent and identically distributed complex Gaussian random processes. Indeed, $h_m(n)$ is zero-mean with a uniformly distributed phase $\theta_m(n)$ on $[0, 2\pi)$ and a Rayleigh distributed envelop $\beta_m(n)$. The variances of $\{h_m(n)\}_{m=1, \dots, M}$ are all assumed equal to σ_h^2 .

To retrieve the desired symbol sequence $b_1(n)$ of the first user, from the received signals $\{r_m(t)\}_{m=1, \dots, M}$, we use the receiver structure presented in [11].

Let us recall the main steps of this receiver: First, the demodulated signal over the m^{th} carrier is processed with a chip-matched filter, which consists of an integrator with duration T_c . The samples are then stored during one bit interval, resulting in the following $N \times 1$ vector:

$$\mathbf{x}_m(n) = \sum_{k=1}^K \sqrt{E_{b_k}} b_k(n) h_m(n) \mathbf{s}_k + \boldsymbol{\eta}_m(n) \quad (4)$$

where $\mathbf{s}_k = [s_k(0) \ s_k(1) \ \dots \ s_k(N-1)]^T$ denotes the normalized spreading vector related to the k^{th} user and $\boldsymbol{\eta}_m(n)$ is an $N \times 1$ vector of AWGN samples.

At that stage, the received vector at the m^{th} carrier is processed by the near-far resistant decorrelating detector [16], which can be written form for user 1 as follows:

$$\mathbf{w}_1 = \sum_{k=1}^K [\mathbf{R}^{-1}]_{1k} \mathbf{s}_k \quad (5)$$

where $\mathbf{R} = [\mathbf{s}_1 \ \mathbf{s}_2 \ \dots \ \mathbf{s}_K]^T [\mathbf{s}_1 \ \mathbf{s}_2 \ \dots \ \mathbf{s}_K]$ is the normalized cross correlation matrix of the spreading vectors and $[\mathbf{R}^{-1}]_{ij}$ denotes the $(i, j)^{\text{th}}$ element of the inverse of the matrix \mathbf{R} .

This decorrelating detector is designed to eliminate the multiple access interference caused by other users and yields the following observation:

$$y_m(n) = \mathbf{w}_1^T \mathbf{x}_m(n) = \sqrt{E_{b_1}} b_1(n) h_m(n) + \xi_m(n) \quad (6)$$

where $\xi_m(n)$ is a zero-mean Gaussian noise with variance $\sigma_\xi^2 = \sigma_\eta^2 [\mathbf{R}^{-1}]_{11}$.

The observations $\{y_m(n)\}_{m=1, \dots, M}$ are combined by using a MRC [17]. This results in the following decision about the desired user data symbol:

$$\hat{b}_1(n) = \text{sgn} \left(\text{Re} \left(\sum_{m=1}^M h_m^*(n) y_m(n) \right) \right) \quad (7)$$

As the fading processes $\{h_m(n)\}_{m=1,\dots,M}$ are unknown, we propose to investigate their estimations in the next section.

3. ADAPTIVE CHANNEL ESTIMATION

3.1. LMS CHANNEL ESTIMATOR

The LMS channel estimator is based on minimizing the Mean Square Error (MSE) criteria $E[|y_m(n) - b_1(n)h_m(n)|^2]$. Given the available observation $y_m(n)$ and the unit energy training sequence $b_1(n)$, the fading process estimate over the m^{th} carrier at time $n+1$ can be obtained as follows:

$$\hat{h}_m(n+1) = \hat{h}_m(n) + \mu[y_m(n) - b_1(n)\hat{h}_m(n)]b_1^*(n) \quad (8)$$

where $\mu > 0$ is the step size.

3.2. RLS CHANNEL ESTIMATOR

The RLS channel estimator is based on minimizing the cost

function $\sum_{i=0}^n \lambda^{n-i} |y_m(i) - b_1(i)h_m(i)|^2$ with a forgetting factor

$0 < \lambda < 1$. The fading process estimate at $n+1$ is given by:

$$\hat{h}_m(n+1) = \hat{h}_m(n) + [y_m(n) - b_1(n)\hat{h}_m(n)]K_m^*(n) \quad (9)$$

where the gain $K_m(n)$ is given by:

$$K_m(n) = [\lambda + P_m(n)b_1^2(n)]^{-1}P_m(n)b_1(n) \quad (10)$$

and $P_m(n)$ is updated recursively as:

$$P_m(n+1) = \lambda^{-1}[1 - K_m(n)b_1^*(n)]P_m(n) \quad (11)$$

3.3. KALMAN CHANNEL ESTIMATOR

3.3.1 AUTOREGRESSIVE MODELING OF RAYLEIGH FADING CHANNELS

The stochastic characteristics of the m^{th} carrier fading process $h_m(n)$ depend on the maximum Doppler frequency:

$$f_d = v f_c / c \quad (12)$$

where v is the mobile speed, f_c is the central carrier frequency and c is the light speed.

According to [5], the theoretical Power Spectral Density (PSD) associated with either the in-phase or quadrature portion of the fading process $h_m(n)$ is band-limited and U-shaped. Moreover, it exhibits two peaks at $\pm f_d$ as follows:

$$\Psi_{hh}(f) = \begin{cases} \frac{1}{\pi f_d \sqrt{1 - (f/f_d)^2}}, & |f| \leq f_d \\ 0, & \text{elsewhere} \end{cases} \quad (13)$$

Thus, the corresponding normalized discrete-time Autocorrelation Function (ACF) satisfies:

$$R_{hh}(n) = J_0(2\pi f_d T_b |n|) \quad (14)$$

where $J_0(\cdot)$ is the zero-order Bessel function of the first kind and $f_d T_b$ denotes the Doppler rate.

Since a p^{th} order AR process, denoted by AR(p), may exhibit up to p peaks in the frequency domain, the fading process along the m^{th} carrier can be modeled as follows:

$$h_m(n) = -\sum_{i=1}^p a_i h_m(n-i) + u_m(n) \quad (15)$$

where $\{a_i\}_{i=1,\dots,p}$ are the AR model parameters and $u_m(n)$ denotes the zero-mean complex white Gaussian driving process with equal variance σ_u^2 along all carriers.

The relationship between the AR parameters and the Jakes model ACF $R_{hh}(n)$ is given by:

$$R_{hh}(n) = \begin{cases} -\sum_{i=1}^p a_i R_{hh}(n-i), & n \geq 1 \\ -\sum_{i=1}^p a_i R_{hh}(-i) + \sigma_u^2, & n = 0 \end{cases} \quad (16)$$

Equation (16) can be represented in a matrix form for $n = 1, \dots, p$ as follows:

$$\underbrace{\begin{bmatrix} R_{hh}(0) & R_{hh}(-1) & \cdots & R_{hh}(-p+1) \\ R_{hh}(1) & R_{hh}(0) & \cdots & R_{hh}(-p+2) \\ \vdots & \vdots & \ddots & \vdots \\ R_{hh}(p-1) & R_{hh}(p-2) & \cdots & R_{hh}(0) \end{bmatrix}}_{\mathbf{R}_{hh}} \underbrace{\begin{bmatrix} a_1 \\ a_2 \\ \vdots \\ a_p \end{bmatrix}}_{\mathbf{a}} = - \underbrace{\begin{bmatrix} R_{hh}(1) \\ R_{hh}(2) \\ \vdots \\ R_{hh}(p) \end{bmatrix}}_{\mathbf{v}} \quad (17)$$

In addition, the variance of the driving process can be expressed as:

$$\sigma_u^2 = R_{hh}(0) + \sum_{i=1}^p a_i R_{hh}(-i) \quad (18)$$

Given $R_{hh}(n)$ in (14), the AR parameters can be determined by solving the set of p YWE in (17). Since \mathbf{R}_{hh} is an autocorrelation matrix, its inverse exists and a unique solution for AR parameters can be calculated by $\mathbf{a} = -\mathbf{R}_{hh}^{-1}\mathbf{v}$. Table 1 shows a typical AR(5) parameters of a fading channel with $f_c = 1800\text{MHz}$, $T_b = 100\mu\text{s}$ and various mobile speeds.

TABLE 1: THE FADING PROCESS AR(5) PARAMETERS FOR $f_c = 1800\text{MHz}$, $T_b = 100\mu\text{s}$ AND VARIOUS MOBILE VELOCITIES.

Mobile velocity (KM/HR)	15	45	75	90
Doppler frequency f_d (Hz)	25	75	125	150
Doppler rate $f_d T_b$	0.0025	0.0075	0.0125	0.015
a_1	-0.79761	-1.4814	-1.8278	-1.9012
a_2	-0.49616	-0.15788	0.075537	0.22188
a_3	-0.19728	0.48294	0.79141	0.79326
a_4	0.09896	0.44077	0.5147	0.3698
a_5	0.39252	-0.28319	-0.55372	-0.48371
σ_u^2	2.102e-5	4.489e-6	6.104e-7	7.122e-7

Unfortunately, due to the band-limited nature of the Doppler fading processes, \mathbf{R}_{hh} will become nearly singular when the driving process variance σ_u^2 gets very small which is the case when increasing the AR model order. Indeed, the YWE will suffer from ill-conditioning starting from very small AR model orders. For this reason and for simplicity purposes, previous studies (e.g., [8][12][13][14]) have focused

only on low order AR models. To solve the ill-conditioning problem, Baddour et al. [15] have suggested a simple heuristic approach to improve the conditioning of \mathbf{R}_{hh} by adding a very small positive bias ε to its main diagonal. This means that the fading process is modeled by an AR process disturbed by an additive white noise. Thus, the first $p+1$ autocorrelation lags of the resulting AR(p) process will satisfy:

$$\hat{R}_{hh}(n) = \begin{cases} R_{hh}(0) + \varepsilon, & n = 0 \\ R_{hh}(n), & n = 1, 2, \dots, p \end{cases} \quad (19)$$

It was demonstrated in [15] that the value of the added bias ε that results in the most accurate AR parameters computation depends mainly on the Doppler rate $f_d T_b$. Typical values of ε , which represent a tradeoff between the improved condition number of \mathbf{R}_{hh} and the bias introduced in the model, are given in Table 2.

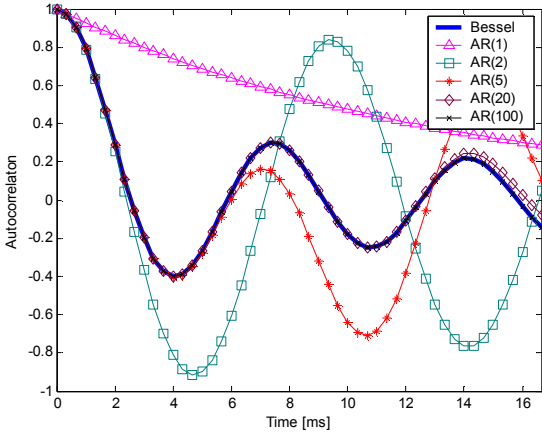


Fig. 1 Autocorrelation function of the Jakes model and that of the fitted AR(p) process with $p=1, 2, 5, 20$, and 100 . $f_d = 150\text{Hz}$ and $f_d T_b = 0.05$.

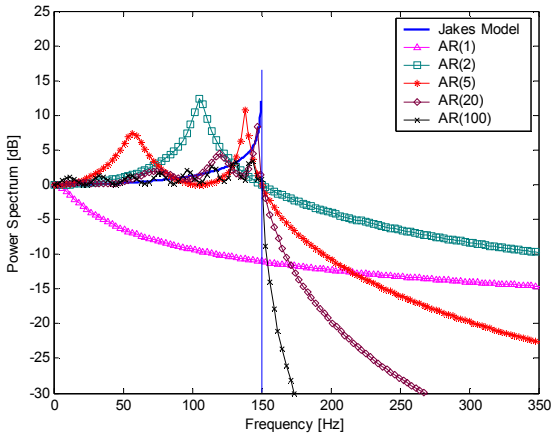


Fig. 2. Power spectral density of the Jakes model and that of the fitted AR(p) process with $p=1, 2, 5, 20$ and 100 . $f_d = 150\text{Hz}$ and $f_d T_b = 0.05$.

As the ill-conditioning problem can be solved by the above approach, dealing with high order AR models will become possible. Indeed, increasing the AR model order will lead to a better fit between the statistics of the resulting AR process and the realistic Jakes channel. This is illustrated in Fig. 1 and Fig.

2, where we, respectively, present the ACF and the PSD of the Jakes model and the fitted AR process whose order is 1, 2, 5, 20, and 100. However, the higher the AR model order, the higher the computational cost. Thus, a happy medium has to be found.

TABLE 2: TYPICAL VALUES OF THE ADDED BIAS ε FOR DIFFERENT DOPPLER RATES.

Doppler rate $f_d T_b$	Added bias ε
0.001	10^{-5}
0.005	10^{-6}
0.01	10^{-7}
0.05	10^{-8}
0.1	10^{-9}
0.2	10^{-9}

3.3.2 ESTIMATION OF FADING PROCESSES

Since our purpose is to estimate the m^{th} carrier fading sequence $h_m(n)$ modeled by a p^{th} order AR process as in (15), the $p \times 1$ state vector is defined as follows:

$$\mathbf{h}(n) = [h(n) \ h(n-1) \ \dots \ h(n-p+1)]^T \quad (20)$$

It should be noted that, for the sake of simplicity and clarity of presentation, the carrier subscript is dropped.

Thus, the resulting state space representation of the m^{th} carrier fading channel system (6) and (15) is given by:

$$\mathbf{h}(n+1) = \mathbf{\Phi} \mathbf{h}(n) + \mathbf{g} u(n) \quad (21)$$

$$y(n) = \mathbf{b}^T(n) \mathbf{h}(n) + \zeta(n) \quad (22)$$

where the state transition matrix $\mathbf{\Phi}$, the input vector \mathbf{g} and the observation vector $\mathbf{b}(n)$ are respectively defined as follows:

$$\mathbf{\Phi} = \begin{bmatrix} -a_1 & -a_2 & \dots & -a_p \\ 1 & 0 & \dots & 0 \\ & \ddots & & \vdots \\ 0 & \dots & 1 & 0 \end{bmatrix}, \quad (23)$$

$$\mathbf{g} = [1 \ 0 \ \dots \ 0]^T, \text{ and } \mathbf{b}(n) = \sqrt{E_{b_i} b_i(n)} [1 \ 0 \ \dots \ 0]^T$$

Given the above state space representation of the system, Kalman filtering can be carried out to provide the estimation $\hat{\mathbf{h}}(n+1/n)$ of the state vector $\mathbf{h}(n+1)$ given the set of observations $\{y(i)\}_{i=1, \dots, n}$ as listed below:

The so-called innovation process $\alpha(n)$ is first obtained:

$$\alpha(n) = y(n) - \mathbf{b}^T(n) \hat{\mathbf{h}}(n/n-1) \quad (24)$$

Its variance is then defined:

$$C(n) = E[\alpha(n) \alpha^*(n)] = \mathbf{b}^T(n) \mathbf{P}(n/n-1) \mathbf{b}(n) + \sigma_\zeta^2 \quad (25)$$

where $\mathbf{P}(n/n-1)$ denotes the so-called error covariance matrix.

The Kalman gain is calculated in the following manner:

$$\mathbf{K}(n) = \mathbf{\Phi} \mathbf{P}(n/n-1) \mathbf{b}(n) C^{-1}(n) \quad (26)$$

The estimation of the state vector $\hat{\mathbf{h}}(n+1/n)$ and the fading process $\hat{h}(n+1/n)$ are respectively given by:

$$\hat{\mathbf{h}}(n+1/n) = \mathbf{\Phi} \hat{\mathbf{h}}(n/n-1) + \mathbf{K}(n) \alpha(n) \quad (27)$$

$$\hat{h}(n+1/n) = \mathbf{g}^T \hat{\mathbf{h}}(n+1/n) \quad (28)$$

The error covariance matrix is updated as follows:

$$\mathbf{P}(n/n) = \mathbf{P}(n/n-1) - \mathbf{P}(n/n-1)\mathbf{b}(n)C^{-1}(n)\mathbf{b}^T(n)\mathbf{P}(n/n-1) \quad (29)$$

and

$$\mathbf{P}(n+1/n) = \Phi\mathbf{P}(n/n)\Phi^H + \mathbf{g}\sigma_u^2\mathbf{g}^T \quad (30)$$

It should be noted that, the state vector and the error covariance matrix are initially assigned to zero vector identity matrix respectively, i.e. $\hat{\mathbf{h}}(0/-1) = \mathbf{0}$ and $\mathbf{P}(0/-1) = \mathbf{I}_p$. The above Kalman filtering algorithm requires a training period during which $b_1(n)$ is known at the receiver to adjust to the channel. Once in the so-called decision-directed mode, the detected symbol $\hat{b}_1(n)$ defined in (7) will be used instead.

4. SIMULATION RESULTS

4.1. SIMULATION PROTOCOLS

In this section, computer simulation results are provided to illustrate the Bit Error Rate (BER) performance of the MC-DS-CDMA system using Kalman channel estimator with high order AR models, under different fading rate scenarios. In addition, the performance of the Kalman estimator is compared with the standard LMS and RLS based ones. We consider a system of $K=10$ multiple-access active users, each using a gold code of length $N=31$. In addition, the fading processes $\{h_m(n)\}_{m=1,\dots,M}$ are generated according to the modified Jakes model [18] with 16 distinct oscillators. They are normalized to have a unit variance, i.e. $\sigma_h^2 = 1$. The average Signal-to-Noise Ratio (SNR) per carrier for the desired user is defined by:

$$\text{SNR} = 10\log_{10}(E_b\sigma_h^2/\sigma_n^2) \quad (31)$$

The bit energy of the desired user is set to $E_b = 1$ and the noise is generated according to the SNR. Moreover, the value of the added bias ε is chosen as in Table 2 for AR models whose order is larger than 4.

4.2. RESULTS AND COMMENTS

Fig. 3 shows the estimated real and imaginary parts of the fading process along the first carrier using the Kalman filter based estimator with AR(5) model, the LMS estimator and the RLS estimator. From this figure one can notice that the Kalman filter based estimator provides much better estimation than the LMS and RLS estimators.

According to Fig. 4, which illustrate the BER performance of the MC-DS-CDMA system versus SNR, the Kalman filter based channel estimator results in much lower BER than the LMS and RLS based ones which tend to an error floor at high SNR. Therefore, exploiting the channel statistics by using AR models in the proposed channel estimator results in significant performance improvement over the model-independent LMS and RLS based estimators. In addition, increasing the AR model order will improve the BER performance of the system with the amount of improvement decreases as the AR model order increases. Furthermore, a significant frequency diversity gain is obtained when increasing the number of carriers from $M=1$ to $M=3$. In Fig. 5, the effects of different fading rates on the BER performance with the various channel estimators are illustrated. For low Doppler rates $f_d T_b < 0.01$, comparable BER performances can be noticed for the various estimators.

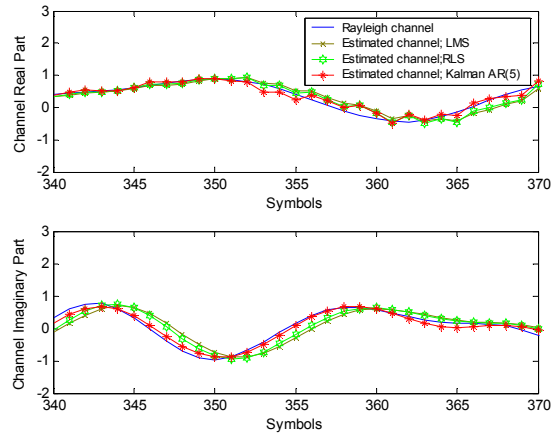


Fig. 3. Real and Imaginary parts of the estimated fading process along the first carrier with the various channel estimators. SNR=20 dB and $f_d T_b = 0.05$.

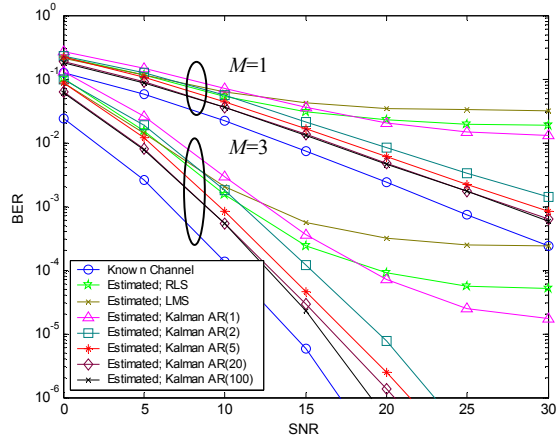


Fig. 4. BER performance of the MC-DS-CDMA system with the various channel estimators for number of carriers $M=1$ and $M=3$. $f_d T_b = 0.05$.

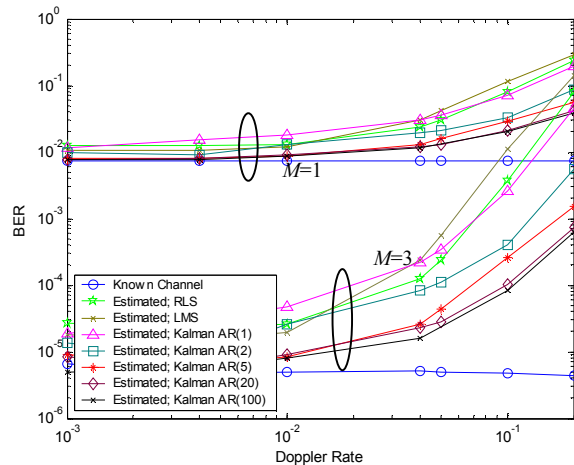


Fig. 5. BER performance of the MC-DS-CDMA system with the various channel estimators versus the Doppler rate for number of carriers $M=1$ and $M=3$. SNR=15 dB.

However, for high Doppler rates $f_d T_b > 0.01$, the Kalman estimator performs much better than the others especially for high order AR models. Therefore, the Kalman estimator is appealing for high Doppler rate environments. Based on and

the various tests we have carried out, a 5th order AR model can provide a trade-off between the accuracy of the model and the computational complexity $O(p^3)$ of the Kalman estimation algorithm.

5. CONCLUSION

The estimation of rapidly time-varying MC-DS-CDMA fading channels based on Kalman, LMS, and RLS filters is considered. The relevance of high order AR models in the Kalman filter based channel estimator is investigated. According to our simulations, an AR(5) model can provide a trade-off between the accuracy of the model and the computational cost.

REFERENCES

- [1] L. Hanzo, L. Yang, E. Kuan and K. Yen, Single and Multi-carrier DS-SS-CDMA, Multiuser Detection, Space Time Spreading, Synchronization and Standard, Wiley & Sons, Ltd., 2003.
- [2] CDMA2000, Physical layer standard for cdma2000 spread spectrum systems. 2001.
- [3] S. Kondo and L. Milstein, "Performance of multicarrier DS-SS-CDMA systems," *IEEE Trans. Commun.*, vol. 44, pp. 238-246, February 1996.
- [4] J. K. Tugnait, Lang Tong and Zhi Ding, "Single-user channel estimation and equalization," *IEEE Signal Processing Magazine*, vol. 17, no. 3, pp. 17-28, May 2000.
- [5] W. C. Jakes, *Microwave Mobile Communications*. New York: Wiley, 1974.
- [6] S. Miller and B. Rainbolt, "MMSE detection of multicarrier CDMA," *IEEE Journal Select. Areas Commun.*, vol. 18, pp. 2356-2362, Nov. 2000.
- [7] D. N. Kalofonos, M. Stojanovic and J. G. Proakis, "Performance of adaptive MC-SS-CDMA detectors in rapidly fading Rayleigh channels," *IEEE Trans. On Wireless Commun.*, vol. 2, no. 2, pp. 229-239, March 2003.
- [8] C. Komminakis, C. Fragouli, A. H. Sayed and R. D. Wesel, "Multi-input multi-output fading channel tracking and equalization using Kalman estimation," *IEEE Trans. On Signal Processing*, vol. 50, no.5, pp. 1065-1076, May 2002.
- [9] M. Tsatsanis, G. B. Giannakis and G. Zhou, "Estimation and equalization of fading channels with random coefficients," *Signal Process.*, vol. 53, pp. 211-229, Sept. 1996.
- [10] W. Gao, S. Tsai and J. S. Lehnert "Diversity combining for DS/SS systems with time-varying, correlated fading branches" *IEEE Trans. Commun.*, vol. 51, no. 2, pp. 284-295, Feb. 2003.
- [11] A. Jamoos, D. Labarre, E. Grivel and M. Najim, "Two cross coupled Kalman filters for joint estimation of MC-SS-CDMA fading channels and their corresponding autoregressive parameters," in *Proc. EUSIPCO'05*, Antalya, 4-8 Sept. 2005.
- [12] H. Y. Wu and A. Duel-Hallen, "Multiuser detectors with disjoint Kalman channel estimators for synchronous CDMA mobile radio channels," *IEEE Trans. Commun.*, vol. 48, no. 5, pp. 752-756, May 2000.
- [13] L. M. Chen and B. S. Chen, "A robust adaptive DFE receiver for DS-SS-CDMA systems under multipath fading channels," *IEEE Trans. Signal Process.*, vol. 49, pp. 1523-1532, July 2001.
- [14] L. Lindbom, A. Ahlen, M. Sternad and M. Falkenstrom, "Tracking of time-varying mobile radio channels. II. A case study," *IEEE Trans. On Communications*, vol. 50, no. 1, pp. 156-167, Jan. 2002.
- [15] K. E. Baddour and N. C. Beaulieu, "Autoregressive modeling for fading channel simulation," *IEEE Trans. On Wireless Commun.*, vol. 4, no. 4, pp. 1650-1662, July 2005.
- [16] S. Verdu, *Multiuser Detection*. Cambridge, U.K., Cambridge University press, 1998.
- [17] J. G. Proakis, *Digital Communications*. New York: McGraw-Hill, 1995.
- [18] P. Dent, G. Bottomley and T. Croft, "Jakes fading model revisited," *IEE Electronics Letters*, vol. 29, no. 13, pp.1162-1163, June 1993.